THE ROLE OF REELIN AFTER TRAUMATIC BRAIN INJURY

By

VALENTINA DAL POZZO

A dissertation submitted to the

School of Graduate Studies

Rutgers, The State University of New Jersey

In partial fulfillment of the requirements

For the degree of

Doctor of Philosophy

Graduate Program in Neuroscience

Written under the direction of:

Gabriella D'Arcangelo

And approved by:

_____

_____

_____

_____

New Brunswick, New Jersey

October, 2019

ABSTRACT OF THE DISSERTATION

THE ROLE OF REELIN AFTER TRAUMATIC BRAIN INJURY

By VALENTINA DAL POZZO

Dissertation Director:

Gabriella D'Arcangelo

Traumatic brain injury (TBI) causes severe cognitive disability or death, resulting from common occurrences as car accidents, falls, high-impact sport, violence, or explosive blasts.

Statistical data indicate that approximately 2 million people are affected annually by TBI in the United States alone. Most of the time, the symptoms are evident immediately or soon after the impact. The injury results in various symptoms, such as seizures, cognitive disability, loss of memory, visual disturbances and other debilitating neurological problems. The patients require long rehabilitative treatments at a high cost for them and their families. At the moment, there are limited treatments available, and no effective cure for cognitive disability after TBI.

In this study, we investigated the potential role of the Reelin protein in neuroprotection and recovery after TBI. Reelin is a glycoprotein that regulates brain development during embryogenesis and synaptic plasticity during adult life. Reelin has been implicated in several developmental brain disorders, including epilepsy and schizophrenia, where its reduced expression may alter neuronal activity. A few studies also suggested that Reelin may play a role in the recovery after brain damage by stimulating adult neurogenesis, protecting tissue from cell death, and promoting tissue

repair by restoring synaptic connectivity. In this work, we used the controlled cortical impact (CCI) technique to model TBI in the mouse brain and found that Reelin expression changes in response to the injury, especially in the hippocampus, an area of the brain that plays an important role in learning and memory. We also conducted *in vitro* experiments using mouse neuronal cultures and observed that exogenous Reelin protects neuronal cells from the toxicity induced by high doses of glutamate, an excitatory amino acid that increases rapidly in the extracellular space after brain injury. Based on these findings, we hypothesize that Reelin may be beneficial for neuroprotection and functional recovery after TBI. To further investigate recovery, we also performed preliminary behavioral studies in mice to establish whether CCI results in cognitive and motor deficits.

The long-term goal of this study is to firmly establish whether Reelin could be a new target for pharmacological intervention aimed at improving the quality of life for people affected by TBI.

Acknowledgements

This work was possible with the support of many people.

First, thank you to Dr. Gabriella D'Arcangelo for her wonderful mentorship. She is the one that made this work possible, always enthusiastic about discussing data or experiments, and not only that. She is a great person, and I was lucky to meet and choose her as my thesis's advisor.

My committee members: Dr. Bonnie Firestein, Dr. Janet Alder, Dr. Ping Xie for all the advises and support for my project. In particular, thank you to Dr. Janet Alder who introduced me to the traumatic brain injury field and helped me at the beginning of the study with the preliminary data and the lateral fluid percussion model. She is always available to help with troubleshooting and advise for experiments and career opportunity.

Thank you to our collaborators. Dr. David Crockett for all the help with the traumatic brain injury model, cortical controlled impact, for all the training hours and the funny talks about experiments, science and life. Dr. George Wagner for the behavioral experiments. A special thank you to Janace Gifford, a Ph.D student in his lab for the training, and help with the Morris Water Maze. Thank you to Dr. Comoletti for the purified Reelin protein.

Thank you to my undergraduate students. Nicholas Briski for the Reelin counting; Khush Patel for the purified Reelin and Natalie Samper that helped me in a different project involving induced pluripotent stem cells from patients affected by Tuberous Sclerosis Complex and siblings. Thank you to my lab members: in particular Beth Crowell, for all the help with the mice and for her funny entertainment stories that make your day

happier. Thank you to Dr. Avery Zucco for working with me in the Tuberous Sclerosis Complex project and for the interesting discussions.

Thank you to all the past D'Arcangelo's lab members. In particular, Dr. Gum Hwa Lee and Dr. Tatiana Kazdoba who trained me when first I joined the lab.

Thank you to my colleague Dr. Ning Chiang, we started and finished together with graduate school.

Thank you to the Neuroscience graduate program at Rutgers University, Robert Wood Johnson Medical School: Dr. John Pintar for his advises and mentorship, Joan Mordes for her great administrative assistance, Neuroconnections club and the student associations.

Thank you to the Cell Biology and Neuroscience department, Rutgers University. Thank you to Dr. Mike Kiledjian for the collaboration with a different project and his lab always available to help me when I need; Dr. Noriko Goldsmith for the technical assistance in the confocal and the INCell analyzer; Dr. Lori Covey, for her kindness and nice talks about science and life in all these years. Thank you to Lauryn Siu and Carolyn Ambrose for administrative assistance.

Thank you to the funding provided by a fellowship from the New Jersey Commission on Brain Injury Research.

Finally, thank you to my family that even far away, they supported me in all my decisions. Thank you to Rafael and the nice surprise in my life. Thank you to all my friends, essential to get through all my Ph.D. life. Special thank you to my best friend Paola, even in a different country, she is always there when I need it, and she would like to be here with me.

Table of Contents

List of Tables

List of Figures

Chapter I: Introduction

1.1 Traumatic Brain Injury

Traumatic brain injury (TBI) is a complex injury often leading to severe neurological disability or death. TBI is largely caused by motor vehicle accidents, falls, violence, sport-related injuries, explosions or gunshot wounds. The injury can result in different levels of damage to the brain, as a blunt trauma or as a penetrating head injury that disrupts normal brain function. In the United States, it is estimated the TBI affects 1.7 million people every year, and the number is increasing every year. It is estimated that 10 million people will be affected annually by 2020 and TBI will be the major cause of death and disability (Humphreys et al., 2013; Hyder et al., 2007). According to the Centers for Disease Control and Prevention (CDC), in 2014 in the United Stated TBI affected 2,8 million people and most of them (85-90%) required emergency department visits, 288,000 hospitalizations, and 56,800 people died (Taylor et al., 2017). TBI has a dramatic economic impact for the society. The estimated annual cost ranges from $60 billion to $221 billion, including medical cost, loss of work and quality of life (Coronado et al., 2012; Faul M, 2010). Most of the insurance companies cover the acute period of the recovery, but a large number of the survivors from a severe brain injury also needs extensive rehabilitation (DeGrauw et al., 2018).

The symptoms caused by TBI are widespread, and the disruption of the brain results in different clinical symptoms such as loss of consciousness, memory loss, dizziness, difficulty in thinking, and other neurological deficits like weakness and loss of balance (Blennow et al., 2016). Based on clinical neurological symptoms, like amnesia or

unconscious status, and brain imaging, TBI can be classified as mild, moderate or severe. The severity of the injury can be categorized based on the Glasgow Coma Scale (GCS) that classifies mild injury (score between 13-15); moderate (between 9-12) or severe (score < 9) in the first 24 hours (Prins et al., 2013) (Table 1).

	Mild TBI	Moderate TBI	Severe TBI
Structural Brain imaging	Normal	Normal or abnormal	Normal or abnormal
Loss of consciousness (duration)	0-30 minutes	30 minutes to 24 hours	>24 hours
Altered mental state (duration)	≤ 24 hours	>24hours	>24 hours
Post-trauma amnesia (duration)	≤ 1 day	1-7 days	>7 days
Glasgow Coma Scale score	13-15	9-12	<9

Table 1. Classification of TBI by the US Department of Veterans Affairs and the US Department of Defense. (Table adapted from Blennow et at., 2016).

Mild to moderate injury represents 80-90% of the total TBI cases (Blennow et al., 2016; Eme, 2017). It is typically caused by non-penetrating head trauma, and the physical symptoms include headaches, dizziness, sleep disruption, nausea and vomiting; cognitive symptoms include poor concentration and amnesia, whereas emotional symptoms include the presence of irritability and loss of consciousness (Prince & Bruhns, 2017). Mild TBI can resolve in 7-10 days, however, TBI can result in long-term cognitive problems like

seizures, anxiety, attention and memory deficits, and visual disturbance. These symptoms can occur soon after the injury, but in many cases, they appear sometime after the injury. If the symptoms persist (> 3 months), the patients are diagnosed with chronic post-concussion syndrome (PCS) that can last up to 12 months (Silverberg & Iverson, 2011). Thus, the injury can affect the quality of life of the patients and their family for extended periods of time (Okie, 2005). Severe injuries cause an accentuation of the symptoms of the mild TBI and often include loss of coordination, slurred speech, persistent headaches and can result in severe disability, vegetative state or death (Dekmak et al., 2018; Mena et al., 2011). Further studies indicate that a severe injury or repetitive mild-moderate injuries can promote the onset of neurodegenerative diseases such as Parkinson's (Crane et al., 2016; Gardner et al., 2015) and Alzheimer's disease (Edwards Iii et al., 2019) associated with the development of a chronic traumatic encephalopathy (CTE). It is difficult to diagnose CTE because pathological examinations of the brain tissue can only be done post-mortem and there are no available biomarkers. However, it seems that in sports with repetitive head trauma, athletes like boxers, football players, ice hockey, and rugby players are more susceptible to the development of CTE (Fesharaki-Zadeh, 2019; Risling et al., 2019; Sahler & Greenwald, 2012). Not only athletes are at risk, but the physiopathology of CTE can also be found in soldiers and veterans (Blennow et al., 2016; Goldstein et al., 2012). Multiple studies reveal that repetitive episodes of TBI followed by the presence of chronic inflammation, pathological *Tau*, axonal damage, neuronal loss, glutamate release and free radicals increase the accumulation of amyloid-β (Aβ) peptides (Gentleman et al., 2004; Kokiko-Cochran & Godbout, 2018; Smith et al., 1999; Wei et al., 2018). Other studies report that the age, sex and the inheritance of the

apolipoprotein E (*APOE)* allele ε4 increases the risk of developing Alzheimer's disease following TBI (Mayeux et al., 1995; O'Meara et al., 1997; Teasdale et al., 2005). However, at the moment, the relationship between contact sports and CTE is incompletely defined, and there are no markers that uniquely differentiate CTE from Alzheimer's disease.

1.1.1 Preclinical animal models of TBI

The incidence of TBI is increasing every year, and many of the patients present impaired cognitive behavior for a long time. Although there are no animal models that can accurately mimic the human injury, these are essential for dissecting the molecular and biochemical events that take place in the brain after TBI (Ma et al., 2019). Animal models have been important tools to replicate various aspects of TBI, understand the neuro-pathophysiology and investigate possible treatments. Brain damage varies as the result of different traumas, like a car accident, fall, sport impact, or explosions in war. In the same way, there are many TBI models that simulate different external mechanical forces to mimic as close as possible the reality of human TBI. Although larger animals such as pigs (Kinder et al., 2019) have brains that are more similar in size and structure to the human brain, rodents are still the animals most widely used in TBI research due to their smaller size, lower cost and standardized behavioral tests.

The most common experimental TBI models are the lateral fluid percussion (LFP), the controlled cortical impact (CCI), weight drop and blast injury.

LFP inflicts an insult by a pendulum that swings against a piston filled with liquid, generating a pressure pulse to the intact dura exposed after craniotomy (Alder et al., 2011). The resulting concussion causes brain tissue deformation and leads to

inflammation. This model mimics TBI without skull fraction, and replicates many acute and chronic features of human TBI like intracranial hemorrhage and brain swelling (Van Putten et al., 2005). LFP also produces a memory deficit that is commonly seen in TBI patients (Fedor et al., 2010).

CCI uses a pneumatic impact device that delivers the injury to the exposed intact dura (Romine et al., 2014; Schwulst & Islam, 2019). This model reproduces cortical tissue loss, acute subdural hematoma, axonal injury, and blood-brain barrier dysfunction seen in TBI patients (Osier & Dixon, 2016). The damage can be widespread and result in acute cortical inflammation, hippocampal and thalamic degeneration (Hall et al., 2005). The CCI model produces many neurobehavioral deficits common in human TBI patients, including long-term cognitive problems and poor scores in functional motor task (Adelson et al., 2013; Chen et al., 2014). It is possible to control the severity of the injury by regulating CCI parameters such as velocity, dwell time and the depth of the impact.

The weight drop model uses a free-falling weight that uses gravitational force to injure the brain, and can be done with or without craniotomy (Kalish & Whalen, 2016). There are several weight drop models of TBI. The Feeney's model generates a focal injury where the weight is dropped directly on the exposed dura (Feeney et al., 1981), whereas in the Shohami's model (closed-head) the weight impacts the intact skull (Shapira et al., 1988), resulting in cortical concussion, hemorrhage, blood-brain barrier damage and activation of immune cells. A diffuse injury is generated in the Marmarou's model (Marmarou et al., 1994), where the injury is delivered to the whole head which is allowed to move, producing brain cell loss, hemorrhage, and diffuse axonal injury. This model is used to mimic a single acceleration impact such as a car accident, or a repetitive

mild injury like that frequently occurring during high-impact sport activity.

The blast model of TBI mimics the diffuse, severe type of injury that can occur in a military environment or battlefield (Xiong et al., 2013). The design consists of a long metal shock tube that is closed on one end, and on the other contains the animal holder (Hue et al., 2016). Air-pressure wave or an explosion is released from the closed end and propagated through the tube. The position of the animal mimics the position of the soldier in the field, like for example supine or prone. The result is a diffuse, closed skull injury, and physically, it can produce a rotation of the head, with tissue distortion and brain swelling (Ma et al., 2019). At the neurological level the injury results in edema, contusion, diffuse axonal injury, hemorrhage, but since it is a whole-body injury it can also affect other organs such the eyes, heart and lungs (Jorolemon MR, 2019).

1.1.2 Pathophysiology and neurochemical changes associated with TBI

Subsequent to the initial mechanic injury, a molecular cascade of events induces an alteration of ions and neurotransmitters leading to further tissue damage (Cater et al., 2007). Insults after TBI can be classified as primary or secondary damage. The primary damage is the direct result of the mechanical insult immediately after the trauma such as skull fractures, hemorrhages, contusions, cerebral laceration. The secondary damage develops over an extended period of time, indirectly as a result of the trauma (Jassam et al., 2017). The first response to TBI is an inflammatory reaction mediated by microglia cells and astrocytes that regulate the recruitment of leukocytes and chemokines to the injured brain (Xiong et al., 2018). In response to tissue damage, the microglia cells change morphology from a “normal” ramified to an “active” ameboid shape, and recruit peripheral macrophages that can further transform into microglia in response to TBI

(Donat et al., 2017). During the secondary damage phase, astrocytes work side by side with microglia to shape the micro-environment of the brain after injury (Barrett et al., 2014). They migrate to the injury side, increase their activity and assume a hypertrophic state by enlarging the cell body and processes (astrogliosis) (Burda et al., 2016). Astrocytes have an important function in maintaining the homeostasis of the cell membranes and can regulate the excitotoxicity by controlling glutamate re-uptake (Karve et al., 2016). However, microglia and astrocytes play a dual role during inflammation. On one hand they promote recovery after TBI through these homeostatic mechanisms, on the other hand, they can cause an excessive inflammatory reaction, thereby increasing brain damage and delaying recovery. In fact, they release cytokines like interleukin (IL)-1β, IL-6, IL-17, tumor necrosis factor-α (TNF-α), interferon-γ (IFN-γ), the macrophage chemotactic protein-1 (MCP-1) (Xiong et al., 2018; Xu et al., 2017) and trigger a positive-feedback system that exacerbates the inflammatory response, causing more damage and cell death (Figure 1). In addition, astrocytes stimulate the TNF-α signaling that upregulates the aquaporin protein, AQPA, increasing the intake of water through the water channel and enhancing edema formation and cranial pressure (Dekmak et al., 2018). The injury and the external force can generate a gradient pressure that stretches and damages the axons. If the damage is extended, it is called diffuse axonal injury (DAI) (Johnson et al., 2013; Mouzon et al., 2012).

After the trauma, the emerging neuropathology includes inflammation, microglia activation, axonal damage, and hemorrhages (Wan et al., 2019). The cerebral damage is directly proportional to the mechanical force applied during the concussion (Blennow et al., 2016). This appears after the physical trauma, not as a secondary effect, and can be

detected immediately after the impact. The force of the impact stretches the axons and disrupts the microtubules, causing the formation of axonal varicosities, impaired axonal transport (Tang-Schomer et al., 2012), and impaired synaptic function. The axons present swelling regions (Johnson et al., 2013) in which axonal transport is discontinuous and there is an accumulation of amyloid precursor protein (APP). It has been suggested that accumulated APP can be used as a marker for axonal injury (Gentleman et al., 1993; Plummer et al., 2016).

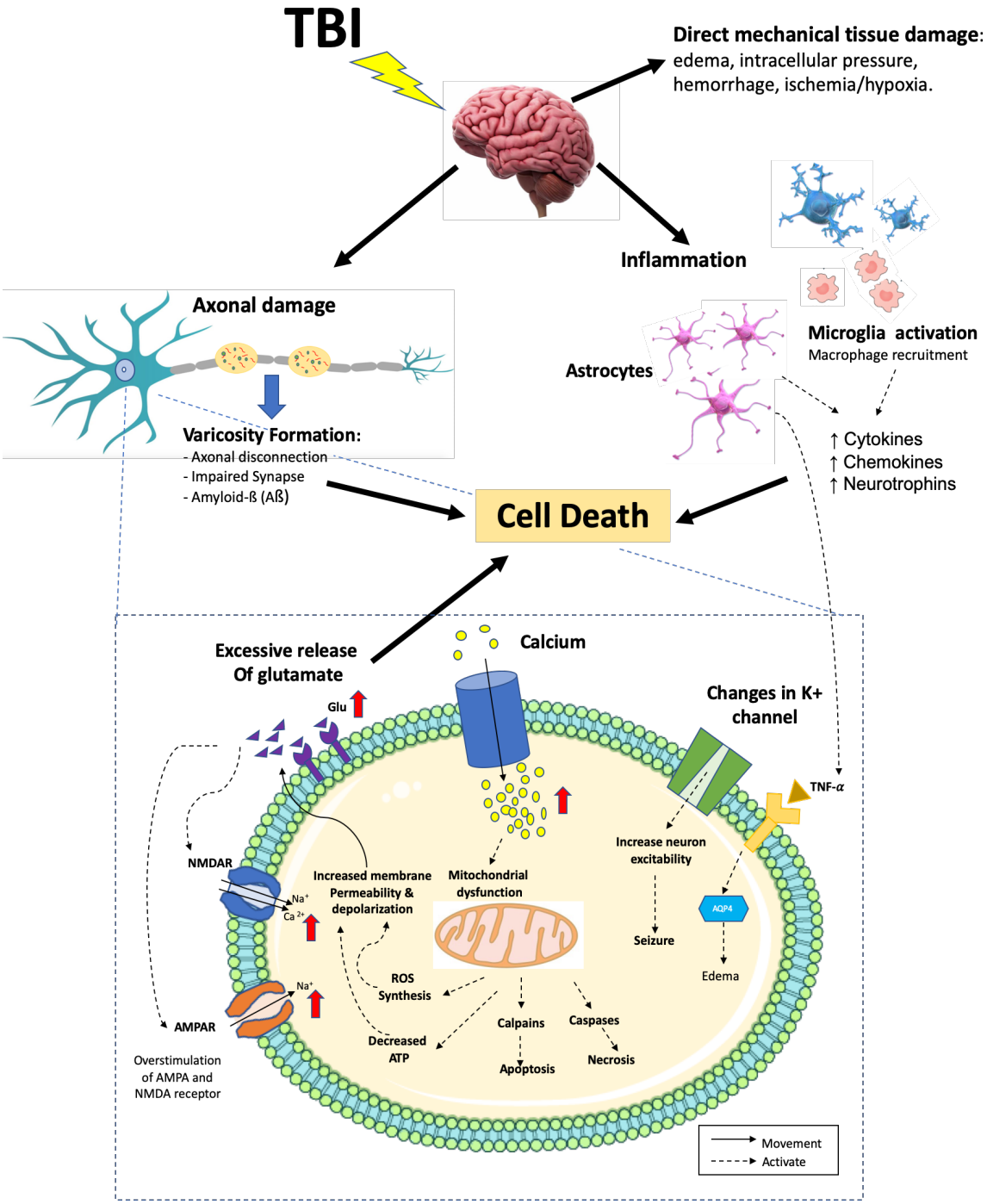

Figure 1. Pathophysiology of TBI.

Following the initial mechanical injury, there is a cascade of events that cause

inflammation (microglia and astrocytes), membrane disruption, axonal damage (varicosity, impaired synapses) and an increased membrane permeability due to the failure of the ATP- dependent ion pumps. This leads to excessive levels of the neurotransmitter glutamate that binds to the glutamate receptors, inducing a perturbation of the membrane homeostasis by altering the $NA^{+}/K^{+}/Ca^{2+}$ ion flux. Glutamate activates ion channels like NMDA and AMPA receptors that increase the depolarization of the cells and elevate the influx of Ca^{2+} and Na^{+}. The excessive level of Ca^{2+} into the mitochondria promotes the synthesis of reactive oxygen species (ROS) that cause oxidative stress in the cells and alter the selective permeability of the membrane. Ca^{2+} also activate the caspases and calpains pathway as a result of apoptotic and necrotic events, cell death and debris accumulation. The change in the K^{+} channel activity makes the neurons more excitable and so more susceptible to seizures. The inflammatory response seems to have a dual role in the brain: astrocytes and microglia mediate the rapid immune response and promote regeneration, but they also cause the activation of several pro-inflammatory factors such as cytokines and neurotrophins such as TNFα that upregulate the aquaporin protein, AQP4. This protein increases the water flux inside the cells and results in edema, intracranial pressure and neuronal degeneration.

Following TBI, there is an increase in membrane permeability that leads to membrane depolarization and excessive release of neurotransmitter like the excitatory neurotransmitter glutamate. This is due to the failure of the ATP-dependent ion pumps that maintain homeostasis, resulting in low levels of ATP, excessive production of lactic

acid and reduced levels of glucose (Dekmak et al., 2018; Werner & Engelhard, 2007). The increased efflux of K^+ renders the neurons more excitable and more susceptible to seizures (Wang et al., 2017). The increased release of glutamate also disrupts the $Na^+/K^+/Ca^{2+}$ flux (Barrett et al., 2014; Mazzeo et al., 2009) and leads to the overstimulation of N-methyl-D-aspartate (NMDA) receptors and α-amino-3-hydroxy-5-methyl-4 isoxazolepropionic acid (AMPA) receptors. This can lead to a neuronal dysfunction and cognitive abnormalities such as learning and memory loss. High levels of glutamate cause neuronal excitotoxicity even if cells are exposed to this neurotransmitter only for brief periods of time. Although the negative effects of the increased concentration of excitatory amino acids have been demonstrated in animal models of TBI (Cantu et al., 2015; Hinzman et al., 2010) the underlying mechanisms and the signaling pathways that are involved are not well understood. NMDA and AMPA receptors regulate Ca^{2+} influx in surrounding neurons and induce the polarization of mitochondrial membranes resulting in mitochondrial dysfunction and the production of reactive oxygen species (ROS) that produce additional damage (Hiebert et al., 2015). The elevated levels of Ca^{2+} activate proteases such as caspases and calpains to induce the apoptotic and necrotic pathways and cause cells death (Kim et al., 2002; Zhang et al., 2005), and this has the potential to further impair cognitive functions. Although glutamate seems to be the main trigger for the excitotoxicity events in traumatic brain injury, glutamate receptor antagonists tested in clinical trials so far have failed to prevent excitotoxicity (Ikonomidou & Turski, 2002). It is possible that other molecular mechanisms are involved in glutamate excitotoxicity, such as, for example, the increase in intracellular calcium mediated by L-type voltage-dependent calcium channels

(VDCCs) (Cater et al. 2007) or other molecular mechanisms that occur as a result of the secondary damage after the injury.

1.1.3 Treatments for TBI

In most TBI cases, current treatments are aimed at stabilizing the patients and improving their chances of survival. Beside initial therapies focused on maintaining an adequate oxygen flow to the brain to reduce death incidence, rehabilitative physical recovery and surgery, to date there is no effective treatment for the neurological defects caused by TBI. Given the complexity of the pathophysiological scenario in TBI, pharmacological treatments have been developed to target specific molecular mechanisms that are altered after TBI, and focus on different temporal stages (Dekmak et al., 2018). For instance, calcium blockers and NDMA receptors antagonists have been used in an attempt to prevent the emergence of neurological deficits in the early post-TBI stage. The calcium blocker *Nimodipine*, for example, has been shown to be effective in rodent models, but not in patients ("Clinical trial of nimodipine in acute ischemic stroke. The American Nimodipine Study Group," ; Vergouwen et al., 2006). NMDA antagonists appeared initially to be promising, but a study was discontinued in phase III of the clinical trial because of inconsistent results (Ikonomidou & Turski, 2002). Similarly, the use of *cyclosporine* to inhibit the entry of calcium in mitochondria, appeared to be promising in animal models (Karlsson et al., 2018), but was not effective in patients with TBI (Hatton et al., 2008). Another form of early stage treatment, namely *hypothermia intervention,* is aimed at reducing the temperature in the affected tissue. This showed promising results, however it must to be used within a specific time window from TBI, and it seems that is not sufficient to prevent damage due to severe injuries (Shaefi et al.,

2016). Another early stage intervention, the treatment with oxygen (*hyperbaric oxygen therapy*), which is focused on normalizing cerebral metabolism, showed some positive neuroprotective effects, but resulted in complications like lung damage and altered vision (Hu et al., 2016). Treatments that aim to combat the later stages of TBI included the use of *statins* as anti-inflammatory, anti-apoptotic and antioxidant agents. Although there were some positive effects in clinical trials, there are still concerns about efficacy (Wible & Laskowitz, 2010). Likewise, *progesterone* was used as a neuroprotective agent, appeared to be very promising in animal models, but failed in clinical trials (Espinoza & Wright, 2011; Stein et al., 2017). Pharmacological treatments such as antidepressants, anti-Parkinson's, anticonvulsants are aimed at reducing specific secondary effects of TBI (Gultekin et al., 2016). Antiepileptic drugs and vagal nerve stimulation were also used to reduce seizures associated with TBI. However, truly effective treatments are still lacking because the cellular and molecular mechanisms that underlie TBI are not completely understood. To date, there is no FDA-approved pharmacological treatment proved to prevent or ameliorate the effects of TBI (Dekmak et al., 2018).

Despite the high impact of TBI on society, very little is known about the molecular basis of cognitive loss and functional recovery. Recent studies support the idea that neuronal progenitor cells (NPCs) present in mammalian brain during the life span, can play an important role in repair and regeneration in response to brain injury (Liu et al., 2014). In the mature mammalian brain, neurogenesis occurs primarily in the subventricular zone (SVZ) and the dentate gyrus (DG) of the hippocampus (Gage et al., 1998; Li et al., 2013). Newborn cells in the adult granule layer of the DG, extend their axons to the CA3 hippocampal area where they establish new synapses onto the hilus and

pyramidal neurons of the CA3 area.

Many TBI patients with cognitive problems present serious damage of the hippocampus area. Recent studies, in rats and mice, showed that TBI increases cell proliferation in SVZ and DG in models of brain injury, including LFP and CCI (Rolfe & Sun, 2015; Sun, 2014). Other studies showed that post-injury neurogenesis is more pronounced in juvenile than adult mice (Sun et al., 2005), and could explain why better functional recovery is observed at younger ages. The adult newborn granule cells integration into the existing hippocampal circuit represents an endogenous innate recovery mechanism following brain injury and they can be used as therapeutic target to induce the endogenous repair in response to TBI (Zheng et al., 2013). Although NPCs have the potential to repair the injured brain, secondary damage effects, like oxidative stress and inflammation, could create a hostile environment for the new neurons. Recently, many studies have focused on the transplantation of embryonic stem cell (ESCs) (Weston & Sun, 2018) or induced pluripotent stem cells (iPSCs), which are advantageous because they avoid the controversial ethical issue related to the use of human embryos, and they can be generated directly from patients without the risk of an immunological rejection. A study showed that rats subjected to CCI and receiving iPSCs exhibited improved motor and cognitive performance (Dunkerson et al., 2014). However, there are also limitations to the use of iPSCs, such as the risk of tumor development. Further studies are necessary to understand the possible application of iPSC-based therapies to treat TBI patients (Gao et al., 2016). Recent data also show that Mesenchymal Stem Cells (MSCs) have potential application to the treatment of TBI. Due to their self-renewal, proliferative and differentiation characteristics, and the capacity to

reduce the inflammation and secrete growth factors that facilitate the regrowth of neurons in the brain, MSCs seem to be the most promising therapy for TBI so far (Hasan et al., 2017). In a recent study mice subjected to CCI and infusion of MSCs cells exhibited improvement in motor skill (Zanier et al., 2011). In a different study, MSCs reduced cell loss and apoptosis and increased levels of the vascular growth factor (VGF) (Chuang et al., 2012). Many research groups are currently searching for additional molecules, hormones, or growth factors that can improve innate recovery and thus can improve cognitive function after TBI. Besides neurogenesis, another focus of current TBI research is to investigate mechanisms that would help to repair the neuronal circuitry after brain damage and to re-establish synaptic connections and network functions. Proteins that are involved in restoring the integrity of cellular systems may play an important role in functional recovery.

1.2 Reelin

Reelin is one of the most important proteins in mammalian brain development, controlling the formation of laminated cortical structures and synaptic circuits (D'Arcangelo et al., 1995). This extracellular protein is essential for cortical and hippocampal layer formation at embryonic stages, and also promotes dendrite growth, synapse formation and synaptic plasticity in the postnatal brain (D'Arcangelo, 2014; Niu et al., 2004). The *Reelin* gene was discovered based on the genetic analysis of *reeler* mutant mice, which lack Reelin expression and are characterized by ataxia and disruption of cortical layers (Lambert de Rouvroit & Goffinet, 1998). The mouse *Reelin* gene is located on chromosome 5 and is composed of 65 exons spanning a region of

approximately 450Kb (Royaux et al., 1997). The first portion of the gene is characterized by large introns and small exons that encode the N terminus, whereas the remaining part presents exons that are close to each other and encode eight Reelin-specific repeats. One microexon close to the 3' coding region is subject to alternative splicing, but the significance of this event is still unknown. *Reelin* mRNA first becomes detectable at embryonic stages, with higher levels present between 1 and 2 postnatal weeks, and then decreases at adult stages (D'Arcangelo et al., 1995). The Reelin protein consists of an N-terminal region that contains a signal peptide, a F-spondin-like domain necessary for the oligomerization (Utsunomiya-Tate et al., 2000), followed by eight unique repeat regions. Each repeat consists of 350-390 amino acids, and contains two sub-repeats A and B, separated by an epidermal growth factor (EGF)-like motif. The C-terminal region has a positively charged sequence of amino acids that is needed for proper protein conformation and secretion (Kohno et al., 2015; Nakano et al., 2007). The full-length mouse protein is a large secreted protein of approximately 450 kDa. The protein is cleaved by proteases mainly at two different sites: the N-terminal cleavage occurs between repeats 2 and 3, whereas the C-terminal cleavage occurs between repeats 6 and 7 (Figure 2). This cleavage results in three main fragments: the N-terminal (N-terminus to repeat 2, ~180 kDa); the central fragment (repeats 3 to 6, ~190 kDa); and the C-terminal (repeats 7 to C terminus, ~80 kDa) (Lambert de Rouvroit et al., 1999). In cultured cell medium containing Reelin and in brain tissue lysates these fragments are readily detectable in addition to intermediate fragments generated by only 1 proteolytic event: N-terminus to repeat 6 (~370 kDa) and repeats 3 to C terminus (~270 kDa) (Jossin et al., 2007). A study showed that the central fragment is sufficient to induce layer formation in

organotypic cortical slice cultures and signal transduction (Jossin et al., 2004). The N-terminal fragment contains a signal peptide region required for secretion, and binds the monoclonal antibody CR50, the first Reelin antibody developed based on the presence of an antigen in wild type, but not *reeler*, Cajal-Retzius cells (D'Arcangelo et al., 1997). The C-terminal fragment is a conserved region (C terminal region = CTR) that is required for the optimal activation of downstream signaling (Nakano et al., 2007).

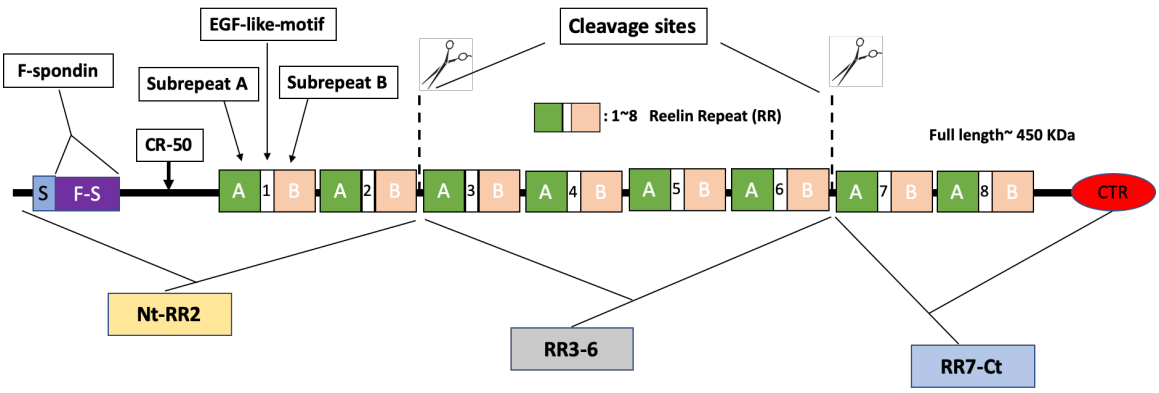

Figure 2. Schematic representation of the Reelin protein.

Reelin is an extracellular matrix protein composed by 3,461 amino acids, with a molecular mass of ~ 450 KDa. The full-length Reelin consists of: a N-terminus (Nt) that contains a signal peptide (S), a F-spondin domain and the antigen recognized region by the CR-50 antibody; eight Reelin Repeat (RR) domains, each consisting of two sub-repeats, A and B, separated by a EGF-like-motif; and a C terminus (Ct) with a C Terminal Region (CTR) containing a positively charged stretch of amino acids. Reelin has two main proteolytic cleavage sites located between repeats RR2-RR3 and RR6-RR7 (scissors). Cleavage at these sites produces three major fragments: N-terminal fragment (Nt-RR2, ~ 180 KDa), a central fragment (CF= RR3-6, ~ 190 KDa), and a C-terminal fragment (RR7-Ct, ~ 80 KDa).

During forebrain development, Reelin is secreted by Cajal-Retzius cells in superficial cortical and hippocampal layers, where it controls radial neuronal migration (D'Arcangelo et al., 1995). Reelin-expressing Cajal-Retzius cells are located in the marginal zone of the neocortex, as well as in the stratum lacunosum moleculare (SLM) of the hippocampus proper, and in the outer molecular layer (OML) of the dentate gyrus (DG) (Alcantara et al., 1998). At postnatal stages, the levels of Reelin decrease drastically in marginal layers as Cajal-Retzius cells die out, but the residual protein still promotes axonal and dendritic outgrowth in these regions. In the postnatal and adult stages, Reelin is mainly secreted by a different cell population, consisting of a subset of inhibitory neurons that are located in all cellular layers throughout the forebrain. In the adult hippocampus, Reelin has been shown to modulate synaptic activity as well as plasticity (Rogers & Weeber, 2008;Trotter et al., 2013). In addition to the forebrain, Reelin is also highly expressed in the cerebellum. In the embryonic cerebellum, Reelin is expressed by granule precursor cells in the external granular layer, where it directs the radial migration of Purkinje cells and the formation of these cells' monolayer. At postnatal stages, as granule precursor cells migrate inward to form the internal granular layer, Reelin expression becomes mainly localized to this region (Hevner, 2008).

Although the function of Reelin in directing radial migration during the development is well established, the role of this protein in the adult brain is not completely understood.

1.2.1 The Reelin signaling pathway

The Reelin signaling activity has been investigated using multidisciplinary approaches, and it was initially elucidated through the analysis of mutant mice. Double

knock-out mice lacking apolipoprotein E receptor-2 (ApoER2) and the very low-density lipoprotein receptor (VLDLR) exhibited a phenotype very similar to *reeler* mice, leading to the suggestion that these proteins may be Reelin receptors (Trommsdorff et al., 1999). Indeed, biochemical assays have demonstrated that full-length Reelin, or its central fragment, has a high binding affinity for ApoER2 and VLDLR on the cell surface or *in vitro* (D'Arcangelo et al., 1999; Hiesberger et al., 1999; Yasui et al., 2007). The receptor binding results in Reelin internalization and activation of Src-family kinases (SFKs). These tyrosine kinases (mostly Fyn and Src) phosphorylate the intracellular adapter protein Dab1 bound to the intracellular domains of the receptors, and this event leads to the activation of other signaling kinases, such as PI3K. The Dab1-dependent activation of PI3K by Reelin causes the downstream activation of Akt, which inhibits Gsk3β and this results in decreased Tau phosphorylation. Accumulation of phospho-Tau is found in *reeler* mice, and this observation could be relevant for the study of neurodegenerative diseases, like Alzheimer's disease, that are associated with high levels of Tau phosphorylation (Wasser & Herz, 2017). The finding that activation of the Reelin pathway decreases the levels of Tau phosphorylation is also relevant to TBI because hyperphosphorylated Tau is a biomarker for brain injury (Ramos-Cejudo et al., 2018; Rubenstein et al., 2017). PI3K and Akt activation by Reelin and Dab1 are also likely to result in neuroprotection, as these kinases are well-known to promote survival in many cellular systems (Bao et al., 2004; Datta et al., 1997; Hossini et al., 2016). Finally, Akt activation results in the phosphorylation and activation of downstream mTORC1, a kinase complex that is very important for neuronal growth and has been previously implicated in axonal regeneration and TBI (Nikolaeva et al., 2016).

In addition to PI3K, Dab1 interacts with actin-binding proteins such as N-WASP and Nckβ, as well as the adapter protein CrkII and the microtubule-interacting protein Lis1. Together these proteins contribute the regulation of neuronal migration by affecting the dynamics of the cytoskeleton during brain development. At the synapse additional signaling mechanisms may be recruited. For example, Reelin-bound ApoER2 forms a complex with the NMDA receptor and the postsynaptic scaffold protein PSD95, leading to increased Ca^{2} influx, neurotransmission and plasticity (Wasser & Herz, 2017). The NMDA receptor increases Ca^{2+} influx and long-term potentiation (LTP), and also promotes the maturation and the insertion of AMPA receptors in the plasma membrane. These mechanisms may be highly relevant to cognitive dysfunction resulting from neurodegenerative diseases and TBI.

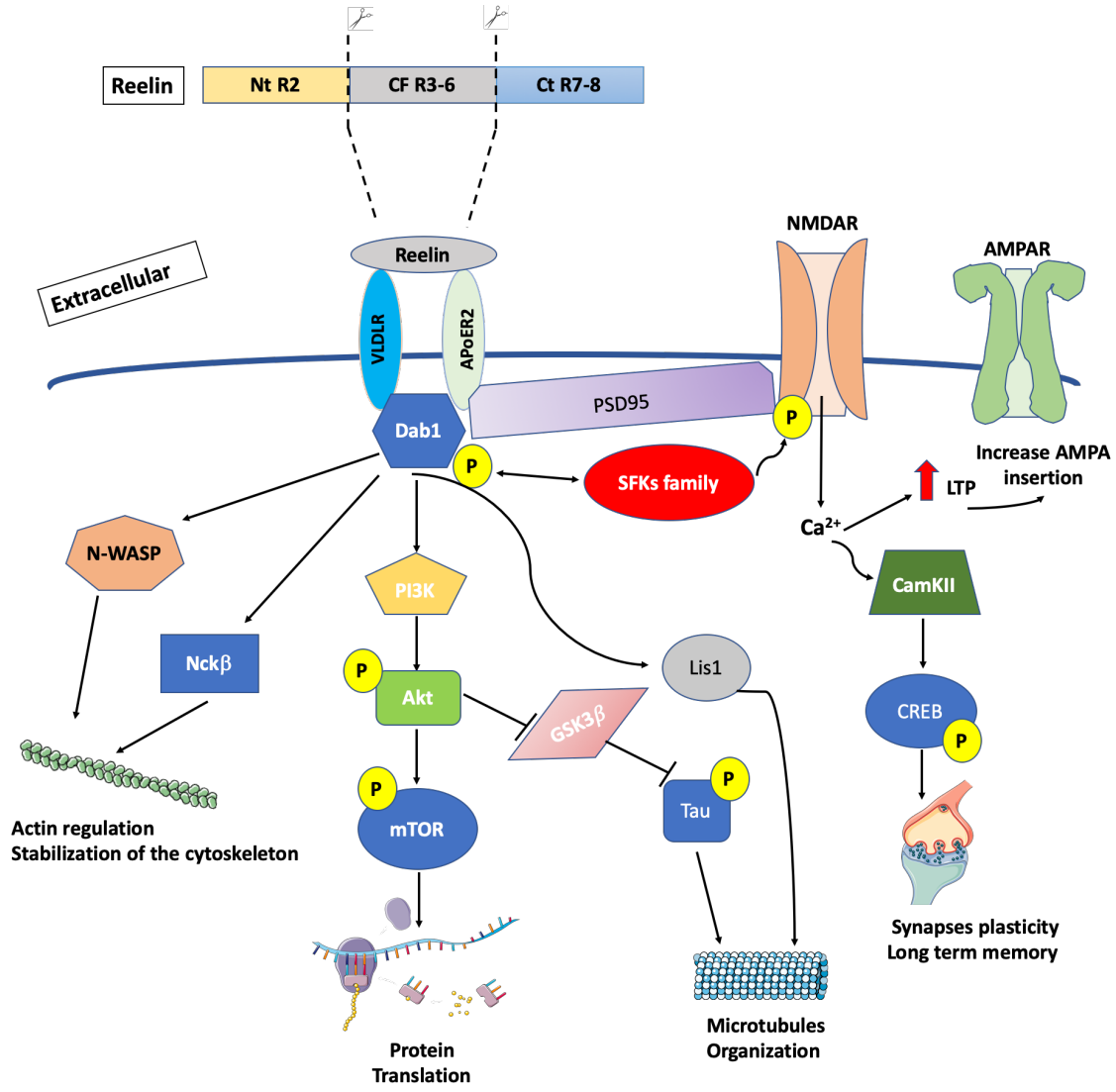

Figure 3. Reelin signaling pathways.

Reelin binds to the VLDLR and ApoER2 receptors and triggers the canonical pathway through the phosphorylation and activation of the adaptor protein Disabled-1 (Dab1) that is mediated by the src-family kinases (SFKs) like Fyn and Src. Phosphorylated Dab1 induces the activation of PI3K that in turn activates Akt. This latter phosphorylates and inhibits Gsk3β, resulting in suppressed levels of Tau

phosphorylation. Akt also upregulates the mTOR pathway and thus increases protein translation. Dab1 also interacts with Lis1 resulting in microtubule stabilization, and with actin-binding proteins such as N-WASP and NcKβ. Finally, Reelin induces synapses plasticity by inducing the formation of a complex between ApoER2 and the scaffold protein PSD95, NMDAR phosphorylation by SFK, Ca^{2+} influx and activation of CaMKII and CREB. The increase of Ca^{2+} influx also enhances LTP and the insertion of AMPAR in the membrane.

1.2.2 Reelin: animal models

The phenotypical analysis of spontaneous or engineered mutant mice has helped tremendously to identify Reelin or components of the Reelin signal pathway and to clarify their biological function (Table 2).

Spontaneous mutant mice completely lacking Reelin expression due to *Reelin* gene deletions (homozygous *reeler*) are characterized by tremor, ataxia, cerebellar hypoplasia and overall disruption of cortical and hippocampal layers (D'Arcangelo et al., 1995), whereas heterozygous *reeler* mice exhibit only reduced synapse formation and alterations in synaptic composition (Niu et al., 2004; Ventruti et al., 2011). In homozygous *reeler* mice, radially-migrating principal neurons fail to reach their laminar destination during the formation of cortical cellular layers in the forebrain and in the cerebellum (Lambert de Rouvroit & Goffinet, 1998). This observation suggested that Reelin affects primarily neuronal migration, and not neurogenesis, during embryonic forebrain or cerebellum development. Double ApoER2 and VLDLR knock-out mice exhibit neuroanatomical characteristics similar to *reeler* mice (Trommsdorff et al., 1999).

Dab1 knock out mice and spontaneous Dab1 mutants *yotari* and *scrambler* (Sheldon et al., 1997) are also indistinguishable from *reeler*. These findings demonstrate that these molecules are essential for Reelin signaling and for its developmental function during layer formation and neuronal migration. Further studies (Teixeira et al., 2012) later demonstrated that Reelin signaling through Dab1 also controls neurogenesis in adult niches such as the subventricular zone of the cerebral cortex and the dentate gyrus.

Mouse	**Gene**	**Characteristics**	**Reference**
reeler-Edinburgh (maintained at The Jackson Labs)	*Reln*	Original spontaneous mutation named *reeler* (large *Reln* gene deletion); displays phenotype consisting of ataxia, dystonic posture and failure of layer formation in cortical structures	(Falconer, 1951)
reeler-Orleans	*Reln*	Spontaneous mutation (small 3' deletion); displays *reeler*-like phenotype	(de Bergeyck et al., 1997)
reeler-transgene	*Reln*	Fortuitous insertion of a *fos* transgene causing *Reln* gene deletion; displays *reeler*-like phenotype	(D'Arcangelo et al., 1995; Miao et al., 1994)
Reln cKO	*Reln*	Engineered gene deletion by CreERT2 (tamoxifen-inducible Reln knockout). Adult-specific mutants appear normal and have normal cortical lamination, but synapses are sensitive to amyloid proteins.	(Lane-Donovan et al., 2015)
yotari and *scrambler*	*Dab1*	Spontaneous mutations (gene deletions causing loss of Dab1); display *reeler*-like phenotype	(Sheldon et al., 1997)
Dab1 KO	*Dab1*	Engineered gene deletion (constitutive *Dab1* knockout). displays *reeler*-like phenotype	(Howell et al., 1997)
Dab1 cKO	*Dab1*	Engineered gene deletion by Cre (promoter-inducible Dab1 knockout). Postnatal-specific mutants appear normal and have normal cortical lamination but show reduction of dendritic spine size, loss of hippocampal LTP and deficit in learning and memory.	(Justin Trotter et al., 2013)
VLDLR and *ApoER2* double	*VLDLR; ApoER2*	Engineered gene deletions (constitutive *VLDLR* and *ApoER2* double knockout);	(Trommsdorff et al., 1999)

KO		display *reeler* like phenotype	
Src and *Fyn* double KO	*Src; Fyn*	Engineered gene deletions (constitutive *Src* and *Fyn* double knockout); display reeler-like phenotype	(Kuo et al., 2005)

Table 2. Mouse mutants for Reelin or other genes involved in the Reelin signaling pathway.

To study the function of Reelin and Dab1, specifically in the postnatal brain, conditional knock out mice (cKO) were generated using the LoxP-Cre recombinase approach. Postnatal forebrain-specific Dab1 cKO mice presented with normal neuronal positioning, dendrite morphology and spine density, but exhibited synaptic plasticity defects as well as cognitive abnormalities (Trotter et al., 2013). Recently, adult-specific inducible Reelin cKO mice were generated that did not exhibit ataxia and performed normally in cognitive tasks (Lane-Donovan et al., 2015). These mice, however, showed increased susceptibility to amyloid-induced synaptic suppression, suggesting that Reelin may not be essential for synaptic function, but it may protect the adult brain from degeneration. The recent availability of inducible Reelin cKO mice now allows investigators to study the consequences of Reelin deficiency specifically in the adult brain, which has not been possible before with traditional animal models that have a defective brain architecture, reduced dendrite growth and abnormal synapses.

1.2.3 Reelin: embryonic, postnatal, adult stage

Reelin is essential for normal neuronal lamination in the neocortex, hippocampus and cerebellum. In the embryonic neocortex and hippocampus, Reelin is secreted by Cajal-Retzius cells and determines the correct locations of newborn principal (excitatory) neurons, which migrate radially from the ventricular zone to occupy specific layers

according to their birthdate (Frotscher, 2010). Similarly, in the developing cerebellum, Reelin is secreted by superficial granule progenitor cells and directs the radial migration of Purkinje cells from the cerebellar ventricular zone into the future Purkinje cell layer. Reelin regulates the formation of forebrain or cerebellar cellular layers by binding the receptors ApoER2 and VLDLR and activating SFKs and several Dab1-dependent signaling pathways, including CrkII and its downstream effectors such as the Rap1 GTPase and N-Cadherin. Through these signaling molecules Reelin controls multiple steps of radial neuronal migration, including the transition to multipolar to bipolar neurons in the intermediate zone, and the somal or terminal translocation of neurons into the upper layers of the developing cortex that is essential for the 'inside-out' pattern of corticogenesis (Chai & Frotscher, 2016).

At early postnatal stages, Reelin is still mainly secreted by the Cajal-Retzius in the forebrain, and promotes the initial growth of axons and dendrites in the marginal layers through the ApoER2/VLDLR/Dab1-dependent activation of the PI3K, which in turn activates Akt and Cdc42 pathways to regulate cytoskeletal dynamics and the stability of the microtubule and actin scaffold to further stimulate the extension of the growth cone (Wasser & Herz, 2017). This function is independent from neuronal migration. For instance, not only homozygous *reeler* mice exhibit reduced dendritic branches and a lower number of spines, but also heterozygous *reeler* mice exhibit this phenotype even though they do not have defects in neuronal positioning (Niu et al., 2004). Furthermore, the function of Reelin in promoting dendrite outgrowth can be observed in neuronal cultures, is impaired in *reeler* or Dab1 mutant neurons, and it is blocked by ApoER2/VLDLR or SFK inhibitors (Niu et al., 2004). The induction of the neurite

outgrowth is believed to be regulated by the activation of the mTOR pathway downstream of PI3K and AKT.

At postnatal ages, Reelin is initially expressed by Cajal-Retzius cells but becomes increasingly expressed by a subpopulation of GABAergic (inhibitory) interneurons as the forebrain matures and Cajal-Retzius cells disappear in the adult stage. In the early postnatal hippocampus, Reelin has been demonstrated to promote targeting and synaptogenesis of entorhinal afferents to form the entorhinal-hippocampal projection (the perforant pathway) that innervates the superficial layers of the hippocampus (where Cajal-Retzius cells are located) (Borrell et al., 1999). This function is completely dependent on Dab1 as hippocampal projections are similarly disrupted in *reeler* and Dab1 KO mutants (Borrell et al., 1999). In heterozygous *reeler* mice, further studies showed that Reelin controls synaptogenesis and the formation of excitatory postsynaptic structures (Ventruti et al., 2011). These mice also present delays in dendritic process formation and spine density (D'Arcangelo, 2014; Liu et al., 2001). These observations are consistent with previous reports that heterozygous *reeler* mice exhibit cognitive and behavioral defects, although they present normal layer formation and no ataxia (D'Arcangelo et al., 1995). Defects on spines were also found in the hippocampus and Dab1 KO mice, demonstrating that this function of Reelin is Dab1-dependent (Niu et al., 2004). Transgenic mice that overexpressed Reelin under the control of CamKII promoter (active in the adult forebrain) also showed increased spine size (Pujadas et al., 2010). Long-term injection of Reelin (5 days) *in vivo* increased spines density, promoting long term potentiation (LTP) and improving performance associated with spatial and learning memory (Rogers et al., 2011). Thus, in the adult hippocampus, Reelin has been

demonstrated to play an important role in modulating synaptic activity as well as plasticity, and it can affect cognitive function. This is relevant to TBI research, since injuries can disrupt hippocampal-dependent functions, and the Reelin pathway could conceivably represent an excellent target for intervention.

1.2.4 Reelin in brain development disorders

The importance of Reelin signaling in brain development and cognitive function is underscored by the findings that reduced Reelin levels have been reported in several developmental brain disorders including epilepsy, schizophrenia, bipolar disorder, and autism. Bosch at al. showed that Reelin overexpression affects the trafficking of NMDA receptors and modulates glutamatergic neurotransmission (Bosch et al., 2016). Another study showed that the loss of Reelin correlated with dentate gyrus granule cells dispersion in epilepsy (Orcinha et al., 2016). These authors showed that the central fragment of Reelin rescues the abnormal migration of dentate gyrus cells, and so established a correlation between Reelin loss and granular cells dispersion in epilepsy. In a different study on temporal lobe epilepsy, the Gong group showed that Reelin supports the integration of the newborn neurons in the neonatal and mature hippocampal formation, and that the lack of Reelin contributes to aberrant plasticity (Gong et al., 2007). Reduced levels of Reelin in GABAergic corticolimbic neurons were also found in post-mortem human tissue from schizophrenia patients. By comparing human post-mortem tissue and animal models, it appears that the Reelin deficit disrupts synaptic connectivity not only in subjects with schizophrenia, but also those with bipolar disorder (Guidotti et al., 2016).

In a different post-mortem human study, it was demonstrated that the

dysregulation of Reelin and Bcl-2 might be responsible for the brain structural and behavioral abnormalities seen in autism (Fatemi et al., 2001). The reduction of Reelin protein and mRNA, and the increase in VLDLR expression, seen in post-mortem studies highlighted the correlation between impairment of Reelin signaling and autism (Fatemi et al., 2005). Finally, the *reeler* phenotype, consisting of cerebellar hypoplasia and perturbed cortical and hippocampal layers, are also seen in humans carrying homozygous mutations in the *REELIN* gene. These patients are afflicted by the developmental disease lissencephaly with cerebellar hypoplasia (Hong et al., 2000).

1.2.5 Reelin in neurogenerative disorders

So far it appears that most, if not all functions of Reelin in the brain are mediated through binding of its 2 receptors, ApoER2 and VLDLR. The downstream pathway promotes synaptic plasticity and the ultimate consequence of this activity in the adult brain has been hypothesized to be the protection of synapses from the deleterious effects of Amyloid-β (Aβ). A recent study using adult-specific, inducible conditional Reelin mutant mice, showed that the absence of Reelin did not disrupt synaptic plasticity or behavior under normal conditions, but exacerbated defects due to Aβ neurotoxicity (Lane-Donovan et al., 2015). The accumulation of this latter protein contributes to loss of cognitive function and memory in Alzheimer's Disease (AD). In AD pathogenesis, tau is hyperphosphorylated, inhibits microtubule stability and the maintenance of the dendritic spines (Sabbagh & Dickey, 2016). Reelin signaling pathway through ApoER2/VLDLR and Dab1/PI3K/Akt inhibits the glycogen synthase kinase-3β (GSK-3β), and this results in the reduction of tau phosphorylation, stabilization of the microtubules, and synaptic plasticity (Wasser & Herz, 2017). These studies are in line with previous findings that

Reelin overexpression ameliorates neuropathology in animal models of AD (Pujadas et al., 2010). Not only did dysregulation of the Reelin/Dab1 pathway leads to a change in the type and morphology of spines (Bosch et al., 2016), but Reelin supplementation by stereotactic injection into the mouse brain was found to increase spine density and ameliorated learning and memory in several animal models (Hethorn et al., 2015; Rogers et al., 2011).

1.2.6 Reelin in neurogenesis: injury and repair

In the adult hippocampus, Reelin has been demonstrated to play an important role in modulating synaptic activity as well as plasticity. Reelin signaling also affects neurogenesis in adult niches such as the subventricular zone of the cerebral cortex and the dentate gyrus of the hippocampal formation (Teixeira et al., 2012). Furthermore, Reelin regulates neurogenesis in the dentate gyrus after epileptogenic insults and maintains the integrity in the newborn neurons (Gong et al., 2007). Although the role of Reelin in migration during the development is well known, the mechanism by which Reelin regulates the migration of neuronal progenitor cells in adult niches needs to be further explored. For instance, Reelin enhances neuronal progenitor cells migration after cortical ischemia (Courtès et al., 2011). It appears that Reelin leads progenitor cells in the subventricular-zone to migrate into the olfactory bulb using a mode of migration distinct from radial migration. In a different study, the level of Reelin was found to increase after injury in the ocular lesion (Pulido et al., 2007). This finding suggests that Reelin could play an active role after injury and may be involved in tissue repair. On the other hand, injuries could potentially disrupt Reelin production potentially leading to abnormal neurogenesis and impaired recovery. The interplay between brain injury, neurogenesis

and Reelin expression is presently unclear.

Project rationale

The Reelin signaling pathway is essential for neural migration and also plays an important role in dendrite branching and the development and maturation of synaptic connections. In the adult brain Reelin also protects synapses from Aβ neurotoxicity, and promotes neurogenesis and integration of newborn neurons in the hippocampus (Teixeira et at., 2012); these findings could have significant implications for the treatment of neurological disorders and brain trauma. The role of Reelin in TBI has not been previously investigated. However, it is conceivable that Reelin may play a role in recovery after brain injury by affecting a number of mechanisms including stimulating adult neurogenesis, protecting neural cells from death, and promoting tissue repair by restoring synaptic connectivity and activity.

My mentor, Dr. D'Arcangelo, discovered Reelin several years ago (D'Arcangelo, 1995) and her lab elucidated many molecular and cellular aspects of its biological activity in the brain (reviewed by D'Arcangelo, 2014). In particular, Dr. D'Arcangelo's lab previously demonstrated that Reelin is important not only during brain development, but also in the postnatal and adult brain where Reelin promotes neuronal maturation, spine formation and modulates synaptic activity. This project focused on TBI and aimed to understand whether Reelin may be involved in the post-injury recovery, a novel area of investigation.

I first explored the potential link between Reelin expression and TBI using a mouse model *in vivo*. The objective of this study is to determinate whether Reelin is

induced after the trauma, and if it is beneficial for the recovery. We analyzed the expression of Reelin in the brain of adult mice that were subjected to lateral fluid percussion (LFP) or controlled cortical impact (CCI), two different TBI paradigms. My *in vivo* data show that Reelin expression in the brain is altered after TBI, especially in the hippocampus area. My *in vitro* data further show that Reelin reduces glutamate-induced excitotoxicity in hippocampal neurons. We reason that Reelin may play an important role in re-establishing neuronal network after TBI. Future goals will be to identify the molecular mechanisms that mediate Reelin-induced neuroprotection after TBI in order to reduced brain damage and improve the cognitive performance of TBI patients.

Chapter II: Material and Methods

Animal Handling

Animals used in this study were handled in accordance with a protocol approved by the Association for Assessment and Accreditation of Laboratory Animal Care (AAALAC) committee at Rutgers, the State University of New Jersey. For the LFP injury, Nestin-GFP transgenic mice on the C57BL/6 background were provided by Dr. Janet Alder at Rutgers University- Robert Wood Johnson Medical School. For the CCI injury and other experiments we purchased mice of the CD-1 strain from Charles River Laboratory.

Lateral Fluid Percussion (LFP) injury model

Adult mice (3-5 month-old) were anesthetized with 4-5% of isoflurane in 100% O_2 and received buprenorphine (0.1 mg/kg) intraperitoneally for preemptive analgesia. The mice were then placed in a stereotaxis frame, the isoflurane flow was maintained at 2%, and the animals were monitored during the entire procedure. An incision was made in the middle from the eyes to the neck and a topical anesthetic was applied on the skull (bupivacaine, 0.025% in saline). A craniectomy was made above the right hemisphere, halfway between bregma and lambda, with a 3 mm diameter trephine. The dura was kept intact and animals which showed herniation or dura damage were discarded. A rigid Luer-lock needle hub (Becton Dickinson) was placed in the skull over the opening and fixed with dental acrylic (Butler Schein). The operated mice received an intraperitoneal saline injection and were placed in a cage for recovery. After 1 hour, some mice were re-anesthetized and connected to the LFP device (Custom Design and Fabrication, Virginia Commonwealth University). When the mice resumed a normal breathing, but were not

completely conscious, they received a pulse generated through the Luer-lock hub with a pressure of 0.9-2.1 atmospheres and the pendulum set to 11.5°. After the impact, the righting reflex time was measured to define the severity of the injury. The injury was considered mild if the righting reflex time was 2-4 minutes, or it was considered moderate if the reflex time was 5-10 minutes. The scalp incision was sealed with Vetbond tissue adhesive (3M) and the animals were placed in the regular housing cage. Animals subjected to craniectomy but not LFP injury were used as shams. Both male and female mice were randomly selected to be included in the sham or LFP injury group. For more details about the LFP procedure see (Alder et al., 2011).

Controlled Cortical Impact (CCI)injury model

To prepare the mice for CCI injury a craniectomy was performed as described in the section above for LFP except that a 2.7 mm diameter trephine was used to remove a piece of the skull just above the parietal cerebral cortex using a stereotaxis apparatus equipped with a micromanipulator (Stoelting). Following craniectomy, the isoflurane anesthesia flow was stopped and the mice were prepared to receive a brain injury by CCI. Under microscopic control, the impactor of a Hatteras Instruments PinPoint Precision Cortical Impactor (Model PCI3000) was positioned over the exposed dura, tilted at a 4-10^0 angle to ensure that the entire surface of the probe was in contact with the dura mater. As soon as the mice regained sternal recumbence the injury was delivered with the following parameters: 1.5 mm depth, 3 m/sec velocity and 500 msec contusion time. This results in a penetrating injury that directly affects the cerebral cortex, but not the underlying hippocampal formation. After delivering the brain injury the skin was closed with Vetbond tissue adhesive (3M) and the mice received an intraperitoneal saline

injection before being allowed to recover in their home cage. Control mice (shams) received the craniectomy, but not the CCI.

Brain tissue section preparation

Mice were sacrificed at different time points after injury. For immunofluorescence experiments they were anesthetized with Avertin (Sigma-Aldrich) and perfused transcardially with saline solution followed by 4% paraformaldehyde (PFA) in phosphate buffered saline (PBS). The brains were dissected, post-fixed in 4% PFA for 4 hours at 4°C and cryoprotected by incubation at 4°C in a 30% sucrose solution in PBS. Brains were mounted onto a sliding microtome using OCT (Tissue-Tek) and sectioned for histology on glass slides.

Immunofluorescence assays

To detect Reelin or cellular markers in the brain, sections were washed in PBS for 5 minutes 2 times to remove the OCT from the slides. Then the slides were permeabilized with 0.1% Triton X-100 in PBS for 20 minutes and incubated with blocking buffer (5% normal goat serum in 0.1 % Triton-X-100 in PBS) for 1 hour. The sections were incubated overnight at 4°C with a primary mouse monoclonal anti- Reelin (clone G10) antibody or another primary cell marker antibodies (see Table 3) diluted in blocking buffer, and then washed with PBS (3 x 5 min).

Antigen	Antibody Isotype	Manufacturer	Catalog#	Application	Working Solution
Calbindin	Rabbit IgG	Cell Signaling	2136	IF	1:250
Calretinin	Rabbit IgG	Abcam	Ab92341	IF	1:250
Doublecortin	Rabbit IgG	Abcam	Ab18723	IF	1:250
GAD67	Mouse IgG2a	Millipore	MAB5406	IF	1:250
Parvalbumin	Rabbit IgG	Abcam	Ab11427	IF	1:250
Reelin	Mouse IgG1 (G10 clone)	Hybridoma cells	D'Arcangelo lab	IF	1:50
Reelin	Mouse IgG1 G10 clone conjugated to Alexa Fluor 488)	Millipore	MAB5364A4	IF	1:500

Table 3. List of primary antibodies.

IF= Immunofluorescence. G10, a mouse monoclonal antibody against Reelin, was

For indirect immunofluorescence assays, sections were incubated with Alexa-Fluor 488- or 647-conjugated secondary antibodies (Invitrogen) for 1 hour at room temperature (Table 4). The sections were then washed again with PBS (3 x 5 min), and coverslips were mounted with Vectashield Mounting Medium containing DAPI (Vector Laboratories). For direct immunofluorescence detection with the Alexa Fluor 488-conjugated Reelin antibodies, coverslips were mounted immediately after washing with PBS (3 x 5 min).

Fluorophore	Antibody type	Manufacturer	Catalog#	Dilution
Alexa Fluor ® 488	Goat anti-mouse IgG	Invitrogen	A11001	1:1000
Alexa Fluor ™ 488	Goat anti-mouse IgG F(ab')2	Invitrogen	A11017	1:1000
Alexa Fluor ™ 488	Goat anti-rabbit IgG	Invitrogen	A11008	1:1000
Cy5 ™	Goat anti-mouse IgG	Invitrogen	A10524	1:1000
Alexa Fluor ™ 647	Goat anti-rabbit IgG	Invitrogen	A21245	1:1000
Alexa Fluor ™ 488	Goat anti-mouse IgG2a	Invitrogen	A21131	1:500
Alexa Fluor ™ 647	Goat anti-mouse IgG1	Invitrogen	A21240	1:500

Table 4. List of secondary antibodies

Multiple sections per brain sample were imaged using a Yokogawa CSU-10 spinning disk confocal head attached to an inverted fluorescence microscope (Olympus IX50) for indirect immunofluorescence, or a Zeiss LSM800 confocal microscope for the direct immunofluorescence detection.

mRNA Isolation and Quantitative Reverse Transcription PCR (*RT-qPCR) Analysis*

Fresh cortical tissue close to the injury area, and hippocampal tissue were collected in the ipsilateral and contralateral side of the brain at different time points after TBI (24h and 72h). The total RNA was purified using the Qiagen RNeasy Kit and transcribed into cDNA using a High-Capacity cDNA Reverse Transcription kit (Applied Biosystems). The resulting cDNA was analyzed by RT-qPCR using primers specific for the genes of interest (Table 5). Some of the primers were designed with the Primer-Blast software, others were reported in the literature. RT-qPCR was performed using the Power

SYBR Green master mix (Applied Biosystems). The expression level of specific genes was normalized to the level of the standard housekeeping gene encoding the ribosomal protein S12 using two Applied Biosystems Real-Time PCR machines. *Reelin, CXCL10 and GFAP* expression was analyzed using the StepOne System and the StepOne Software v2.3, whereas *Gad1, Parvalbumin, Somatostatin and Map2* expression was analyzed using the QuantStudio 3 and the QuantStudio Design&Analysis V1.4.3 software.

Gene	**Sequence**	**Reference**
CXCL10	F 5-ACCCAAGTGCTGCCGTCATT-3' R 5-ATTCTCACTGGCCCGTCATC-3'	(Israelsson et al., 2009)
Gad1	F 5'-CGCTTGGCTTTGGAACCGACAA-3' R 5'-GAATGCTCCGTAAACAGTCGTGC-3'	NM_008077
GFAP	F 5'-CGGGAGTCGCCAGTTACCAG-3' R 5'-TTTCCTGTAGGTGGCGATCTC-3'	(Israelsson et al., 2009)
Map2	F 5'-GCCAGCCTCGGAACAAACA-3' R 5'-GCTCAGCGAATGAGGAAGGA-3'	(Jones et al., 2018)
Reelin	F 5'-CCCAGCCCAGACAGACAGTT-3' R 3'-CCAGGTGATGCCATTGTTGA-3'	(Heinrich et al., 2006)
Parvalbumin	F 5'-TGTCGATGACAGACGTGCTC-3' R 5'-TTCTTCAACCCCAATCTTGC-3'	(Filice et al., 2016)
Somatostatin	F 5'-TCTGCATCGTCCTGGCTTT-3' R 5'-CTTGGCCAGTTCCTGTTTCC-3'	(Córdoba-Chacón et al., 2011)
S12	F 5'-GGCATAGCTGCTGGAGGTGTAA-3' R 5'-GGGCTTGGCGCTTGTCTAA-3'	(Heinrich et al., 2006)

Table 5. Primer sequences for RT-qPCR analysis.

F = Forward. R= Reverse.

Reelin Protein Expression and Purification

Reelin conditioned medium was collected as the supernatant of a stable mammalian cell line (CER) derived from 293-EBNA cells (Invitrogen) that were transfected with a plasmid encoding the full length *Reelin* cDNA (pCER) cloned into the pCEP4 vector (Invitrogen). Hygromycin B-resistant clones were selected and tested for *Reelin* expression, and then pooled to generate the CER cell line (Niu et al., 2004). The cells were cultured in a serum free Neurobasal medium (Gibco by Life Technologies). The Reelin conditional medium (CER) and the mock control medium from the parental cell line (EBNA) were collected and stored at 4 °C with HEPES buffer (20nM) (Gibco by Life Technologies) until use.

Full length mouse Reelin protein was purified by affinity chromatography from transiently transfected mammalian cells in the Comoletti's laboratory according to an established protocol (Lee et al., 2014). The highly concentrated purified protein was detected by SDS-PAGE followed by Coomassie staining, whereas the more diluted Reelin protein present in the CER medium was detected by SDS-PAGE (4-12% gradient gel, ThermoFisher) followed by Western blot analysis using the G10 mouse monoclonal antibody.

Dissociated cortical and hippocampal neurons

The cerebral cortex and hippocampus were dissected from the brain of embryonic day (E) 16 CD-1 wild type mice, and cells were dissociated using Papain (Worthington) in HBSS buffer with the supplement of 1M of EDTA and 0.5M of $CaCl_2$. Neurons were cultured in 24-well plates (1.0×10^5 cells/ well) coated with poly-L lysine in Neurobasal medium supplemented with 2% B-27 supplement and 0.5 mM L-glutamine (Invitrogen).

Cell Death Staining and Analysis.

After 6 days *in vitro* (DIV) for cortical neurons, or 10-13 DIVs for hippocampal neurons, cells were pretreated with purified Reelin (50nM) or CER medium for 30 minutes and then exposed to 30μM of glutamate to induce excitotoxicity. EBNA mock medium was used as a control for CER. 24 hours after glutamate exposure, cells were stained with 10 mg/mL Propidium Iodide (PI) (Fluka) to label the nuclei of dead cells, and with Hoechst stain (1:1000, ThermoFisher) to label all cell nuclei. Cultures were stained with these fluorescent dyes for 15 minutes in PBS at 37°C, and then washed 2 times with PBS. Stained cells were imaged at the 10x magnification with an automated confocal fluorescence microscope (INCell Analyzer 6000, GE Healthcare). Multiple image fields (9 per well) were selected at random, and stained nuclei were manually counted in blind. The fraction of co-labeled PI/Hoechst over total Hoechst-labeled cells were calculated in each treatment group from multiple wells as an index of cell death.

Locomotion test: rotarod

Two different rotarod devices were used in two independent experiments. In the first experiment, the mice were placed on a rod rotating at 12 cycles/ minutes. The rod was positioned approximately 100 cm above a bedding-filled box. The latency time to fall from the rod was measured. The mice were subjected to 3 trials of 1 minute each. The mice were tested before the injury (to obtain a baseline) and 3 days after the injury.

In a second experiment, the mice were placed in a different rotarod device with an automatic accelerator from 4 to 40 cycles/ minutes and 5 minutes for each trial. The mice were subjected to 3 trials the day before injury (baseline), 1 day and 3 days after injury.

Morris Water Maze (MWM)

The water maze is a task designed for assessing memory impairment. Mice were placed in one quadrant of a ~70 cm diameter tub (small pool) or a ~120 cm diameter (bigger pool) filled with room-temperature water made opaque with non-toxic latex paint. In another quadrant of the tub, submerged just under the surface, a platform was placed (6 cm diameter). The task during a 4 days training period (memory acquisition) consists of finding the platform from any point in the tub. Mice were released into the tub and allowed to swim to the platform in a 60 secs maximum trial. When they failed to find it, they were placed on the platform for a 30 secs intertrial interval. There was 5 trials/day with the critical measure being latency to find the platform. Mice were dried before being returned to their home cage. At the completion of this learning phase, the mice were tested for their ability to remember the location of the platform (probe test); this consisted of a 60 sec probe trial (conducted on day 7) in which there the platform had been removed from the pool. The performance of the mice was measured as percentage of time spent in the correct (target) quadrant compared to the time spent in other quadrants, using the behavioral tracking software ANY-maze (Anymaze). Two weeks after the probe trial, the mice were introduced back into the water maze for a one trial memory retention test with the platform available submerged.

Statistical Analysis

All data were plotted as the mean values for each group (+/- SEM), and statistically analyzed using the GraphPad Prism7 software. $p<0.05$ was considered significant.

For the distribution of Reelin expression in the cortex and hippocampus after CCI the indirect immunofluorescence signal was analyzed in 6 serial coronal sections cut near the injury site (–1.06 to -2.54 mm from bregma) and was measured as the average of the intensity values of the ROIs (6 for the cortex and 3 for the hippocampus) using the measurement tool of ImageJ. The sham samples were shown for comparison but they were not included in the analysis because they were obtained only from one subject. The data were analyzed by two-way ANOVA (Distance and Injury Type as factors) followed by Sidak's multiple comparisons test of CCI Ipsilateral (Ipsi) vs CCI Contralateral (Contra).

For the direct fluorescence, the density of Reelin positive cells/ROI in the cortex or the total number of Reelin-positive cells in the entire hippocampus was manually determined using 3 different sections/mouse at the -1.50, -2.00, -250 mm distance from bregma. Outliers identified with the ROUT test were eliminated from the analysis. The data were first analyzed for normality distribution with the Shapiro's test. If the distribution was normal the values were analyzed by ordinary one-way ANOVA or, if it not normal, by the non-parametric Kruskal-Wallis test. The data were analyzed by using paired t-tests (if normal distribution) or Wilcoxon matched-paired tests (if not normal distribution) comparing contralateral (C) and ipsilateral (I) values from the same CCI mice, or one-way ANOVA to compare all groups including shams.

RT-qPCR data were analyzed by paired t-test or Wilcoxon matched-paired tests to compare contralateral (C) and ipsilateral (I) values within Sham or CCI groups.

For the behavioral data in the Morris Water Maze, repeated measures (RM) 2-way ANOVA with Turkey's multiple comparison was used for the training data. One-way

ANOVA with Turkey's multiple comparison was used for the analysis of the probe test, whereas the non-parametric Kruskal-Wallis test with Dunn's multiple comparison was used for the retention test when all groups were compared to each other.

Ordinary one-way ANOVA was used for the statistical analysis of glutamate excitotoxicity data using hippocampal or cortical neurons treated with glutamate +/- purified Reelin or conditioned medium.

Chapter III: Results

The objective of this study is to investigate the possible link between Reelin activity and TBI, and specifically to understand whether Reelin expression is altered by the trauma and whether this protein is beneficial for neuroprotection or functional recovery.

Expression of Reelin after TBI using the LFP model

In order to establish whether Reelin expression is altered by trauma we initially used lateral fluid percussion (LFP) as a TBI paradigm. For LFP experiments our collaborator, Dr. Janet Alder at Rutgers University- Robert Wood Jonson Medical School, provided direct training and technical support. The LFP experiments were conducted in Dr. Alder's laboratory after performing a small craniotomy on anesthetized mice. The animals that after craniotomy showed damage in the dura were excluded from the study. Mice that were 2-5 month-old were subjected to LFP or sham surgery (see Materials and Methods section for details). To determine whether LFP alters Reelin protein expression, we prepared coronal brain sections using a cryostat, and performed indirect immunofluorescence staining with a highly specific anti-Reelin mouse monoclonal antibody (G10) (de Bergeyck et al., 1998), which was produced in our lab from a hybridoma cell line. Secondary anti-mouse IgG antibodies were conjugated to either Alexa-Fluor488 or Alexa- Fluor647. Images were collected from multiple sections with a confocal or an epifluorescence microscope.

The results of these experiments were variable. In 19 mice subjected to LFP, 9 mice showed no detectable Reelin signal, 5 mice showed a high level of Reelin

expression, and 4 mice showed few Reelin-positive cells. In some cases, Reelin appeared to be upregulated in the injured brain of mice exposed to LFP even in regions distant from the injury. For example, in a few experiments Reelin expression was clearly detected in some cells of the dentate gyrus on the side ipsilateral to the injury 24h after LFP, but it was barely detectable in the contralateral side (Figure 4). However, when these experiments were repeated using additional mice, the results were quite variable, and Reelin expression was similar in both side.

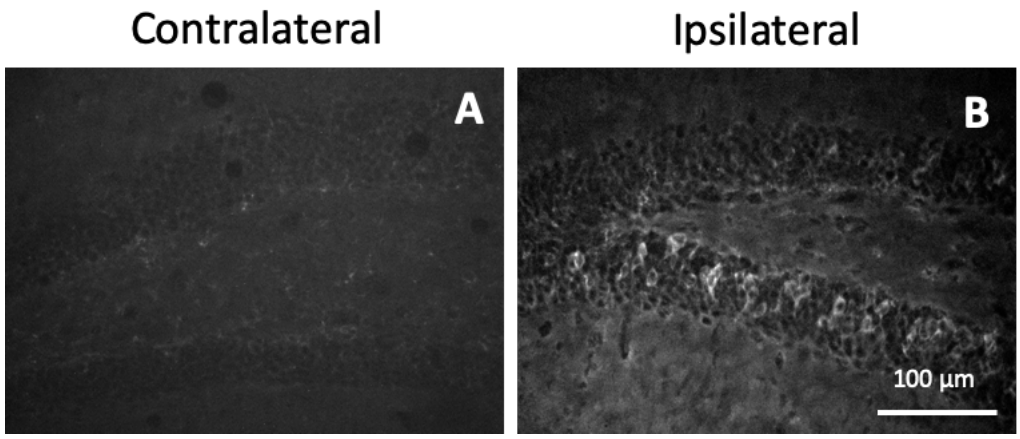

Figure 4. Reelin expression after LFP.

Reelin immunofluorescence using G10 antibody in coronal brain sections from 3 month-old mice. High levels of Reelin expression were detected in the dentate gyrus on the ipsilateral side (**B**). Few and faint Reelin-positive cells were detected in the contralateral side (**A**). Scale bars: 100 µm.

Identification of the cell types that express Reelin after TBI

Even though the levels of Reelin expression were not consistently increased after TBI using the LFP model, we nevertheless set out to identify the cell types that expressed Reelin in samples that clearly showed positive cells after injury.

Since some Reelin positive cells were clearly in the dentate gyrus where neurogenesis occurs even at adult ages, we first investigated whether they might be neuronal progenitor cells. This idea was based on previous studies that showed an increase in neurogenesis in the subventricular zone (SVZ) of the cortex and in the hippocampus after brain injury in a rat LFP model (Chirumamilla et al., 2002). Also, the activation of the neurogenic niche was reported in the mature brain of several models of brain injury (Chang et al., 2016).

To visualize neural progenitor cells, we took advantage of transgenic Nestin-GFP mice, provided by our collaborator Dr. Alder. In these mice, the green fluorescent protein (GFP) is expressed specifically in neural progenitor cells under the control of the nestin promoter. Coronal brain slides were obtained from these mice after LFP, and processed by indirect double immunofluorescence using anti-Reelin G10 (mouse IgG) and anti-GFP (rabbit IgG) antibodies to amplify the signal in nestin-positive cells. The Reelin signal did not co-localize with GFP, indicating that Reelin-expressing cells after TBI are not neuronal progenitor cells (Figure 5, A-C). We also considered the possibility that Reelin positive cells in the dentate gyrus might newly born, immature neurons. However, they do not co-label with antibodies against doublecortin (Figure 5, D-F), a marker for immature neurons.

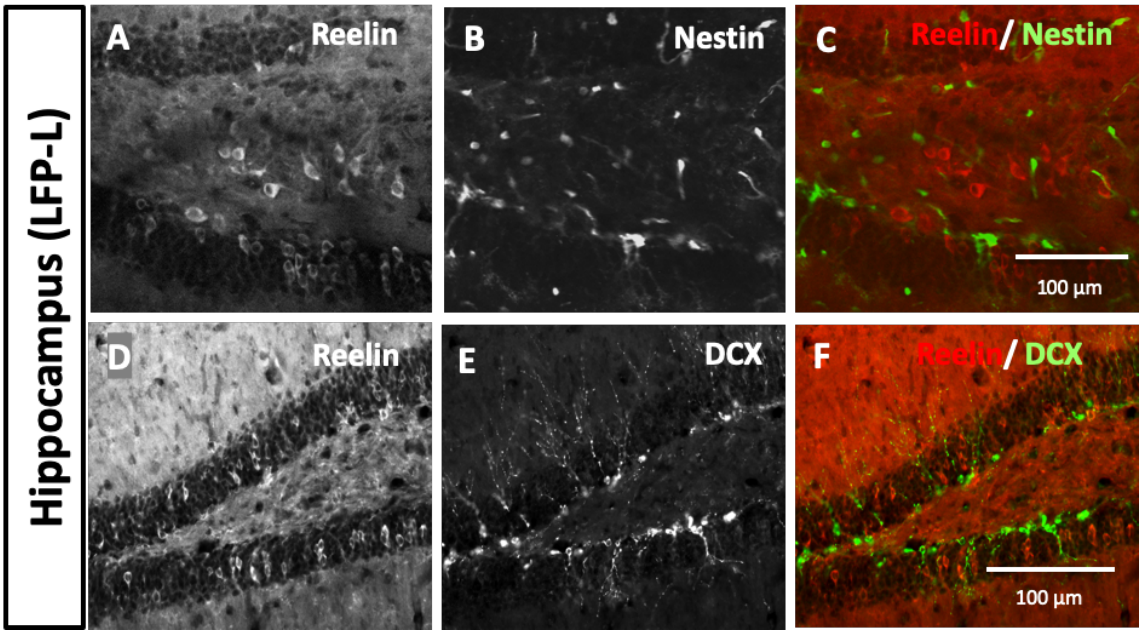

Figure 5. Reelin does not colocalize neuronal progenitor cells and immature neurons.

Indirect immunofluorescence of coronal brain sections after TBI (LFP) in the ipsilateral side (Ipsilateral=L). In the hippocampus Reelin did not colocalize with the neuronal progenitor marker Nestin (**A-C**), nor with the immature neuron marker Doublecortin (DCX) (**D-F**). Scale bars: 100 µm.

Next, we hypothesized that Reelin-positive cells after TBI may represent the same subset of GABAergic interneurons that normally express this protein in the intact adult brain (Alcantara et al., 1998). To test this hypothesis we conducted indirect immunofluorescence experiments using several inhibitory neuronal markers, including GAD67 (which labels all interneurons), calbindin (which labels a subset of interneurons that partially overlaps with the Reelin-expressing subset), and parvalbumin (which labels a different subset of interneurons not expressing Reelin). We double labeled brain slides

obtained from mice subjected to LFP or CCI with rabbit antibodies against these interneuron markers and mouse monoclonal antibodies against Reelin (G10). The results show that many of the cells that are positive for Reelin are also positive for GAD67 (Figure 6,A-C) and calbindin (Figure 6, G-I), but not parvalbumin (Figure 6, D-F). These data suggest that after injury Reelin is expressed by the same cells that normally express this protein in the intact forebrain, namely a subset of interneurons (Alcantara et al., 1998; D'Arcangelo, 2014; Pohlkamp et al., 2014).

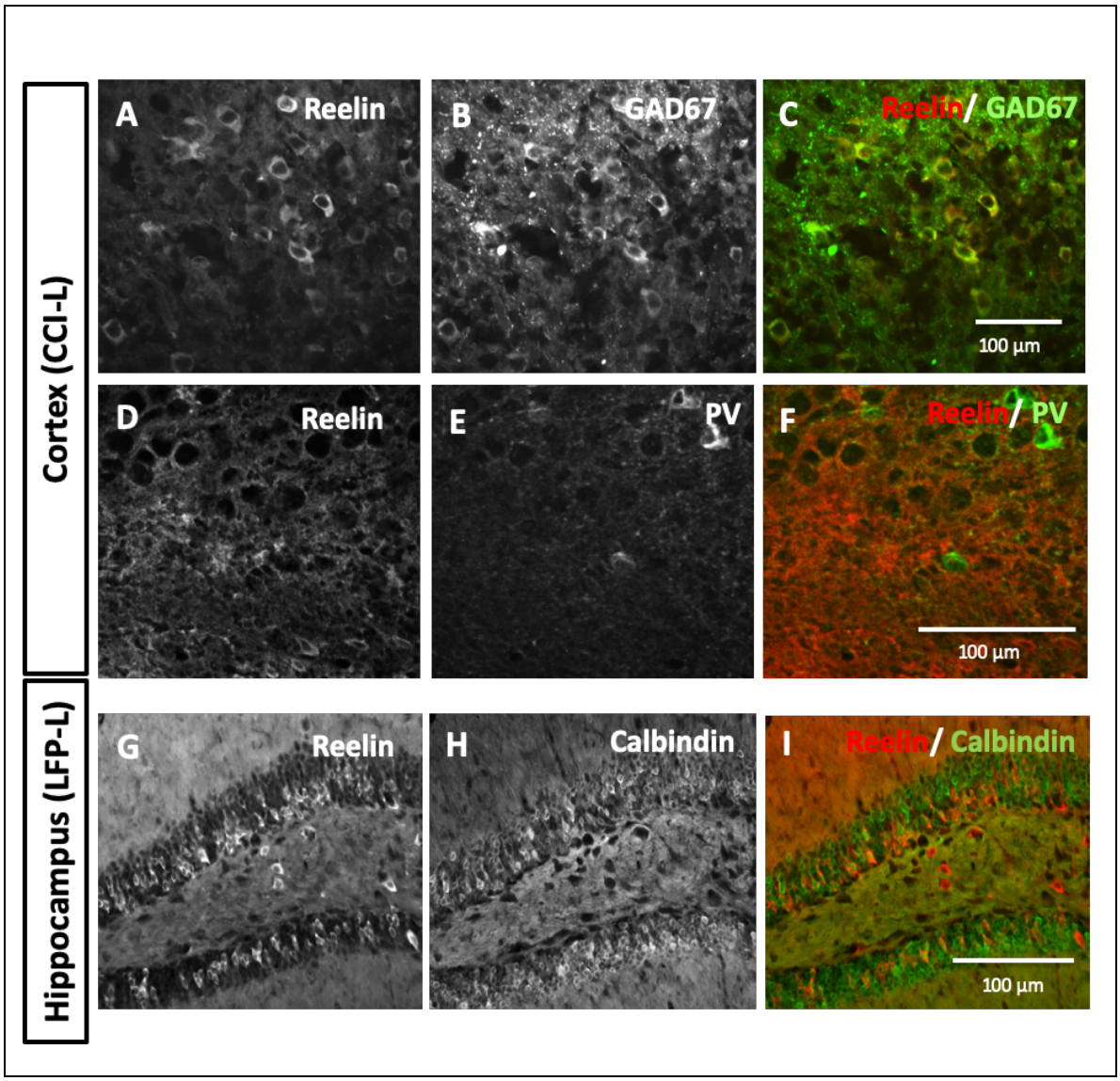

Figure 6. Reelin colocalization with interneuron markers.

Indirect immunofluorescence of coronal brain sections after TBI (LFP and CCI) in the ipsilateral side (Ipsilateral=L). Reelin-positive cells (red) were readily detected and co-labeled primarily with cortical interneurons expressing GAD67 (**A**-**C**), but not with the subpopulation of interneurons positive for Parvalbumin (PV) (**D**-**F**). In the hippocampus Reelin partially colocalized with the interneuron subpopulation expressing Calbindin (**G**-**I**). Scale bars: 100 μm.

Expression of Reelin after TBI using the CCI model

We suspected that the variability of our immunofluorescence results may be due at least in part to the variability of the injury inflicted by LFP. Therefore, after a pilot experiment, we decided to switch to the controlled cortical impact (CCI) model of TBI, which reportedly confers reproducible injuries (Lu & Mao, 2019; Osier & Dixon, 2016; Siebold et al., 2018).

Our collaborator Dr. David Crockett, at Rutgers University- Robert Wood Johnson Medical School, provided the necessary training and equipment to use the CCI model after craniectomy (sham injury). All the mice subjected to CCI in this study were young adult (1-2 month-old) mice of the CD-1 strain. The parameters for CCI were selected based on previous literature, and were as follows: 1.5 mm depth, 3m/sec velocity and 500 ms dwell time (Figure 7). The craniectomy size was 2.7 mm and the impactor tip diameter was 2 mm. Based on the velocity and the depth of the impact used for the procedure, this injury was considered moderate (Ma et al., 2019; Siebold et al., 2018)

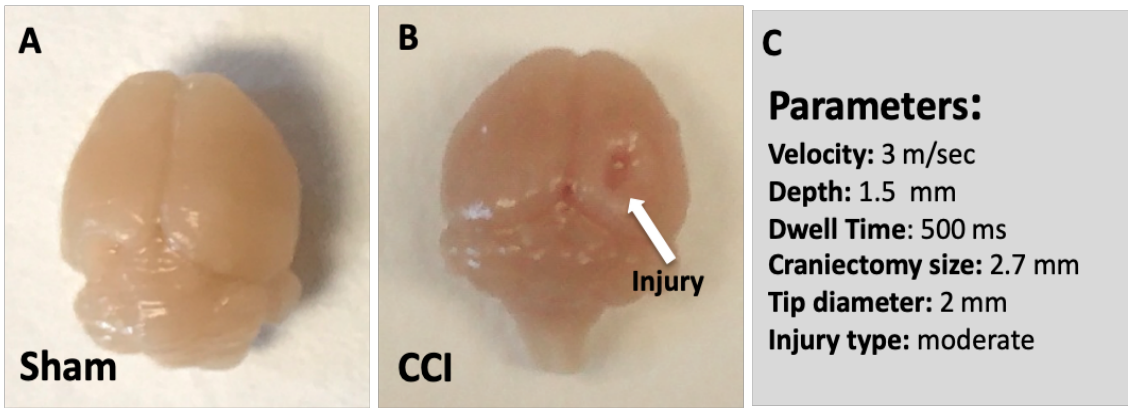

Figure 7. The Controlled Cortical Impact (CCI) model.

Representative images of whole mouse brains 24h following injury (CCI) (**B**) or craniectomy only (Sham) (**A**). The injury was delivered to the right hemisphere, in the somatosensory cortical area, approximately halfway between bregma and lambda (arrow). (**C**) Parameters used for this CCI model. Based on the velocity and the depth of the impact used for the procedure, this injury was considered moderate.

To examine Reelin expression after CCI we used the same indirect immunofluorescence method described above for LFP experiments. Preliminary results indicated that mice subjected to CCI appeared to have a dramatic increase in Reelin expression in the injury side on the hippocampus and cortex (Figure 8), compared to the contralateral side or to sham controls. These results were in agreement with our LFP results and with previous findings from other groups that showed that Reelin is upregulated around the injury lesion in an ischemia mouse model (Courtès et al., 2011) and after ocular tissue injury (Pulido et al., 2007).

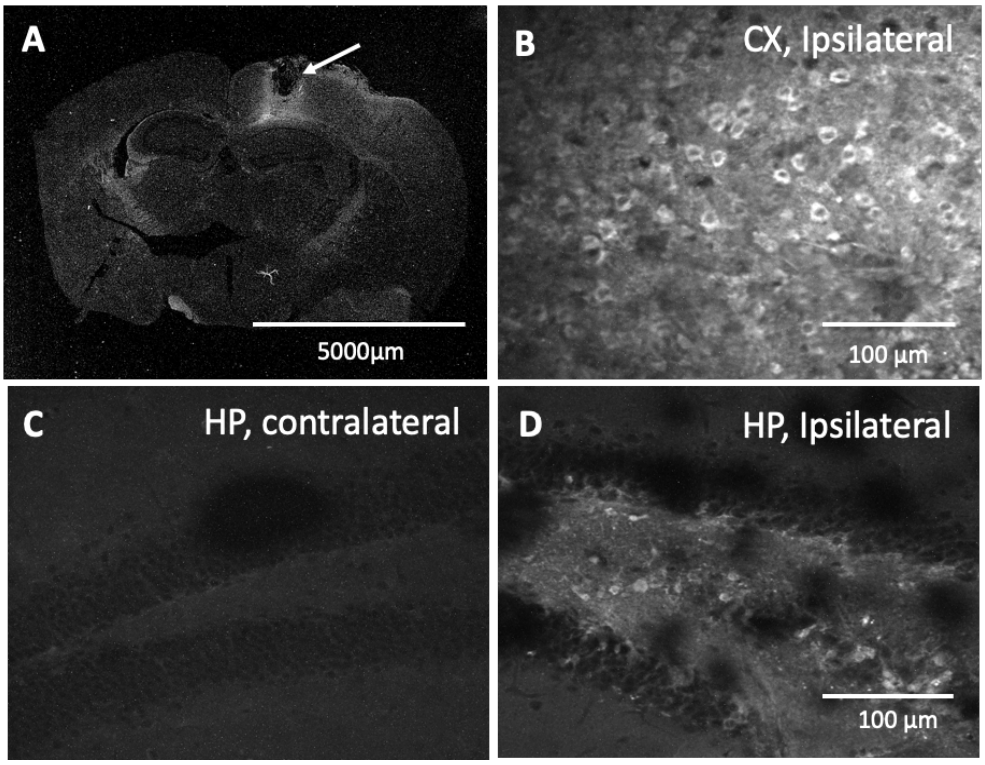

Figure 8. Reelin indirect immunofluorescence after CCI.

Indirect immunofluorescence of coronal brain sections using the Reelin G10 mouse monoclonal antibody followed by anti-mouse IgG secondary antibody conjugated to Alexa-Fluor 488. (**A**) Low magnification image reveals high signal in the cortex surrounding the site of injury (arrow). High magnification images show many cells with high levels of fluorescence signal in the dentate gyrus (**D**) and in the cortex on the ipsilateral side (**B**). Few and faint Reelin-positive cells were detected in the contralateral side (**C**). CX= Cortex; HP = Hippocampus. *Scale bars*: 5000 µm (**A**) and 100 µm (**B**, **C**, **D**).

Quantitative analysis of Reelin expression in response to TBI by indirect immunofluorescence

In order to examine in detail the levels of overexpression, the timing and the spatial distribution of Reelin-expressing cells after injury, we subjected a set of mice to CCI or sham injury. Brain samples were collected 24h or 72h after injury, sectioned serially with cryostat at the 20 μm thickness, and 6 coronal sections per brain were mounted on each slide. To obtain these sections we selected 6 locations surrounding the injury using as reference the mouse brain atlas, at the following distances from bregma: -1.06, -1.22, 1.46, -1.70, -2.06, and -2.54. For each immunofluorescence experiment all slides were processed at the same time with primary mouse monoclonal Reelin antibodies (G10) and fluorophore-conjugated secondary anti-mouse-IgG antibodies. Images were collected with a confocal microscope at the same exposure time. For each slide we analyzed Reelin expression in the ipsilateral and contralateral hippocampus and neocortex, using three different ROIs (regions of interest) selected at random for each structure, and averaging the fluorescence intensity value of the ROIs. The levels of fluorescence intensity were determined using the Image-J software, plotted and statistically analyzed using two-way ANOVA (distance and injury side as factors). Thus, CCI-Ipsilateral (experimental) values from n=3-4 mice per time point were compared to CCI-contralateral (control) values at each distance from bregma. Values obtained from sham mice were shown for comparison but were not included in the analysis because they were obtained from only one mouse. The results showed that the Reelin signal was significantly induced in the injury side of both the neocortex and hippocampus at 24h, and in the neocortex only at 72h after injury (Figure 9). The results also showed a

distribution of the Reelin cortical signal intensity that was more intense close to the injury. These results suggested that TBI causes an upregulation of Reelin expression in the cerebral cortex and hippocampus and led us to hypothesize that this may have functional significance in protecting the brain from the deleterious effects of the injury and promoting recovery.

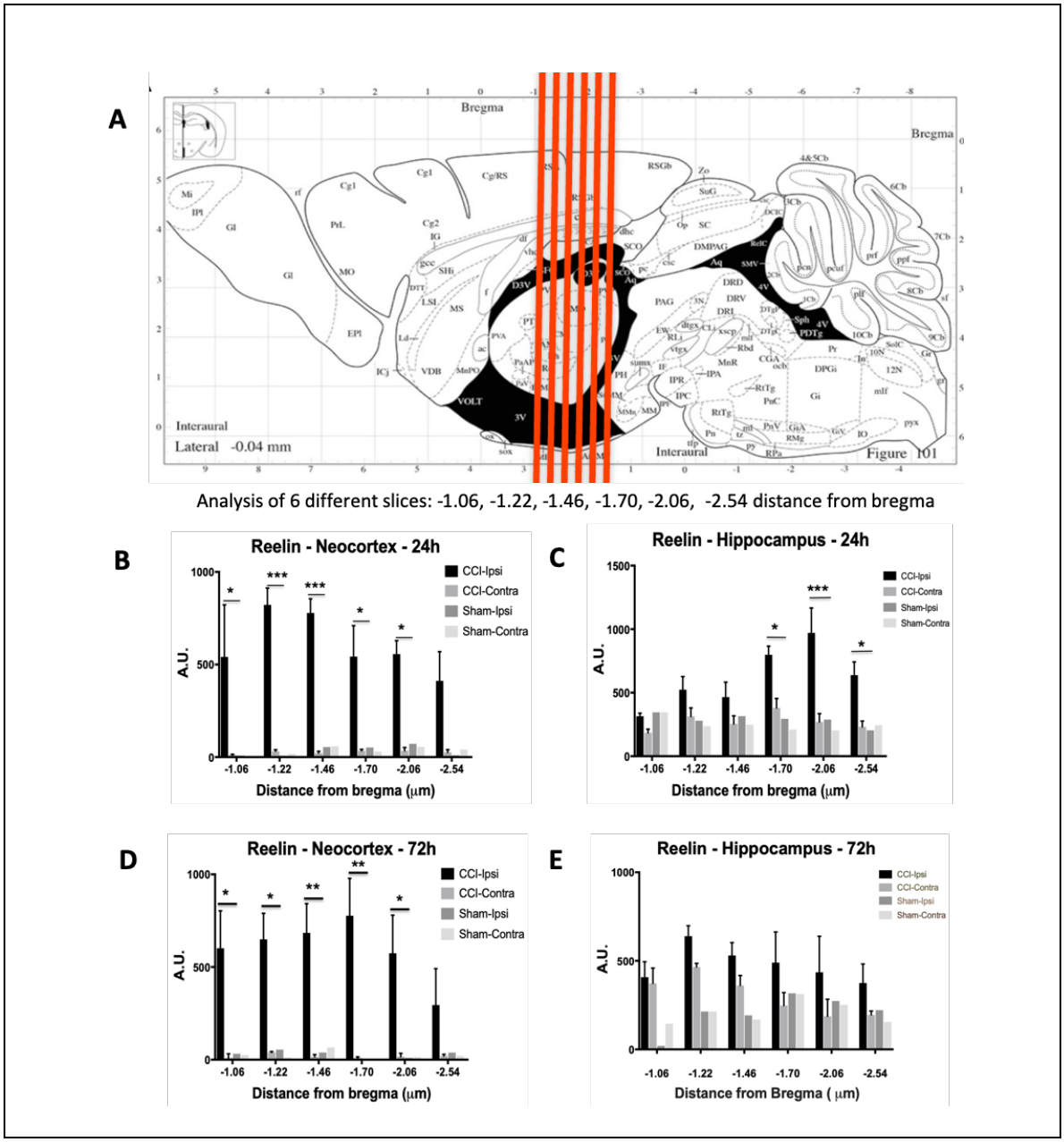

Figure 9. Quantification of Reelin expression after CCI.

Analysis of the indirect immunofluorescence Reelin signal intensity using 6 serial coronal sections cut near the injury site (–1.06 to -2.54 mm from bregma) (see **A**). In the cortex the Reelin signal was stronger in the ipsilateral side of the injury than in the contralateral side or sham samples at 24h or 72h after CCI (**B, D**). In the hippocampus the Reelin signal was also stronger in the ipsilateral side at 24h (**C**), but less so at 72h (**E**). For the 24h data point n=4 CCI and n=1 sham mice were used. For the 72h point n=3 mice CCI and n=1 sham were used. Statistical test: two-way ANOVA (Distance and Injury Type) followed by Sidak's multiple comparisons test of CCI Ipsilateral (Ipsi) vs CCI Contralateral (Contra) values. *$p \leq 0.05$, **$p < 0.01$, ***$p < 0.001$.

Problems with indirect immunofluorescence experiments

The results of the experiments described above strongly suggested that Reelin expression is upregulated in the brain tissue surrounding the injury. However, we noted that the tissue ipsilateral to the injury was very frail and tended to break during processing, suggesting that cell permeability may be altered. To ensure that the signal was specific, we conducted further immunofluorescence experiments including controls consisting of samples incubated only with the fluorophore-conjugated secondary anti-mouse IgG antibodies used to detect Reelin primary antibodies. Surprisingly, secondary anti-mouse IgG antibodies produced a strong immunofluorescence signal in the ipsilateral side even in the absence of primary anti-Reelin antibodies (Figure 10).

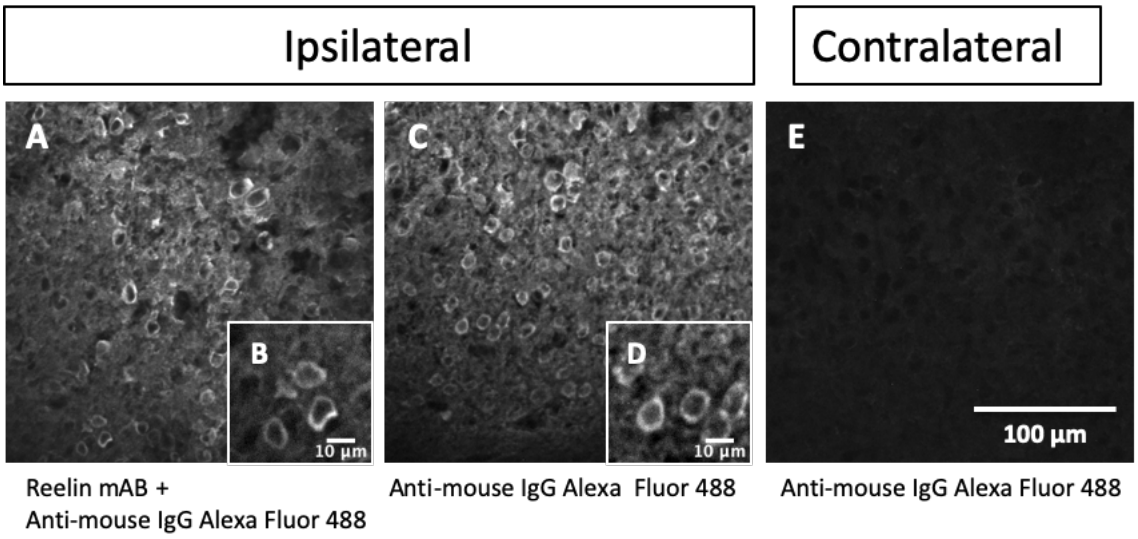

Figure 10. Secondary anti-mouse IgG antibody artifact.

Coronal brain sections from mice subjected to CCI were processed of indirect immunofluorescence with a primary mouse monoclonal antibody (mAB) against Reelin (clone G10), followed by Alexa Fluor 488 (H+L) secondary anti-mouse IgG antibodies **(A, B)** or by secondary antibodies alone as a control **(C, D)**. An intense signal was detected in many cortical cells in the ipsilateral injury side using either both primary and secondary antibodies or secondary antibodies alone. No cells were labeled by secondary antibodies alone in the contralateral side **(E)**. Scale bars: 100 µm (**A**, **C**, **E**) and 10 µm (**B**, **D**).

This artefactual signal was present only near the injury and only in conjunction with anti-mouse IgG secondary antibodies. Secondary antibodies directed against the contralateral side (Figure 10, E) or a different species, such as fluorophore-conjugated

anti-rabbit IgG antibodies, did not produce the artefactual signal. It is possible that anti-mouse IgG secondary antibodies labeled injury-induced immunoglobulins produced by macrophages, raising doubts on the specificity of the signal we had measured by indirect immunofluorescence.

We considered different ways to circumvent the technical problem related to the use of secondary anti-mouse-IgG antibodies. A simple solution would have been to use a Reelin antibody produced in a different host species, but unfortunately, at the time of these experiments, the only available Reelin antibodies suitable for immunofluorescence experiments were raised in mice. We tried to minimize the problem using secondary anti-mouse IgG antibodies conjugated to a different fluorophore, or secondary antibodies raised against the antigen-binding fragment (Fab) of the mouse immunoglobulin. We also tried to block the tissue prior to the staining with serum obtained from a different serum, but the problem remained. Finally, a newly developed Reelin mouse monoclonal antibody (same G10 clone) that is already conjugated with the Alexa-Fluor 488 fluorophore became commercially available. This reagent enabled us to perform direct immunofluorescence experiments, thereby avoiding the use of anti-mouse IgG secondary antibodies altogether. We performed a pilot experiment with mice subjected to CCI and determined that the Reelin signal obtained with this approach was now clear and unequivocal in both, the contralateral and ipsilateral side of the brain (Figure 11). However, there was no apparent difference in expression between the injury sides, prompting us to re-examine the issue of Reelin expression after TBI in a new set of experiments.

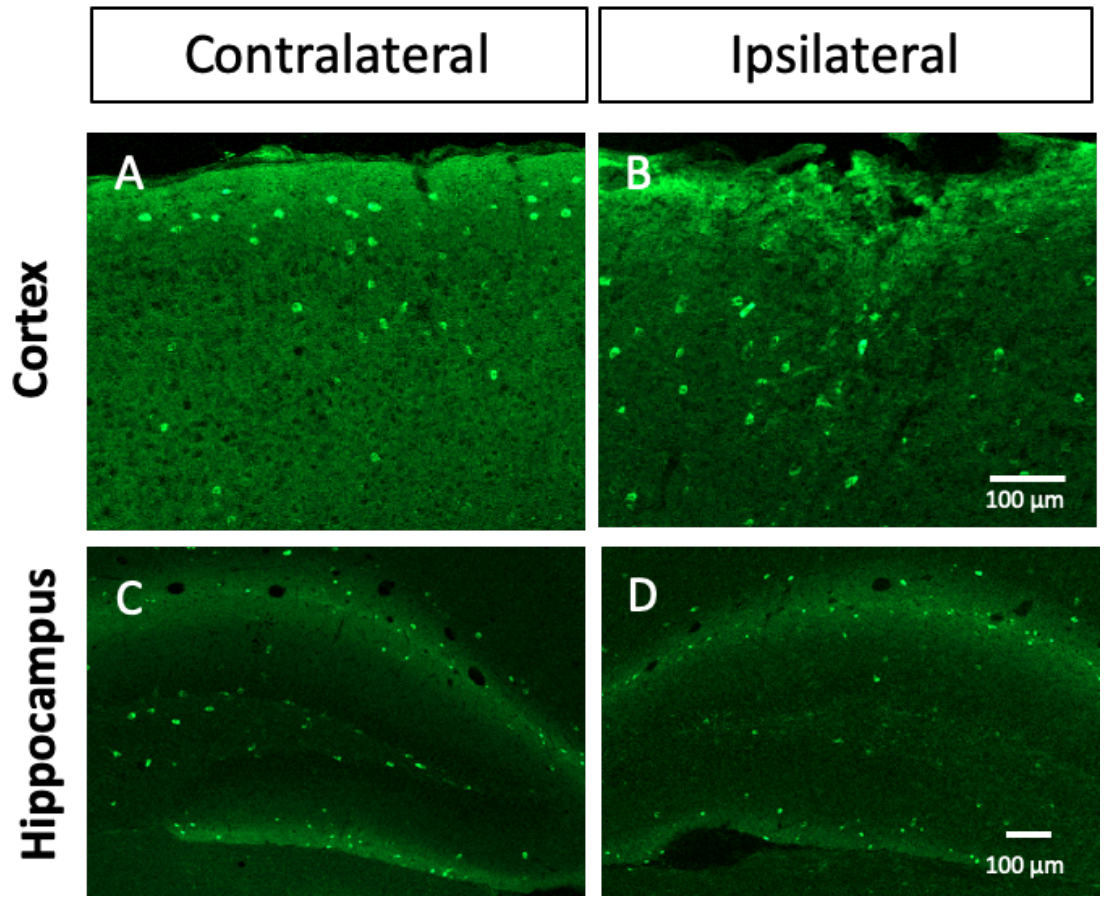

Figure 11. Detection of Reelin by direct immunofluorescence.

Reelin-positive cells were unequivocally identified in mouse coronal brain sections after CCI using only a primary mouse monoclonal anti-Reelin antibody (clone G10) directly conjugated to Alexa Fluor 488. Reelin-positive cells were clearly detected in the ipsilateral cortex and hippocampus (**A**, **C**) as well as in the contralateral cortex and hippocampus (**B**, **D**). Scale bars for all panels: 100 µm.

Analysis of protein expression by direct immunofluorescence reveals loss of hippocampal Reelin-expressing cells after CCI

Using this improved direct immunofluorescence approach, we conducted a new set of experiments to have a good understanding of whether Reelin protein expression changes or not after injury. We collected brain samples and analyzed Reelin expression data at 3 different time points (24h, 72h, and 7 days) after CCI injury or sham surgery, in both the ipsilateral and contralateral sides. To analyze expression in the neocortex for each group we counted the number of Reelin+ cells in 6 ROIs/section and 3 different sections/brain collected at -1.50, -2.00, -250 μm distance from bregma; we then divided these values by the total area of the ROIs to obtain density values (# of Reelin+ cells/μm^2 cortex). Using the same brain sections, we also measured the total number of Reelin+ cells in the entire hippocampus proper and in the dentate gyrus. All counts were done in blind by 2 different persons. We then plotted and statistically analyzed the data using the GraphPad Prism 7 software. When data in each CCI or sham group were normally distributed, we compared contralateral and ipsilateral values in the same mice using paired t-tests. Data that were not normally distributed were analyzed using Wilcoxon matched-paired tests. The results show that the density of Reelin+ cells was not altered 24h after injury (n= 3-4 CCI and n=4 sham mice) (Figure 12, D).

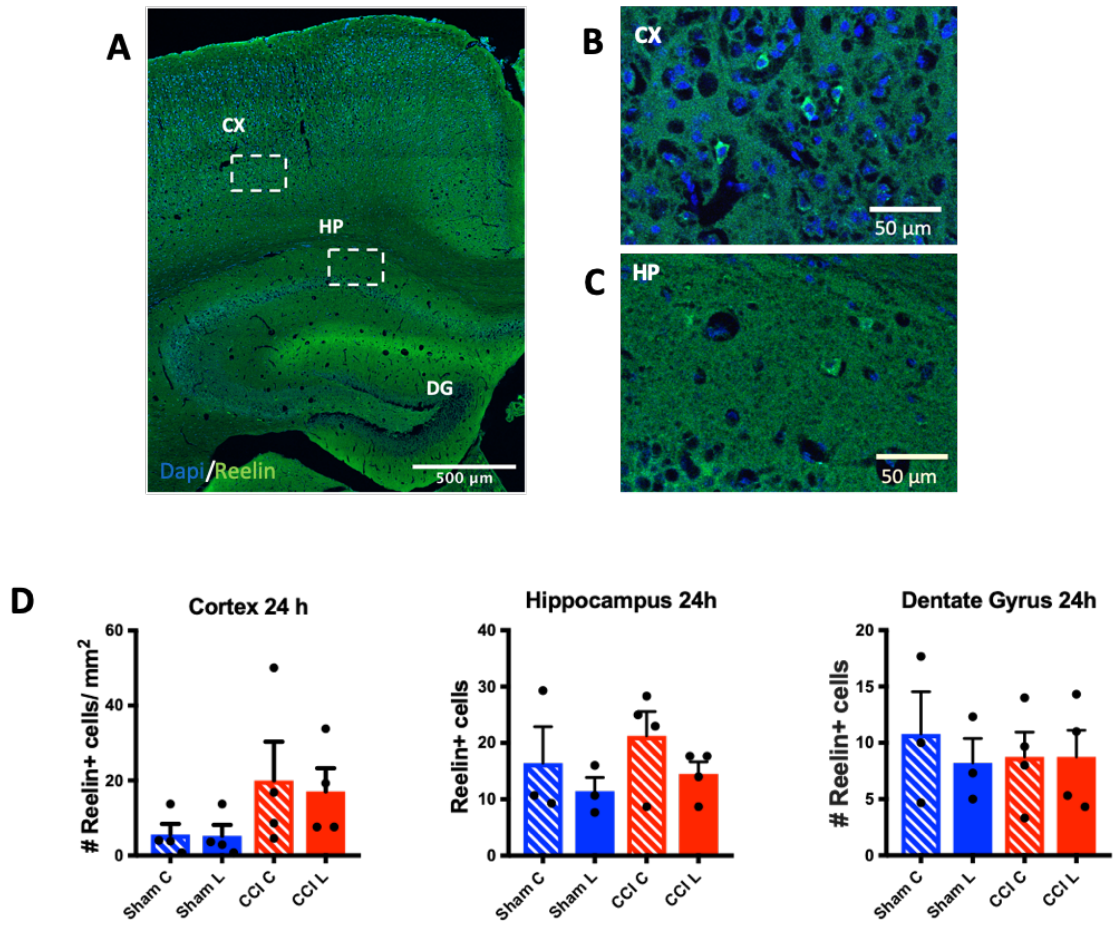

Figure 12. No change in the number of Reelin+ interneurons 24h post-CCI.

Direct immunofluorescence with a Reelin antibody conjugated to Alexa Fluor 488 using brain sections 24h post-injury. **(A)** Representative image at low magnification of the contralateral injury side, double labeled with Reelin antibodies (green) and Dapi (blue). High magnification images showing Reelin+ cells in the cortex (**B**) and hippocampus (**C**). (**D)** Quantification of the density of Reelin+ cells in *n*=4 CCI or *n*=3-4 Sham mice. The analysis is based on 3 different sections/mouse at -1.50, -2.00, -250 mm distance from bregma. Cortex data includes 6 image fields/section for each group. Hippocampus and Dentate Gyrus data include all Reelin+ cells identified in the entire structure in each

section. No statistical difference was found comparing contralateral (C) and ipsilateral (I) CCI groups using paired t tests, or CCI (I) versus CCI (C) and Sham samples using ordinary one-way ANOVA. The scatter plots show each mouse data point and the mean value of each group (+/- SEM). CX= cortex; HP= hippocampus; DG= dentate gyrus.

A similar result was obtained at 72h post-TBI in all regions analyzed (*n*= 3 CCI and *n*=4 sham mice) (Figure 13).

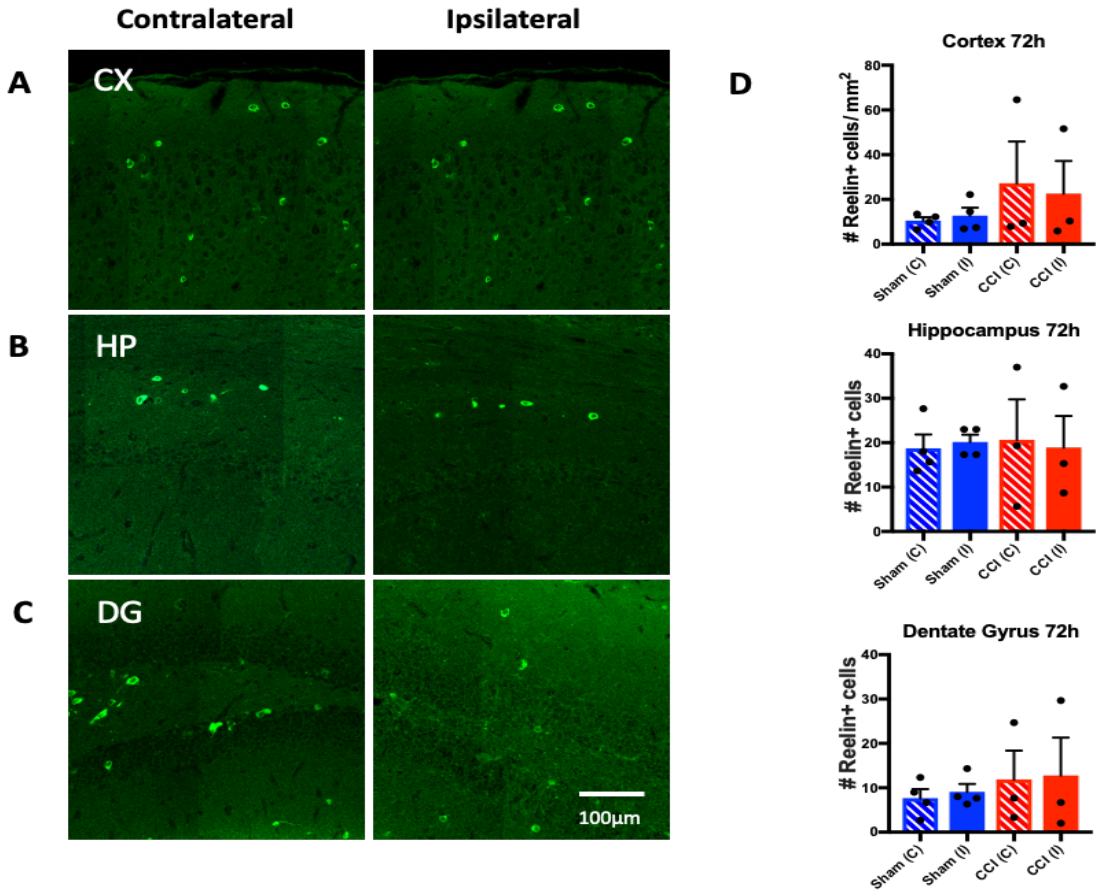

Figure 13. No change in number of Reelin+ interneurons 72h post-CCI.

Direct immunofluorescence with a Reelin antibody conjugated to Alexa Fluor 488 using brain sections collected 72h post-injury. Representative images showing Reelin+ cells (green) in the cortex (CX) (**A**), hippocampus (HC) **(B)** or dentate gyrus (DG) **(C)**. **(D)** Quantification of the density of Reelin+ cells in *n*=3 CCI and *n*=4 Sham mice. The analysis is based on 3 different sections/mouse at -1.50, -2.00, -250 mm distance from bregma. Cortex data includes 6 image fields/section for each group. Hippocampus and dentate gyrus data include all Reelin+ cells identified in the entire structure in each

section. No statistical difference was found comparing contralateral (C) and ipsilateral (I) CCI groups using paired t tests or Wilcoxon tests, or CCI (I) versus CCI (C) and Sham samples using ordinary one-way ANOVA or non-parametric Kruskal-Wallis test. *Scale bar for all panels*: 100 μm.

However, 7 days after injury the number of Reelin+ cells were significantly reduced, but only in the hippocampus, whereas it remained unaltered in the cortex and dentate gyrus (*n*= 4 CCI and *n*=2 sham mice) (Figure 14). These results are similar to those obtained in a recent study (June 2019) where mice showed reduced levels of Reelin expression 14 days after cryoinjury in the motor cortex and no difference 1 day after the injury (Arimitsu et al., 2019).

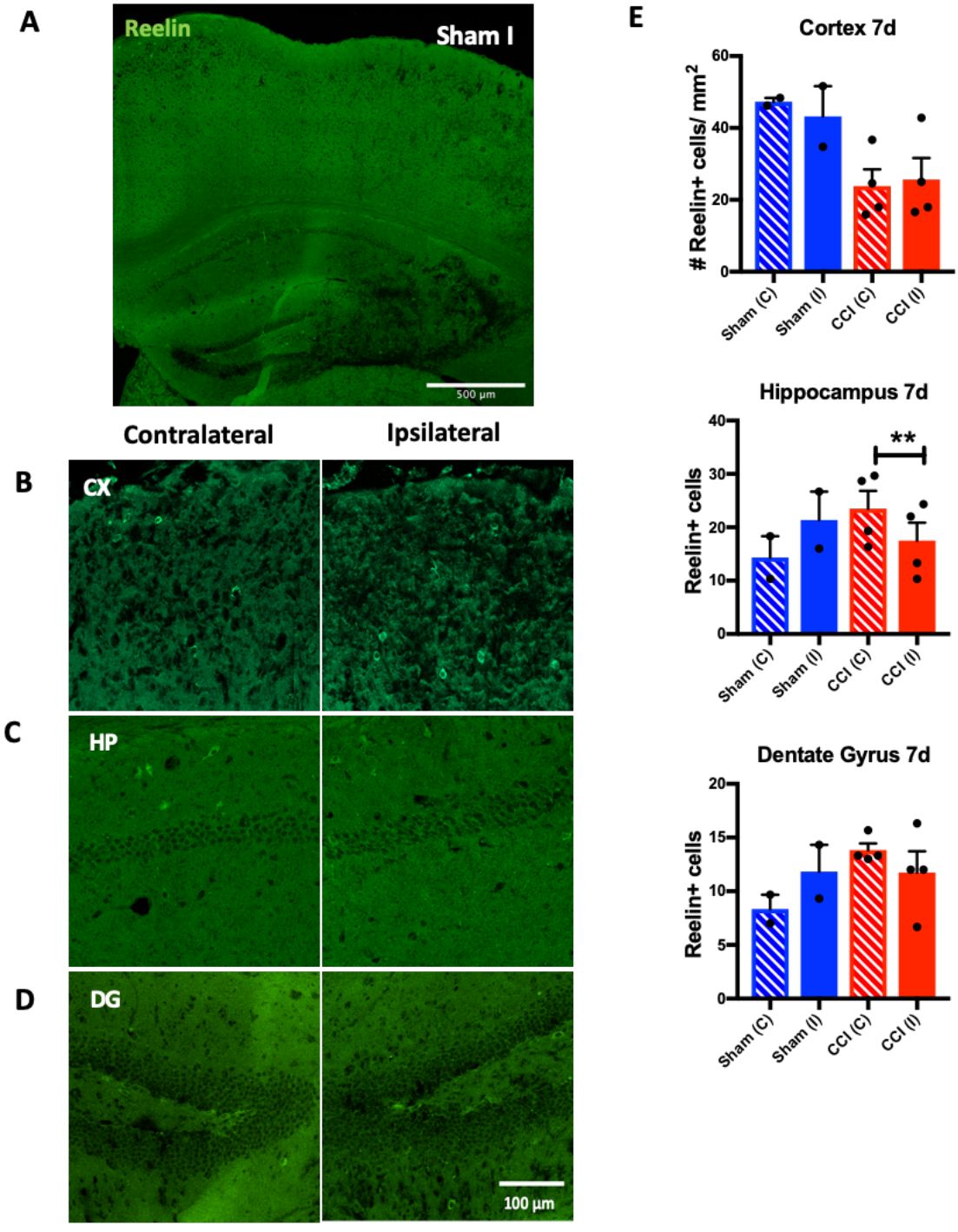

Figure 14. Loss of Reelin+ hippocampal interneurons 7 days post-CCI.

Direct immunofluorescence with a Reelin antibody conjugated to Alexa Fluor 488 using brain sections collected 7 days post-injury. (**A**) Representative low magnification image of a Sham brain on the ipsilateral injury side labeled with Reelin antibodies (green). High magnification images showing Reelin+ cells in the cortex (CX) (**B**), hippocampus (HC) (**C**) and dentate gyrus (DG) (**D**)**.** (**E**) Quantification of the density of Reelin+ cells from *n*=4 CCI and *n*=2 Sham mice. The analysis is based on 3 different sections/mouse at -1.50, -2.00, -250 mm distance from bregma. Cortex data includes 6 image fields/section for each group. Hippocampus and Dentate Gyrus data includes all Reelin+ cells identified in the entire structure in each section. The density of Reelin+ cells in the hippocampus was significantly reduced in ipsilateral CCI (I) compared to contralateral CCI (C) samples (p= 0.0031). No significant differences were found between CCI groups in the cortex or dentate gyrus. The scatter plots show each mouse data point and the mean value of each group (+/- SEM). *Statistical analysis*: paired t-tests comparing CCI (C) and CCI (I) values for cortex and hippocampus data; Wilcoxon matched-pairs test for dentate gyrus data **p<0.01. *Scale bars*: 500 μm (A) and 100 μm (B-D).

In summary, these results contradicted my preliminary results obtained by indirect immunofluorescence, and the idea that injury may upregulate Reelin expression. Rather, the direct immunofluorescence data revealed that brain injury causes a delayed loss of Reelin expression that specifically affects the hippocampus. Given the role of this structure in cognition and memory, and the critical function of Reelin in maintaining the adult hippocampal circuitry and synaptic plasticity (Jiang et al., 2016; Trotter et al.,

2013), the data suggest that learning and memory deficits after TBI may be due at least in part to loss of Reelin.

TBI leads to decreased mRNA levels of Reelin and other inhibitory neuron markers

To further investigate the effect of TBI on the expression of Reelin and other markers of inhibitory neurons, we performed RT-qPCR at 24h and 72h after injury. We collected freshly dissected brain samples from CCI, Sham or naive mice and extracted the total mRNA. Since the level of Reelin is high in the embryonic brain and decreases at postnatal ages, we used as a positive control a wild type mouse cortex and hippocampus sample collected at postnatal day (P) 5. The data were normalized first to the internal qPCR control S12, and then to the P5 reference sample or to the average of sham contralateral values. The data were then plotted and statistically analyzed in a paired fashion, comparing contralateral to ipsilateral values in each mouse brain.

At 24h after injury, the level of *Reelin* mRNA was unaltered in the ipsilateral side of the cortex and hippocampus (Figure 15, C and D). This result is in agreement with the previous analysis of Reelin expression by immunostaining. We also measured the expression level of other inhibitory markers such as *Somatostatin, Parvalbumin, and Gad1* (the gene encoding GAD67). The expression of all these inhibitory neuron markers was similar between ipsilateral and contralateral samples in the CCI and sham groups. Also, *Map2*, a marker for all mature neurons, is unaltered by the injury at the 24h time point (*n*=4-7 CCI, *n*=1-3 sham, *n*=naïve).

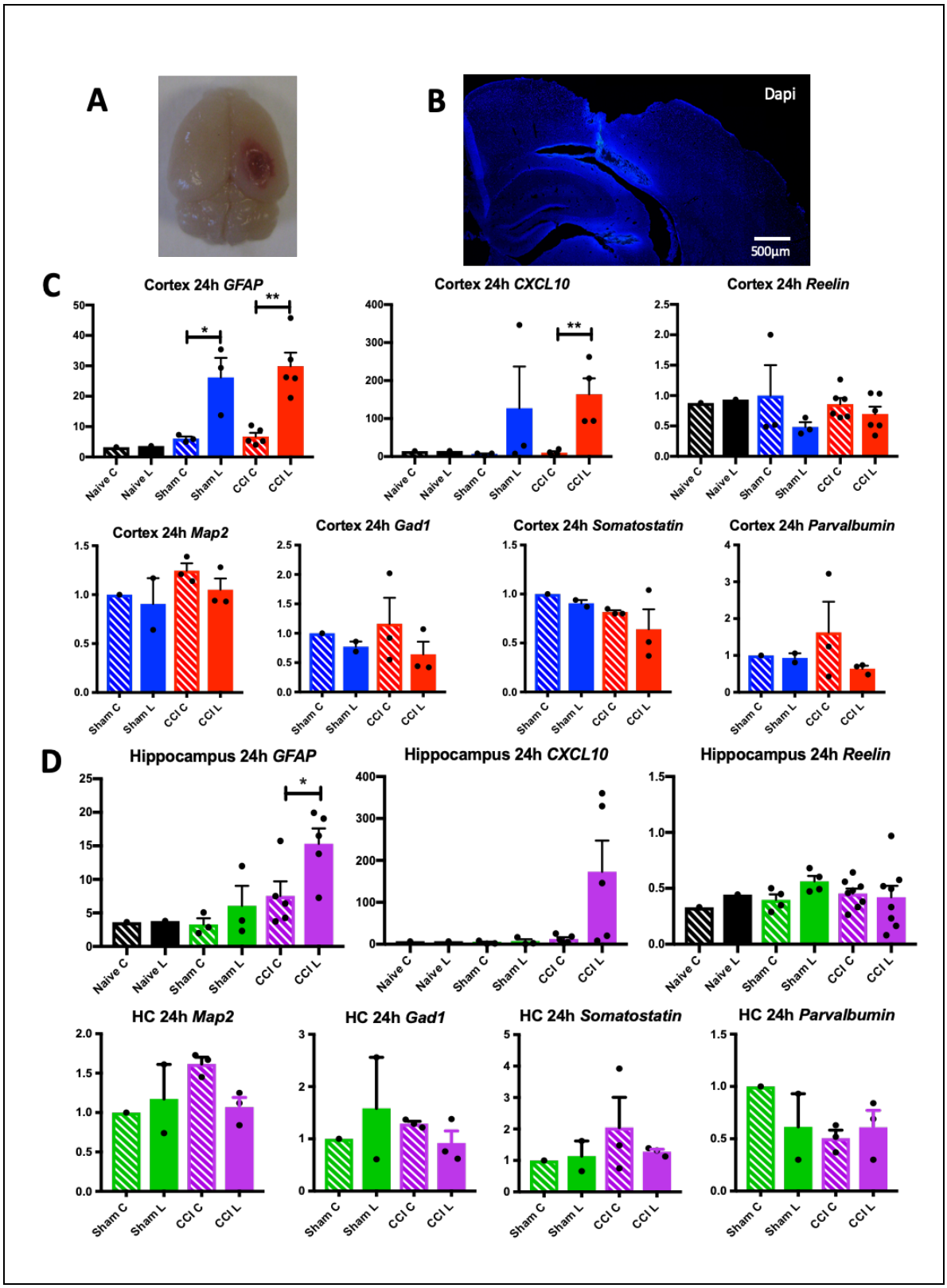
A
B
Dapi
500µm
C
Cortex 24h GFAP
Cortex 24h CXCL10
Cortex 24h Reelin
Cortex 24h Map2
Cortex 24h Gad1
Cortex 24h Somatostatin
Cortex 24h Parvalbumin
Naive C
Naive L
Sham C
Sham L
CCI C
CCI L
D
Hippocampus 24h GFAP
Hippocampus 24h CXCL10
Hippocampus 24h Reelin
HC 24h Map2
HC 24h Gad1
HC 24h Somatostatin
HC 24h Parvalbumin

Figure 15. RT-qPCR shows inflammation but no change in Reelin or other neuron marker gene expression 24h post-CCI.

RT-qPCR analysis of mRNA expression of inflammatory markers (GFAP, CXCL10), Reelin, a pan-neuronal marker (Map2), and interneuron markers (Gad1, Somatostatin, Parvalbumin) in the cortex and hippocampus 24h after injury. (**A**) Representative image of the whole brain 24h post-CCI. (**B**) Low magnification image of the ipsilateral side of a brain section stained with the nuclear dye Dapi (blue). Analysis of the RT-qPCR data in the cortex (**C**) or hippocampus (HC) (**D**) shows increased levels of GFAP and CXCL10 in ipsilateral CCI (I) versus contralateral CCI (C) samples, consistent with the induction of inflammatory response by injury. The expression of Reelin, Map2 or interneurons markers was not significantly altered by the injury in CCI or Sham mice. RT-qPCR data for each gene were normalized to the gene encoding ribosomal protein S12 (a housekeeping gene). Data for GFAP, CXCL10 and Reelin: n=3-8 CCI, n=3-4 sham and 1 naïve mouse was used. These data were further normalized to a postnatal day 5 WT mouse sample used as a reference. Data for interneuron markers (Somatostatin, Parvalbumin, Gad1) and Map2 data: n= 3 CCI and n=2 Sham mice were used, and the data were normalized to the average Sham (C) value. The scatter plots show each mouse data point and the mean value of each group (+/- SEM). Statistical analysis: when data were normally distributed, a paired t-test was used to compare contralateral (C) and ipsilateral (I) values within Sham or CCI groups. For data that were not normally distributed the Wilcoxon matched-pairs test was used instead. *$p<0.05$, **$p<0.01$.

As positive controls for the injury, we also performed a RT-qPCR to detect the levels of *GFAP* (Okonkwo et al., 2013) and *CXCL10* (Israelsson et al., 2010), two mRNAs that are known to be activated by the immunological response after injury. The *GFAP* levels were indeed strongly and significantly elevated in mice subjected to CCI. In the cortex, the sham ipsilateral group also showed high levels of *GFAP* expression compared to the contralateral. The levels of *CXCL10* were also elevated in the cortex in the ipsilateral side of the CCI mice and in the sham group, but the difference was not statistically significant due to a large sample variation. In the hippocampus *GFAP* levels were significantly elevated in CCI mice on the ipsilateral side (Figure 15, C and D). *CXCL1*0 levels were also elevated, but the difference was not statistically significant. Together these results indicate that 24h after injury there is substantial inflammatory response to CCI in both the cortex and hippocampus, and some inflammation is also present in the cortex as a result of the craniectomy alone. Despite this, the expression of *Reelin* or other neuronal markers is not altered at this early time point.

To determine whether TBI causes a delayed change in gene expression, we conducted similar RT-qPCR experiments at 72h post injury. At this time point inflammation (as indicated by the increased *GFAP* expression) persisted both in the ipsilateral cortex and hippocampus of CCI samples, but it was no longer present in Sham samples (Figure 16, C). We analyzed the levels of *Reelin* mRNA in CCI samples and found that they were significantly lower in the ipsilateral side of the cortex and hippocampus compared to the contralateral values (Figure 16, C). No change was seen in Sham samples. We also performed RT-qPCR analysis with inhibitory neuron markers to see whether they are affected by injury or sham surgery. *Gad1*, a marker for all inhibitory

neurons was significantly downregulated in the CCI cortex and hippocampus in the ipsilateral side. *Parvalbumin* was also reduced after TBI in the cortex (Figure 16, C). In the hippocampus, the level of *Parvalbumin* was reduced in the ipsilateral side, but the difference was not statistically significant compared to the contralateral values. The level of *Somatostatin*, another gene expressed in a different set of inhibitory neurons, was downregulated but only in the ipsilateral hippocampus 72h after CCI. These data are consistent with a recent study showing that cortical GABAergic interneurons expressing Parvalbumin or Somatostatin are decreased in mice 2-4 week after TBI by immunostaining analysis (Cantu et al., 2015). No change in any gene expression was detected in Sham samples.

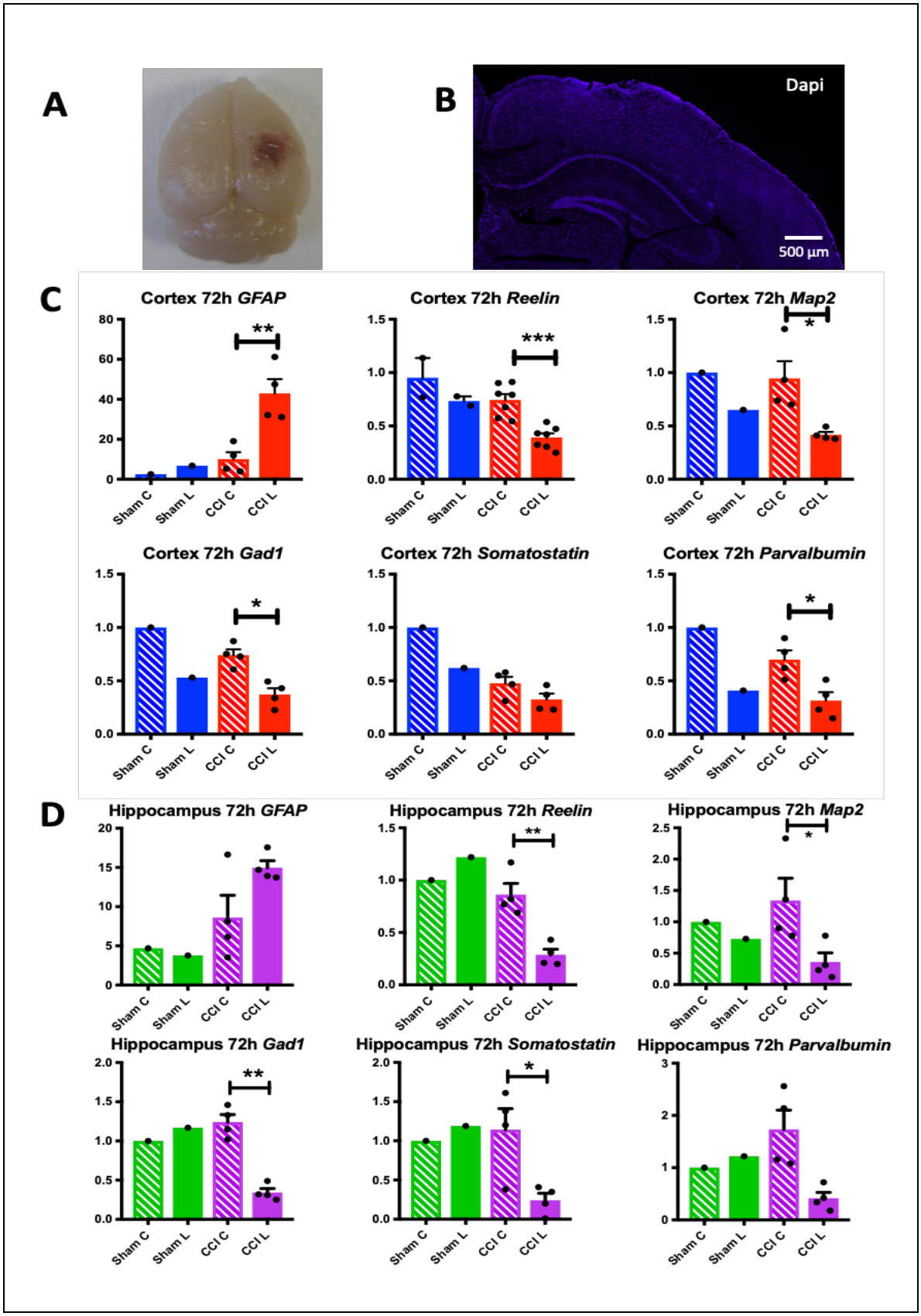
A
B
Dapi
500 µm
C
Cortex 72h GFAP
Cortex 72h Reelin
Cortex 72h Map2
Cortex 72h Gad1
Cortex 72h Somatostatin
Cortex 72h Parvalbumin
Sham C
Sham L
CCI C
CCI L
D
Hippocampus 72h GFAP
Hippocampus 72h Reelin
Hippocampus 72h Map2
Hippocampus 72h Gad1
Hippocampus 72h Somatostatin
Hippocampus 72h Parvalbumin

Figure 16. RT-qPCR shows a decrease in the expression of Reelin and other neuronal genes 72h post-CCI.

RT-qPCR analysis of mRNA levels of an inflammatory marker (GFAP), Reelin, a pan-neuronal marker (Map2), and interneuron markers (Gad1, Somatostatin, Parvalbumin) in the cortex and hippocampus 72h after injury. (**A**) Representative image of the whole brain 72h post-CCI. (**B**) Low magnification image of the ipsilateral side of a brain section stained with the nuclear dye Dapi (blue). Analysis of the RT-qPCR data in the cortex **(C)** or hippocampus **(D)** shows increased levels of GFAP in ipsilateral CCI (I) versus contralateral CCI (C) samples, indicative of a persistent inflammatory response. This difference however, was statistically significant only in the cortex. Reelin expression was significantly downregulated in CCI (I) samples in both cortex and hippocampus. All other markers analyzed were also downregulated, although the values did not always reach statistical significance. All RT-qPCR data for each gene were first normalized to the gene encoding ribosomal protein S12. Cortical data for GFAP and Reelin: n=4-7 CCI, n=1-2 sham and 1 naïve mouse was used. These data were further normalized to a reference postnatal day 5 WT mouse. Data for cortical interneuron markers (Somatostatin, Parvalbumin, Gad1) and Map2, n= 4 CCI and n=1 Sham mice were used, and the data were normalized to the Sham (C) value. For all hippocampal data: n= 4 CCI and n=1 Sham mice were used; GFAP data were normalized to a WT reference, whereas all other genes were normalized to Sham (C). The scatter plots show each mouse data point and the mean value of each group (+/- SEM). Statistical analysis: all data were normally distributed and a paired t-test was used to compare contralateral (C) and

ipsilateral (I) values within Sham or CCI groups. *p<0.05, **p<0.01.

We wondered whether brain injury affected gene expression specifically in interneurons or in all neurons. The level of the pan-neuronal marker *Map2* was also reduced in the ipsilateral side of CCI samples compared to the contralateral side, but not in Sham samples, indicating that the effects of the injury on gene expression were not limited to the interneuron population. Together, these data suggest that CCI caused a delayed downregulation of many neuronal markers, including *Reelin*, possibly leading to alterations of neuronal structure and functional

Behavioral analysis of mice after CCI

The experiments above raised the possibility that loss of Reelin may contribute to the deficit in memory and cognitive function after TBI. This may be because, even though Reelin expression is low in the adult brain, it still plays an important function in the control of synaptic formation, activity and plasticity (D'Arcangelo, 2014; Trotter et al., 2013). Mice subjected to CCI have been previously reported to display motor and cognitive impairment (Fox et al., 1998; Xiong et al., 2013). They fall off more quickly from the rotarod (Bajwa et al., 2016) and they exhibit learning and memory deficits in the Morris water maze (Washington et al., 2012). The deficits can persist up to one year post CCI, and are often associated with brain atrophy (Dixon et al., 1999).

To investigate the contribution of Reelin expression loss to the CCI sequela, we had planned to use adult-specific inducible conditional mutant mice that exhibit complete loss of Reelin in the brain after tamoxifen induction (cKO). These mice were generated in the laboratory of Dr. Joachim Herz, University of Texas Southwestern Medical Center,

Dallas, and would be suitable for this study because they do not exhibit a developmental phenotype that would confound the analysis of the injured, adult brain (Lane-Donovan et al., 2015). Before acquiring the cKO Reelin mice, we set out to reproduce the reported deficits in locomotion and cognitive function after TBI. We tested a group of wild type mice subjected to CCI and conducted behavioral experiments, including the Rotarod as a test for locomotion to assess motor function, and the Morris Water Maze (MWM) to assess learning and memory abilities. We performed behavioral tests (see Figure 17 for the experimental design) under the supervision of an experienced collaborator, Dr. George Wagner and his research group in the Department of Psychology at Rutgers University.

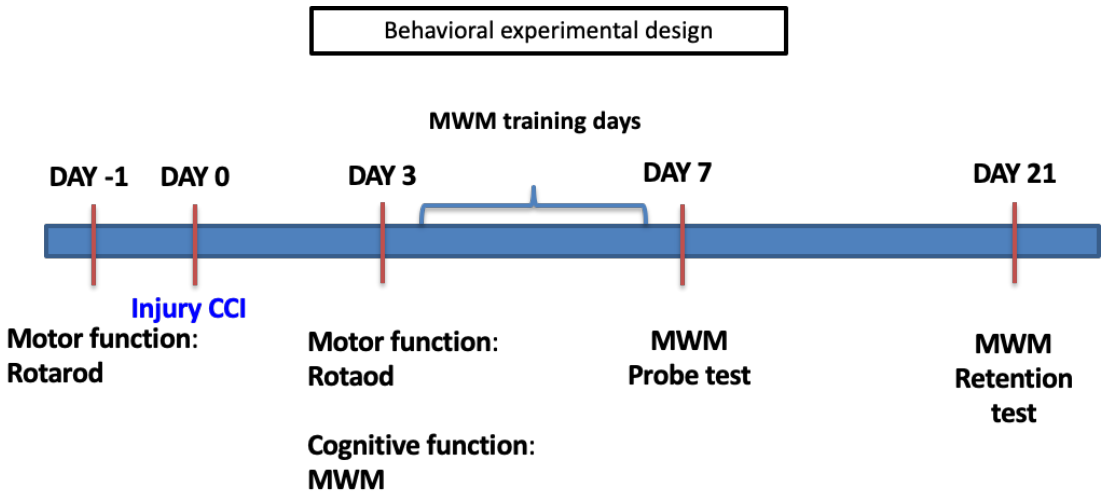

Figure 17. Timeline of the behavioral testes.

CCI is inflicted on day 0. To test for motor function the rotarod test is performed 1 day before (baseline) and 3 days after the injury (3 trials, 60s each). Morris water maze (MWM) is used to assess cognitive functions. The training period starts 3 days after injury and lasts for 4 consecutive days (5 trials, 60s each). A probe test is conducted 1 day after the end of the learning period (7 days after injury), and a memory retention test is conducted after 14 additional days (21 days after CCI).

A first pilot experiment was conducted using CD-1 mice that were 2 month-old. Groups were as follows: completely naïve mice (n=3); naïve-iso, (n=4) (control mice subjected to 5 minutes of isoflurane anesthetic similar to that used during the CCI and sham surgery); sham (n=4) (craniectomy surgery only but no cortical impact); CCI mice (n=4). The rotarod test was performed one day before the surgery to set up a baseline and to get the mice familiar with the apparatus; we used 3 trials, 60 seconds each, at the 12

RPM speed. The rotarod was used again 3 days after injury to see whether CCI or other control conditions caused a locomotion deficit. Surprisingly, the CCI mice did not show any locomotion deficit (Figure 18). One possible explanation for this result is that the rotarod parameters were not optimal; alternatively, it is possible that locomotion was not affected because we delivered the injury to the somatosensory cortical area, a brain region that does not primarily affect motor control.

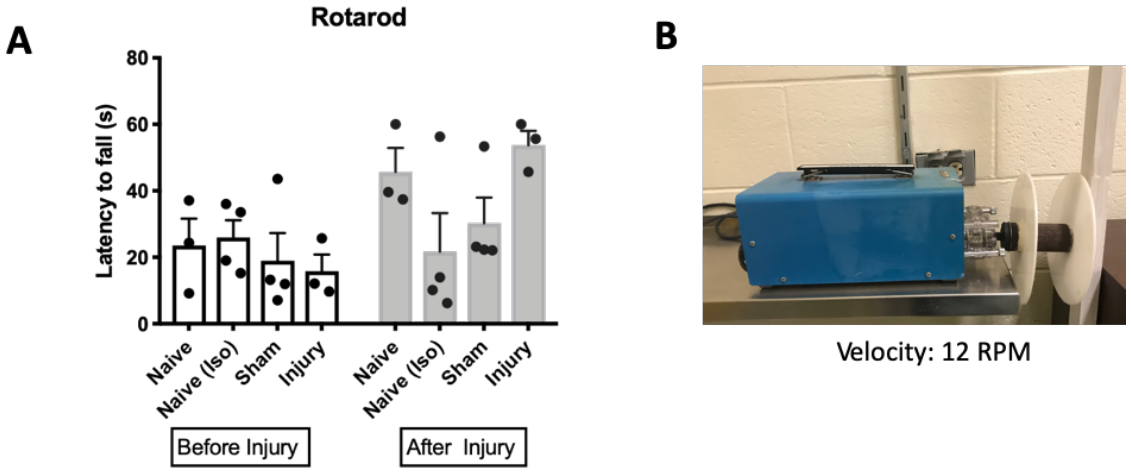

Figure 18. No motor function defect after CCI injury.

To test for motor function, the rotarod test was performed on 2 month-old wild type mice one day before injury (baseline) and 3 days after injury (3 trials/60s each). Groups consist of *n*=3-4 mice/each: **Naïve**, **Naïve (Iso)** (control mice exposed to 5 minutes of isoflurane anesthetic), **Sham**, and **Injury** (CCI). The latency to fall off the rotating rod was recorded (in seconds). (**A**) The scatter plot shows the quantification of the data from

a single experiment; each dot represents the average latency from 3 trials in each mouse, and the error bars show the mean values of each group (+/- SEM). No group shows any deficit in locomotion after injury compared to baseline values. (**B**) The image shows the rotarod apparatus used for this analysis (12 RPM speed for each trial).

The same mice were used for the Morris Water Maze (MWM) test using a small swimming pool (~70 cm in diameter) containing an elevated platform. On day3, after the surgery, the mice were subject to a training period for 4 consecutive days, involving 5 trials of 60 seconds each. During the training period, the mice are supposed to learn in which quadrant of the pool the platform is located. The mice were released inside the pool facing the edge of the pool; visual clues were placed around the pool to provide spatial information to help them locate the platform. The CCI mice performed consistently poorly for all 4 days of the training period compared to all control groups (naïve, naïve-iso and sham), which performed very similarly and learned the location of the platform somewhat on the first day (Figure 19, A and B). However, controls mice did not show a definite learning curve (improvement) during the training period, indicating that the experimental set up was not optimal. A probe test in which the platform was removed to assess whether mice remembered the location of the platform was performed on the 5th day. The ANY-maze software was used to measure the time that the mice spent in the quadrant were the platform used to be during the training period (target quadrant). The injury mice spent significantly less time in the target quadrant compared to the naïve (iso) controls (Figure 19, C). Other control groups also appeared to perform better than CCI mice, suggesting that the brain injury disrupted the mice learning and memory.

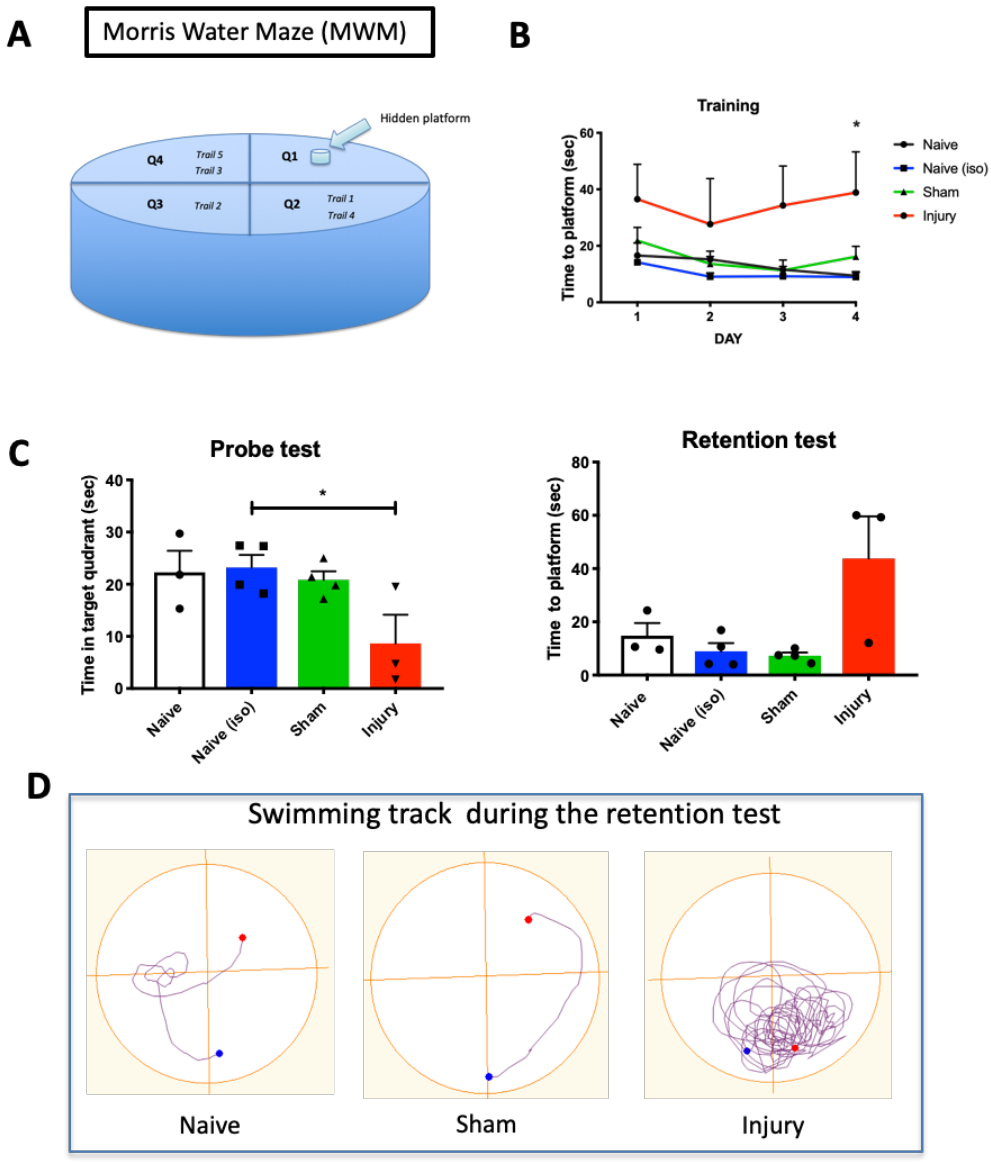

Figure 19. Cognitive defects detected after CCI using the MWM test.

(A) Schematic representation of the swimming pool used for the Morris Water Maze (MWM) test. A small pool (~ 70 cm in diameter) is divided in four equal quadrants (Q1-4). One of the quadrant contains a hidden platform, placed about 1cm below the water surface. Tempera is added to the water to render it opaque. The test is designed to test

spatial acquisition and long-term memory by recording the latency time required for each mouse to reach the hidden platform. The acquisition time is a training period (lasting 4 days) during which the platform is hidden, and the mice learn where it is located in 5 trials per day. **(B)** Quantification of the learning curve for each indicated group during the training period. The values represent the mean latency time (± SEM) to reach the platform. Mice were CD1 WT, 2 month- old (female and male). All groups did not improve significantly during the training period. However, injury mice, n=4 (in red) exhibited a longer latency compared to all control mice (naïve, n=3; naïve (iso), n=4; and sham, n=4). **(C)** Quantification of the probe and retention tests. For the probe test the platform was removed and the mean (± SEM) time spent in the quadrant in which the platform was located during the training days was measured. The injury mice spent significantly less time in the correct quadrant compared to the naïve (iso) controls. For the retention test (performed 14 days after the probe test) the platform was placed back in the pool and the mean (± SEM) time to find the platform was measured. The injury mice required more time to find the platform compared to all controls, although the difference was not statistically significant. The panels in **(D)** show the swimming track of individual representative mice during the retention test obtained with ANY-maze tracking software. Naïve and Sham mice reach the platform in a shorter time compared to injury mice. Statistical analysis. For training data: repeated measures (RM) 2-way ANOVA with Turkey's multiple comparison, *$p<0.05$ (Injury vs Naïve or Naïve (iso)). For the probe test: ordinary one-way ANOVA with Turkey multiple comparison. All groups were compared to each other, *$p<0.05$ (Injury vs Naïve (Iso)). For the retention test: Kruskal-Wallis test with Dunn's multiple comparison.

A memory retention test was also performed 7 days after the probe test. For this test the platform was added back and hidden in the same quadrant as for the training period. The test tracks the latency time that the mice take to reach the platform. Injury mice took longer to find the platform compared to the controls, although considerable subject variation was present (Figure 19,C and D).

Because control mice did not show the expected learning curve during the acquisition time in this first pilot experiment, we decided to perform the MWM experiment again using a bigger pool with double diameter (~120 cm) (Figure 20, A), testing the same mice 21 days after injury.

This time, the control mice showed a learning curve by improving the latency time to find the platform every day from day 1 to day 4 of the training period. This indicated that the larger pool set up was more appropriate to the size of the adult mice than the original one. On the other hand, as in the first MWM experiment, the injury mice performed similarly for the entire duration of the training period (Figure 20, C), suggesting that the injury affects the acquisition of spatial memory for at least 3 weeks after the trauma. A probe test was conducted on these mice after removing the platform. Again, CCI mice on average performed worse than all control groups, although the difference was not statistically significant due to a larger subject variation.

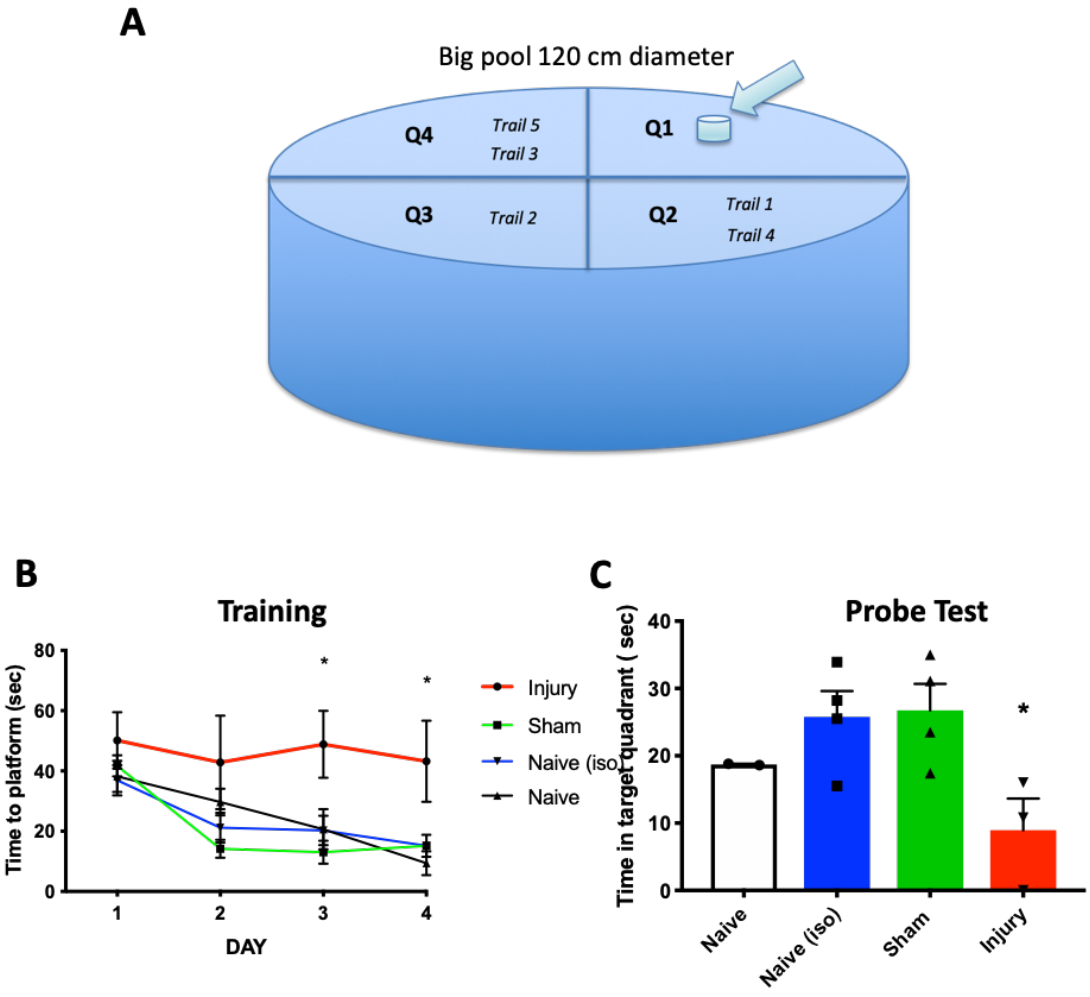

Figure 20. Repeated MWM experiment in a bigger swimming pool.

The MWM experiment in figure 16 was repeated using the same animal groups, but with a bigger pool (~120 cm diameter) (**A**). (**B**) Quantification of the data during the 4 days training period. The control mice, naïve n=3, naïve (iso) n=4, and sham n=4 showed an improvement in the latency time to find the platform compared to the first day of training (day 1). The injury mice n=4 did not improve during this learning phase, and performed very similarly each day, with a longer latency time to find the platform at day 3 and 4

compared to the control groups. **(C)** Quantification of the probe test. The injury mice show impaired learning and memory and spend less time in the quadrant with the platform compared to the controls. Statistical tests. For the Training data: mean ± SEM, RM 2-way ANOVA with Dunnett's multiple comparison test. Injury and Sham values were compared to Naïve (iso), *p<0.05 Injury vs Naïve(iso). For the probe test: ordinary one-way ANOVA with Dunnett's multiple comparison (Naïve group was excluded). Sham or Injury groups were compared to Naïve (iso) control. *p<0.05 Injury vs control.

Having optimized the experimental conditions, we conducted more behavioral tests with a second cohort of CCI and sham mice. The cohort again consisted of CD-1 mice (female and male, as previously), however this time the mice were younger (1 month-old). Groups were: naïve (n=4); sham (n=4); CCI (n=4). The rotarod test was performed as above prior to the injury, then again one day and 3 days after the injury, except that we used a different equipment and different experimental conditions in an effort to reveal possible motor defects that had previously gone undetected. The test consisted of 3 trials with auto accelerator from 4 RPM to 40 RPM for 5 minutes. The result confirmed that injury mice did not have any motor dysfunction and performed similar to the control mice (sham and naïve) (Figure 21, B).

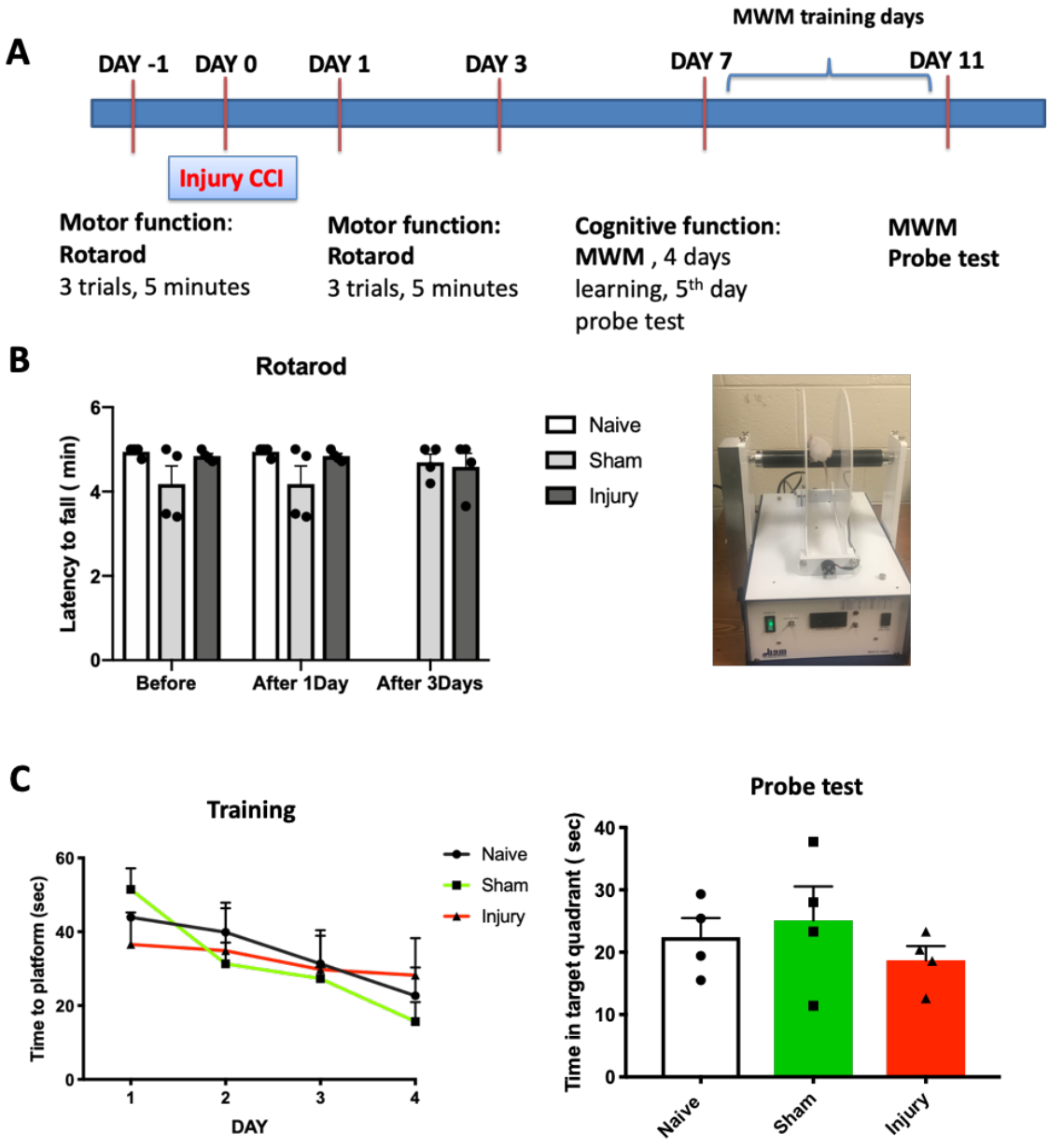

Figure 21. Normal behavioral performance in a one month-old CCI mouse cohort.

In **(A)** schematic representation of the experimental design used in the behavioral analysis of a one month-old CD-1 mouse cohort. Mice performed the rotarod test before injury (baseline), 1 day and 3 days after injury. The MWM training began 7 days after

injury (acquisition time). Probe test was conducted 1 day after the end of the training period, 11 days after injury. Naïve: n=4, sham: n=4, injury: n=4. The rotarod test does not show any motor dysfunction after the injury (**B**). The plot shows the mean latency time to fall ± SEM. (**C**), quantification for the MWM test. The training test and the probe test do not show any difference in learning and memory tasks between injury and controls. Statistical analysis: for the training test: mean ± SEM, repeated measurements 2 way ANOVA with Turkey's multiple comparison. For the probe test: mean ± SEM, ordinary one-way ANOVA with Turkey's multiple comparison.

To probe for spatial memory dysfunction in this young CCI cohort, we again conducted the MWM test in the bigger pool, using the same set up as for the previous experiment. Unexpectedly, we found that the injury mice performed similarly to the controls during the training period, learned the location of the platform and gradually improved up to day 4, similarly to controls. Also, in the probe test with the removed platform, the CCI mice performed very similarly to the controls (Figure 21, C). This result suggests that perhaps younger mice (2nd cohort) recover from the injury faster than older mice (1st cohort) possibly because they have more brain plasticity and can more efficiently re-build neuronal circuits in the damaged brain. Indeed, a visual inspection of the whole brain dissected from the 2nd mouse cohort used for behavioral analysis suggests that the brain tissue heals faster in younger mice (Figure 22).

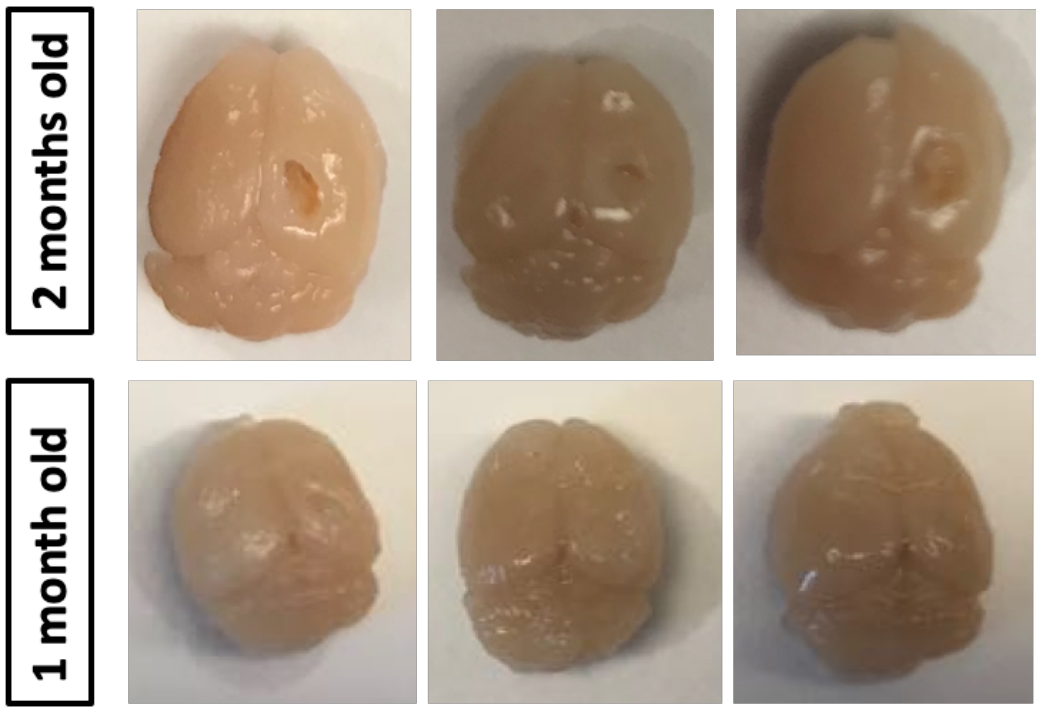

Figure 22. One month-old mice recovery faster from CCI than older mice.

Representative pictures of the whole brain of mice injured at 2 months (top) or 1 month (bottom) of age. All mice were subjected to the same CCI injury and behavioral tests. By macroscopic tissue's examination, it seems that the injury heals better in younger mice.

Given the conflicting results obtained with the 2 cohorts of mice analyzed, we could not conclusively determine whether or not CCI results in behavioral abnormalities. Unfortunately, due to technical difficulties and time limitations, we were not able to perform additional behavior experiments and resolve this issue; thus we did not pursue the initially proposed studies with the cKO mice to determine if the lack of Reelin affects functional recovery after injury.

Reelin protecs hippocampal neurons from glutamate excitotoxicity in vitro

In addition to the initial mechanical insult, TBI causes a secondary cascade of chemical insults that take place in neighboring cells or even in cells further away from the initial site of injury (Kwak & Nakamura, 1995). One of the best-known secondary effects of TBI is the transient increase in excitatory amino acids, such as glutamate, which causes widespread excitotoxic cells death. To determine whether Reelin can protect brain cells from glutamate excitotoxicity we conducted a set of *in vitro* experiments using cortical and hippocampal neuronal cultures that were treated with Reelin prior to glutamate exposure (see Figure 23 for experimental design). Two sources of recombinant Reelin were used in these experiments: conditioned medium and purified protein. Reelin conditioned medium was collected from a stably transfected cell line (CER) that was previously established in our laboratory (Niu et al., 2004). Mock medium from a parental cell line (EBNA) was used as a control. Purified Reelin was obtained as previously described and provided from our collaborator Dr. Davide Comoletti at Rutgers University- Robert Wood Johnson Medical School, Child Health Institute of New Jersey (Lee et al., 2014). Purification buffer was used as a control for this reagent. The quality of the Reelin reagents was verified by SDS-PAGE followed by Coomassie staining for the purified protein, or by Western blot for the conditioned medium (Figure 24, A and B). As expected, these reagents contain a mixture of full-length Reelin protein, as well as several proteolytic fragments. We collected hippocampal and cortical neurons from wild type CD-1 pregnant mice at embryonic stage E16, cultured hippocampal neurons for 10-13 days in vitro (DIV) and cortical neurons for 6 DIV in a serum-free medium (Figure 24).

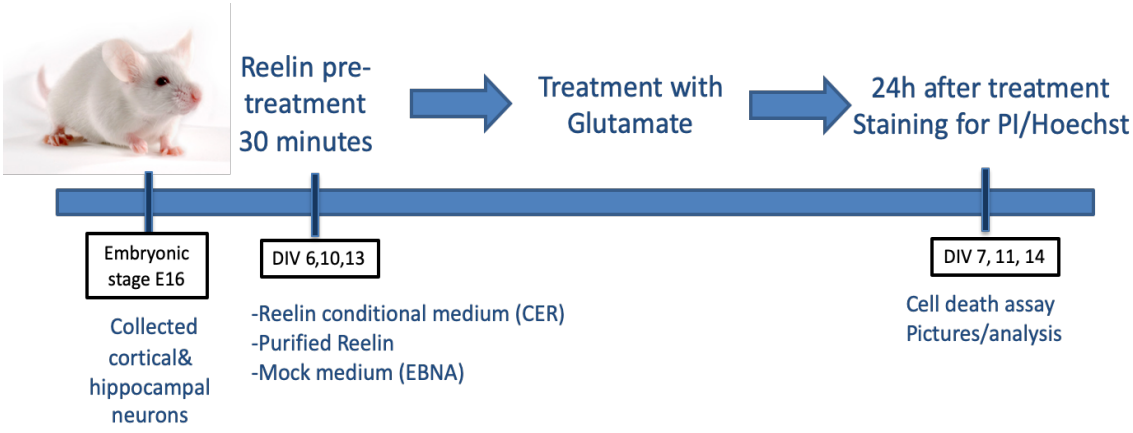

Figure 23. Schematic representation of the experimental design for glutamate neurotoxicity studies in vitro.

Cortical and hippocampal neurons are collected at the embryonic stage E16 from WT CD-1 mice. After several days in vitro (DIV) (DIV 6 for cortical neurons or DIV 10-13 for hippocampal neurons) the cells are pre-treated with Reelin conditional medium, purified Reelin protein or appropriate mock medium or buffer controls for 30 minutes, and then exposed to 30μM glutamate or buffer control overnight. 24h later, the cells are stained with Propidium iodide (PI, red fluorescent) to label dead cells, and Hoechst dye (blue fluorescent) to label all cell nuclei. The ratio of PI+/Hoechst+ cells is calculated to determine the fraction of dead cells in each treatment group.

Cultures were pretreated with purified Reelin or conditioned/mock medium for 30 min, and then exposed to 30 μM Glutamate overnight. We then performed a cell death assay involving staining the cultures with propidium iodide (PI, red fluorescent) to label

the nuclei of dead cells, and Hoechst stain (blue fluorescent) to label all nuclei, collected images from multiple random fields, and measured the fraction of cell death. For the hippocampal neurons the different conditions analyzed were: control untreated cells, glutamate alone, Reelin alone, glutamate plus Reelin, CER alone, CER with glutamate, EBNA (mock medium) alone, and EBNA plus glutamate. We performed two independent experiments with hippocampal neurons and analyzed 15-20 fields in n=4 wells for each condition in blind. In these two experiments, Reelin caused a significant reduction in cell death compared to the glutamate alone group (Figure 24, C), suggesting that Reelin protects hippocampal neurons from glutamate-induced excitotoxicity. This is an exciting and novel result and future experiments are planned to test whether Reelin treatment helps neurons retain their cell morphology, such as the complexity of dendritic branching measured by Scholl analysis, after glutamate exposure.

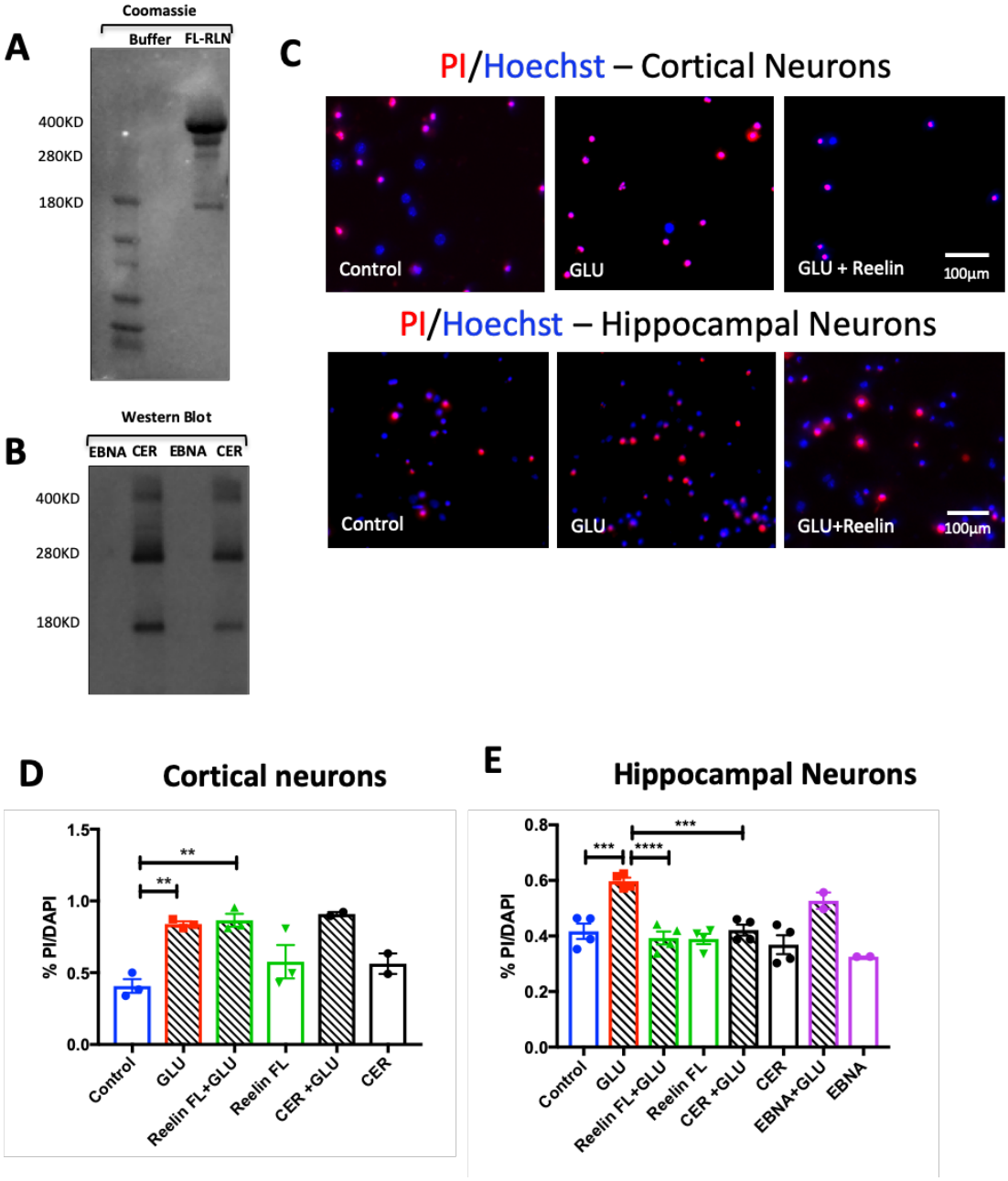

Figure 24. Reelin protects hippocampal neurons, but not cortical neurons, from glutamate-induce excitotoxicity.

(A) Coomassie staining of purified full-length (FL) Reelin protein analyzed by SDS-PAGE. The purification buffer was used as a negative control. FL Reelin consists of a

major high MW band (~400 kDa). Proteolytic fragments of lower MW are also detected. **(B)** Western blot analysis of conditioned medium from a stably-transfected cell line expressing FL Reelin (CER). FL Reelin plus proteolytic fragments are detected using the mouse monoclonal G10 antibody. Mock medium (EBNA) from a parental cell line was used as control. **(C)** Cortical neurons or hippocampal neurons were pretreated with 50 nM purified FL Reelin or Reelin conditioned medium (CER) for 30 minutes and then exposed to 30μM glutamate (GLU) overnight. The cells were stained 24h later with PI (red, dead nuclei) and Hoechst (blue, all nuclei). Representative images were randomly acquired using the INCell Analyzer 6000. **(D)** Quantitative analysis of DIV6 cortical neurons treated as indicated and imaged as above. The ratio of PI/Hoechst-positive nuclei in each condition was measured in blind from 5 fields/well and n=3 wells/group in 1 culture experiment. CER and CER+GLU groups contained only 2 measurements and were excluded from the analysis. GLU alone or GLU+Reelin caused a significant increase in cell death compared to control. Reelin alone (FL or CER) had no effect. Ordinary one-way ANOVA, **$p<0.01$. **(E)** Quantitative analysis of DIV9-13 hippocampal neurons treated and imaged as above. The ratio of PI/Hoechst-positive nuclei in each condition was measured in blind from 5 fields/well and n=4 wells/group in 2 independent culture experiments. EBNA alone and EBNA+GLU groups contained only 2 measurements and were excluded from the analysis. GLU alone caused a significant increase in cell death compared to control, but the addition Reelin in Reelin FL+GLU or CER+GLU resulted in cell death values that were significantly reduced compared to GLU alone. Reelin alone (FL or CER) had no effect. Ordinary one-way ANOVA, ***$p<0.001$, ****$p<0.0001$.

However, we did not see the same neuroprotection effect in cortical neurons. In the only experiment in which we were able to detect a significant increase in cell death due to Glutamate exposure, but Reelin treatment did not reduce cell death (Figure 24, D).

Together, these findings suggest that Reelin specifically protects hippocampal neurons from glutamate excitotoxicity. However, further experiments are necessary to confirm these data and to define the molecular mechanism that mediates Reelin-induced neuroprotection.

Chapter IV: Discussion

In this work, we investigated the potentially novel link between Reelin and TBI using *in vivo* mouse models of TBI to examine Reelin expression and behavior, and *in vitro* neuronal culture models to study the effect of Reelin on glutamate-induced excitotoxicity, a secondary effect of TBI. Our initial *in vivo* studies were conducted using the LFP model of TBI. However, due to the experimental variability we encountered, we later switched to the CCI model that is reported in the literature to generate more reproducible injuries (Schwulst & Islam, 2019; Kim et al., 2018; Osier & Dixon, 2016).

Our preliminary *in vivo* indirect immunofluorescence data with both the LFP and the CCI models appeared to show that Reelin expression was strongly induced in the ipsilateral cerebral cortex and hippocampus 1-3 days after TBI. This exciting result was in line with the data published by other groups, showing that Reelin was upregulated in two different lesion models: unilateral cortical ischemia and focal demyelination (Courtès et al., 2011). Reelin immunoreactivity was also reported to be increased in the mouse cornea and retina following ocular injury (Pulido et al., 2007). However, further control experiments demonstrated that the Reelin signal obtained with indirect fluorescence in the ipsilateral side of the injured brain was largely an artefact resulting from the secondary fluorophore-conjugated anti-mouse IgG antibodies used in our assays. This technical problem specifically affected the damaged, injured brain tissue (ipsilateral), and confounded the interpretation of our initial immunofluorescence results. Other groups previously reported cellular autofluorescence after TBI, and cautioned that this can hinder immunofluorescence analysis (Turtzo et al., 2015; Turtzo et al., 2013). In addition, intact

blood cells are known to be autofluorescent, and in fact, can be used to detect hemorrhages in postmortem studies (Cullen et al., 2005). Also, in hemorrhagic areas, clotted chromo-lipids called “hemoceroids” are ingested by macrophages that give out autofluorescence (Edelson et al., 1985). However, it seems unlikely that autofluorescence was responsible for the artifact we detected, since this was not observed when secondary anti-rabbit IgG antibodies were used. It appears that the artifact was specifically linked to the use of anti-mouse IgG antibodies in damaged brain tissue. It is conceivable that these secondary antibodies bind to endogenous immunoglobulin-like antigens expressed or exposed specifically in damaged brain cells. Because the only available Reelin antibodies reported to work in immunofluorescence assays were monoclonals produced in mouse, we were not initially able to circumvent this problem. Finally, a new reagent became commercially available that enabled us to perform direct, instead of indirect, immunofluorescence assays, avoiding the use of secondary anti-mouse IgG antibodies altogether. The same Reelin mouse monoclonal antibody (G10 clone) used in our previous assays was conjugated to the Alexa Fluor 488 fluorophore, and generated a strong and highly specific Reelin signal with virtually no background or artefactual signal even in damaged brain tissue.

The results of this improved direct immunofluorescence approach were surprising and showed that Reelin expression was either unaffected or decreased after TBI, contrary to our previous interpretation. Specifically, our direct immunofluorescence data demonstrated that the density of Reelin-positive cells was unaltered in the cerebral cortex at any time point examined, but it was reduced in the hippocampus at a late time point (7 days after TBI). These new results contradicted the initial hypothesis that the injury may

upregulate Reelin expression. The fact that other studies reported the upregulation of Reelin after ischemia and demyelination in the corpus callosum could be explained by differences in the injury model or brain region. Our findings that the number of Reelin-positive cells decrease in the hippocampus after CCI are consistent with a previous study that showed decreased Reelin protein levels after cerebral ischemia by Western blot analysis (Stary et al., 2015). Interestingly, this study also showed that ischemia causes the upregulation of the microRNA miR-200c, which targets and suppresses *Reelin* gene expression, suggesting that this could contribute to stroke-induced injury. Reelin was also shown to be targeted by miR27b-3p, a microRNA that is elevated in cerebrospinal fluid (CSF), blood and saliva of TBI patients (Atif & Hicks, 2019). These studies raise the intriguing possibility of targeting *Reelin*-suppressing microRNAs after TBI to prevent Reelin downregulation and improve clinical outcome.

Our immunofluorescence data revealed that brain injury causes a delayed loss of Reelin expression that specifically affects the hippocampus. These data are consistent with the literature, showing that GABAergic neurons are particularly susceptible to injury and become compromised by the increased glutamate excitability following TBI (Cantu et al., 2015; Nichols et al., 2018). One study reported that Calretinin-positive cells (a subpopulation of interneurons) exhibit reduced dendrite length 7 days post injury, concurrent with a reduction in the frequency of miniature inhibitory postsynaptic currents in layer V of the neocortex (Brizuela et al., 2017).

In the adult forebrain, Reelin is expressed mostly by inhibitory neurons (Alcantara et al., 1998; Gabriella D'Arcangelo, 2014). A previous study showed that the number of inhibitory neurons positive for parvalbumin and somatostatin decreases 2-4 weeks after

injury (Cantu et al., 2015). The results of our RT-qPCR are consistent with this finding and showed that *Reelin* and other inhibitory markers like *Gad1, Parvalbumin and Somatostatin* were unaltered 24h after TBI, but were significantly decreased in the injury side of the cortex and hippocampus 72h post-injury. Also, most inhibitory markers, including *Reelin,* were reduced in the injured cortex at this later time point. These data suggested that TBI results in a global deficit of inhibitory neurons, which may alter connectivity and function in both the cortex and hippocampus. Indeed, one study provided evidence that the loss of inhibitory neurons following TBI leads to hyperexcitability and epilepsy (Cantu et al., 2015). However, we found that the expression of the pan-neuronal marker *Map2* was also reduced 72h post-injury, suggesting that neuronal loss after TBI is not limited to interneurons. This widespread cell loss may relate to the activation of cells death mechanisms following the secondary effect of brain injury, namely glutamate excitotoxicity. Our novel finding that Reelin expression is reduced in the forebrain after injury suggests that this event may contribute to the cortical and hippocampal circuit dysfunction, leading to cognitive defects or memory loss after TBI. These observations also imply that recovery after TBI may be facilitated by molecules that can prevent Reelin downregulation or re-activate the Reelin signaling pathway.

Our *in vitro* data indicate that Reelin reduces glutamate-induced excitotoxicity in hippocampal neurons. We found that the addition of Reelin to the medium of cultured hippocampal neurons exposed to glutamate significantly suppressed cells death. However, the same effect was not found in cultured cortical neurons. Possible explanations for the discrepancy in our findings could be related to the age or the type of

culture, since we used older (DIV 10-13) hippocampal neurons and younger (DIV 6) cortical neurons. Reelin regulates the homeostasis of NMDAR in hippocampal neurons through SFK and Dab1 signaling (Chen et al., 2005). It is possible that these receptors mediate the neuroprotective effect of Reelin in older cultures, but may not be expressed at high levels in younger cultures. Alternatively, hippocampal neurons may express different signaling molecules that make them especially responsive to Reelin. The age of the cultures may also dictate which signaling events can be activated by Reelin. For example, although the Reelin canonical pathway (Dab1- and Akt-dependent) can be readily activated in young neurons at DIV 4-5, Reelin is known to also activate a non-canonical Erk-dependent pathway leading to increased gene expression of *c-Fos* and other immediate-early genes preferentially in mature cortical neurons (10-12 DIV) (Lee et al., 2014). Finally, it should be noted that our *in vitro* data are very preliminary, and is based only on 2 hippocampal cultures and 1 cortical neuron culture.

Further studies are necessary to confirm the findings and to identify the molecular mechanisms that mediate neuroprotection by Reelin.

In conclusion, based on our findings, we reason that Reelin may play an important role in restoring the function of forebrain neuronal networks after TBI, and reducing the extent of glutamate-induced cells death in the hippocampus. It would be interesting in the future to understand the mechanisms that lead to the decrease in *Reelin* expression and the loss of Reelin-positive cells in the hippocampus. Similarly, it would be interesting to understand how Reelin protects hippocampal neurons from excitotoxicity, and to investigate how the Reelin signaling could be exploited to facilitate functional recovery in TBI patients.

Future directions

In this study we were able to demonstrate that cognitive deficits are present in our CCI model at 2 months of age. These young adult mice exhibited spatial learning and memory deficits as assessed by the Morris Water Maze (MWM) test up to 3 weeks after injury. However, we were not able to reproduce these findings in a younger cohort (1 month-old). It is presently unclear whether this is simply the result of experimental variability, or whether our CCI paradigm is not sufficient to induce significant cognitive abnormalities in the juvenile brain, which may be more plastic and recover more readily from injury than the adult brain.

Although Reelin overexpression in the adult brain is known to induce hypertrophic dendritic spines in the hippocampus (Pulido et al., 2007) and hippocampal slices treated with Reelin show increased LTP (Weber et al., 2001), it is presently unclear if Reelin actually promotes functional recovery after TBI. We were not able in this study to address this point due to space and time limitations. However, future experiments involving the injection of purified Reelin (provided by our collaborator Dr. Davide Comoletti), stereotaxically in the brain just before CCI could be conducted to determine if this protein improves the mice performance in behavioral tests. A complementary approach to study the role of Reelin in functional recovery would be to use adult-specific inducible Reelin mutant mice that exhibit completely loss of Reelin in the brain after tamoxifen injection (Lane-Donovan et al., 2015). Because these mice do not exhibit brain structural abnormalities or behavioral deficits, it should be possible to determine whether they perform better or worse (as we hypothesize) than wild type mice in behavioral tasks.

In addition to behavioral analysis, future experiments could address the specific role of Reelin in reducing cell death or alleviating the neuroinflammation resulting from TBI. Cell death could be assayed in wild type mice after Reelin injection, or in Reelin cKO, by immunofluorescence with markers such as Caspase 3. Neuroinflammation could be analyzed by immunofluorescence or by RT-qPCR analysis of *GFAP* and *CXCL10* mRNA levels, which are strongly induced by CCI as we have already shown in this study.

Reelin is crucial for neuronal migration during brain development, and the Dab1-dependent canonical signaling pathway is essential for this function (Honda & Nakajima, 2016). A recent study showed that Reelin canonical signaling also critically controls the migration of neural stem/progenitor cells (NSPCs) transplanted in the adult motor cortex after cryogenic injury, and the functional recovery of hemiplegic mice (Arimitsu et al., 2019). The effect is entirely dependent of Dab1 signaling since *yotari* (Dab1-mutants) NSPCs failed to migrate into the cortex and contribute to functional recovery.

These findings raise the exciting possibility that Reelin signaling may be exploited in the future to aid stem cells therapy as a possible approach for treating TBI patients

Bibliography

Adelson, P. D., Fellows-Mayle, W., Kochanek, P. M. & Dixon, C. E. (2013). Morris water maze function and histologic characterization of two age-at-injury experimental models of controlled cortical impact in the immature rat. *Childs Nerv Syst, 29*(1), 43-53. doi:10.1007/s00381-012-1932-4

Alcantara, S., Ruiz, M., D'Arcangelo, G., Ezan, F., de Lecea, L., Curran, T., . . . Soriano, E. (1998). Regional and cellular patterns of reelin mRNA expression in the forebrain of the developing and adult mouse. *J Neurosci, 18*(19), 7779-7799.

Alder, J., Fujioka, W., Lifshitz, J., Crockett, D. P. & Thakker-Varia, S. (2011). Lateral fluid percussion: model of traumatic brain injury in mice. *J Vis Exp*(54). doi:10.3791/3063

Arimitsu, N., Takai, K., Fujiwara, N., Shimizu, J., Ueda, Y., Wakisaka, S., . . . Suzuki, N. (2019). Roles of Reelin/Disabled1 pathway on functional recovery of hemiplegic mice after neural cell transplantation; Reelin promotes migration toward motor cortex and maturation to motoneurons of neural grafts. *Exp Neurol, 320*, 112970. doi:10.1016/j.expneurol.2019.112970

Atif, H. & Hicks, S. D. (2019). A Review of MicroRNA Biomarkers in Traumatic Brain Injury. *J Exp Neurosci, 13*, 1179069519832286. doi:10.1177/1179069519832286

Bajwa, N. M., Halavi, S., Hamer, M., Semple, B. D., Noble-Haeusslein, L. J., Baghchechi, M., . . . Obenaus, A. (2016). Mild Concussion, but Not Moderate Traumatic Brain Injury, Is Associated with Long-Term Depression-Like Phenotype in Mice. *PLoS One, 11*(1), e0146886. doi:10.1371/journal.pone.0146886

Bao, S., Ouyang, G., Bai, X., Huang, Z., Ma, C., Liu, M., . . . Wang, X. F. (2004). Periostin potently promotes metastatic growth of colon cancer by augmenting cell survival via the Akt/PKB pathway. *Cancer Cell, 5*(4), 329-339.

Barrett, E. C., McBurney, M. I. & Ciappio, E. D. (2014). omega-3 fatty acid supplementation as a potential therapeutic aid for the recovery from mild traumatic brain injury/concussion. *Adv Nutr, 5*(3), 268-277. doi:10.3945/an.113.005280

Blennow, K., Brody, D. L., Kochanek, P. M., Levin, H., McKee, A., Ribbers, G. M., . . . Zetterberg, H. (2016). Traumatic brain injuries. *Nat Rev Dis Primers, 2*, 16084. doi:10.1038/nrdp.2016.84

Borrell, V., Del Rio, J. A., Alcantara, S., Derer, M., Martinez, A., D'Arcangelo, G., . . . Soriano, E. (1999). Reelin regulates the development and synaptogenesis of the layer-specific entorhino-hippocampal connections. *J Neurosci, 19*(4), 1345-1358.

Bosch, C., Masachs, N., Exposito-Alonso, D., Martinez, A., Teixeira, C. M., Fernaud, I., . . . Soriano, E. (2016). Reelin Regulates the Maturation of Dendritic Spines, Synaptogenesis and Glial Ensheathment of Newborn Granule Cells. *Cereb Cortex, 26*(11), 4282-4298. doi:10.1093/cercor/bhw216

Brizuela, M., Blizzard, C. A., Chuckowree, J. A., Pitman, K. A., Young, K. M. & Dickson, T. (2017). Mild Traumatic Brain Injury Leads to Decreased Inhibition and a Differential Response of Calretinin Positive Interneurons in the Injured Cortex. *J Neurotrauma, 34*(17), 2504-2517. doi:10.1089/neu.2017.4977

Burda, J. E., Bernstein, A. M. & Sofroniew, M. V. (2016). Astrocyte roles in traumatic brain injury. *Exp Neurol, 275 Pt 3*, 305-315. doi:10.1016/j.expneurol.2015.03.020

Cantu, D., Walker, K., Andresen, L., Taylor-Weiner, A., Hampton, D., Tesco, G. & Dulla, C. G. (2015). Traumatic Brain Injury Increases Cortical Glutamate Network Activity by Compromising GABAergic Control. *Cereb Cortex, 25*(8), 2306-2320. doi:10.1093/cercor/bhu041

Cater, H. L., Gitterman, D., Davis, S. M., Benham, C. D., Morrison, B., 3rd & Sundstrom, L. E. (2007). Stretch-induced injury in organotypic hippocampal slice cultures reproduces in vivo post-traumatic neurodegeneration: role of glutamate receptors and voltage-dependent calcium channels. *J Neurochem, 101*(2), 434-447. doi:10.1111/j.1471-4159.2006.04379.x

Chai, X. & Frotscher, M. (2016). How does Reelin signaling regulate the neuronal cytoskeleton during migration? *Neurogenesis (Austin), 3*(1), e1242455. doi:10.1080/23262133.2016.1242455

Chang, E. H., Adorjan, I., Mundim, M. V., Sun, B., Dizon, M. L. V. & Szele, F. G. (2016). Traumatic Brain Injury Activation of the Adult Subventricular Zone Neurogenic Niche. *Frontiers in Neuroscience, 10*(332). doi:10.3389/fnins.2016.00332

Chen, Y., Beffert, U., Ertunc, M., Tang, T.-S., Kavalali, E. T., Bezprozvanny, I. & Herz, J. (2005). Reelin Modulates NMDA Receptor Activity in Cortical Neurons. *The Journal of Neuroscience, 25*(36), 8209-8216. doi:10.1523/jneurosci.1951-05.2005

Chen, Y., Mao, H., Yang, K. H., Abel, T. & Meaney, D. F. (2014). A modified controlled cortical impact technique to model mild traumatic brain injury mechanics in mice. *Front Neurol, 5*, 100. doi:10.3389/fneur.2014.00100

Chirumamilla, S., Sun, D., Bullock, M. R. & Colello, R. J. (2002). Traumatic brain injury induced cell proliferation in the adult mammalian central nervous system. *J Neurotrauma, 19*(6), 693-703. doi:10.1089/08977150260139084

Chuang, T. J., Lin, K. C., Chio, C. C., Wang, C. C., Chang, C. P. & Kuo, J. R. (2012). Effects of secretome obtained from normoxia-preconditioned human mesenchymal stem cells in traumatic brain injury rats. *J Trauma Acute Care Surg, 73*(5), 1161-1167. doi:10.1097/TA.0b013e318265d128

Clinical trial of nimodipine in acute ischemic stroke. The American Nimodipine Study Group. (1992). *Stroke, 23*(1), 3-8. doi:10.1161/01.str.23.1.3

Córdoba-Chacón, J., Gahete, M. D., Castaño, J. P., Kineman, R. D. & Luque, R. M. (2011). Somatostatin and its receptors contribute in a tissue-specific manner to the sex-dependent metabolic (fed/fasting) control of growth hormone axis in mice. *American Journal of Physiology-Endocrinology and Metabolism, 300*(1), E46-E54. doi:10.1152/ajpendo.00514.2010

Coronado, V. G., McGuire, L. C., Sarmiento, K., Bell, J., Lionbarger, M. R., Jones, C. D., . . . Xu, L. (2012). Trends in Traumatic Brain Injury in the U.S. and the public health response: 1995-2009. *J Safety Res, 43*(4), 299-307. doi:10.1016/j.jsr.2012.08.011

Courtès, S., Vernerey, J., Pujadas, L., Magalon, K., Cremer, H., Soriano, E., . . . Cayre, M. (2011). Reelin controls progenitor cell migration in the healthy and pathological adult mouse brain. *PLoS One, 6*(5), e20430. doi:10.1371/journal.pone.0020430

Crane, P. K., Gibbons, L. E., Dams-O'Connor, K., Trittschuh, E., Leverenz, J. B., Keene, C. D., . . . Larson, E. B. (2016). Association of Traumatic Brain Injury With Late-Life Neurodegenerative Conditions and Neuropathologic Findings. *JAMA Neurol, 73*(9), 1062-1069. doi:10.1001/jamaneurol.2016.1948

Cullen, K. M., Kocsi, Z. & Stone, J. (2005). Pericapillary haem-rich deposits: evidence for microhaemorrhages in aging human cerebral cortex. *J Cereb Blood Flow Metab, 25*(12), 1656-1667. doi:10.1038/sj.jcbfm.9600155

D'Arcangelo, G. (2014). Reelin in the Years: Controlling Neuronal Migration and Maturation in the Mammalian Brain %J Advances in Neuroscience. *2014*, 19. doi:10.1155/2014/597395

D'Arcangelo, G., Homayouni, R., Keshvara, L., Rice, D. S., Sheldon, M. & Curran, T. (1999). Reelin is a ligand for lipoprotein receptors. *Neuron, 24*(2), 471-479.

D'Arcangelo, G., Miao, G. G., Chen, S. C., Soares, H. D., Morgan, J. I. & Curran, T. (1995). A protein related to extracellular matrix proteins deleted in the mouse mutant reeler. *Nature, 374*(6524), 719-723. doi:10.1038/374719a0

D'Arcangelo, G., Nakajima, K., Miyata, T., Ogawa, M., Mikoshiba, K. & Curran, T. (1997). Reelin is a secreted glycoprotein recognized by the CR-50 monoclonal antibody. *J Neurosci, 17*(1), 23-31.

Datta, S. R., Dudek, H., Tao, X., Masters, S., Fu, H., Gotoh, Y. & Greenberg, M. E. (1997). Akt phosphorylation of BAD couples survival signals to the cell-intrinsic death machinery. *Cell, 91*(2), 231-241. doi:10.1016/s0092-8674(00)80405-5

de Bergeyck, V., Naerhuyzen, B., Goffinet, A. M. & Lambert de Rouvroit, C. (1998). A panel of monoclonal antibodies against reelin, the extracellular matrix protein defective in reeler mutant mice. *J Neurosci Methods, 82*(1), 17-24.

de Bergeyck, V., Nakajima, K., Lambert de Rouvroit, C., Naerhuyzen, B., Goffinet, A. M., Miyata, T., . . . Mikoshiba, K. (1997). A truncated Reelin protein is produced but not secreted in the 'Orleans' reeler mutation (Reln[rl-Orl]). *Brain Res Mol Brain Res, 50*(1-2), 85-90.

DeGrauw, X., Thurman, D., Xu, L., Kancherla, V. & DeGrauw, T. (2018). Epidemiology of traumatic brain injury-associated epilepsy and early use of anti-epilepsy drugs: An analysis of insurance claims data, 2004-2014. *Epilepsy Res, 146*, 41-49. doi:10.1016/j.eplepsyres.2018.07.012

Dekmak, A., Mantash, S., Shaito, A., Toutonji, A., Ramadan, N., Ghazale, H., . . . Zibara, K. (2018). Stem cells and combination therapy for the treatment of traumatic brain injury. *Behav Brain Res, 340*, 49-62. doi:10.1016/j.bbr.2016.12.039

Dixon, C. E., Kochanek, P. M., Yan, H. Q., Schiding, J. K., Griffith, R. G., Baum, E., . . . DeKosky, S. T. (1999). One-year study of spatial memory performance, brain morphology, and cholinergic markers after moderate controlled cortical impact in rats. *J Neurotrauma, 16*(2), 109-122. doi:10.1089/neu.1999.16.109

Donat, C. K., Scott, G., Gentleman, S. M. & Sastre, M. (2017). Microglial Activation in Traumatic Brain Injury. *Front Aging Neurosci, 9*, 208. doi:10.3389/fnagi.2017.00208

Dunkerson, J., Moritz, K. E., Young, J., Pionk, T., Fink, K., Rossignol, J., . . . Smith, J. S. (2014). Combining enriched environment and induced pluripotent stem cell therapy results in improved cognitive and motor function following traumatic brain injury. *Restor Neurol Neurosci, 32*(5), 675-687. doi:10.3233/rnn-140408

Edelson, J. D., MacFadden, D. K., Klein, M. & Rebuck, A. S. (1985). Autofluorescence of alveolar macrophages: problems and potential solutions. *Med Hypotheses, 17*(4), 403-407.

Edwards Iii, G. A., Zhao, J., Dash, P. K., Soto, C. & Moreno-Gonzalez, I. (2019). Traumatic brain injury induces tau aggregation and spreading. *J Neurotrauma*. doi:10.1089/neu.2018.6348

Eme, R. (2017). Neurobehavioral Outcomes of Mild Traumatic Brain Injury: A Mini Review. *Brain Sci, 7*(5). doi:10.3390/brainsci7050046

Espinoza, T. R. & Wright, D. W. (2011). The role of progesterone in traumatic brain injury. *J Head Trauma Rehabil, 26*(6), 497-499. doi:10.1097/HTR.0b013e31823088fa

Falconer, D. S. (1951). Two new mutants, 'trembler' and 'reeler', with neurological actions in the house mouse (Mus musculus L.). *J Genet, 50*(2), 192-201.

Fatemi, S. H., Snow, A. V., Stary, J. M., Araghi-Niknam, M., Reutiman, T. J., Lee, S., . . . Pearce, D. A. (2005). Reelin signaling is impaired in autism. *Biol Psychiatry, 57*(7), 777-787. doi:10.1016/j.biopsych.2004.12.018

Fatemi, S. H., Stary, J. M., Halt, A. R. & Realmuto, G. R. (2001). Dysregulation of Reelin and Bcl-2 proteins in autistic cerebellum. *J Autism Dev Disord, 31*(6), 529-535.

Faul M, X. L., Wald MM, Coronado VG. (2010). Traumatic Brain Injury in the United States: Emergency Department Visits, Hospitalizations and Deaths 2002-2006. *Atlanta (GA): Center for Disease Control and Prevention, National Center for Injury Prevention and Control*.

Fedor, M., Berman, R. F., Muizelaar, J. P. & Lyeth, B. G. (2010). Hippocampal theta dysfunction after lateral fluid percussion injury. *J Neurotrauma, 27*(9), 1605-1615. doi:10.1089/neu.2010.1370

Feeney, D. M., Boyeson, M. G., Linn, R. T., Murray, H. M. & Dail, W. G. (1981). Responses to cortical injury: I. Methodology and local effects of contusions in the rat. *Brain Res, 211*(1), 67-77. doi:10.1016/0006-8993(81)90067-6

Fesharaki-Zadeh, A. (2019). Chronic Traumatic Encephalopathy: A Brief Overview. *Front Neurol, 10*, 713. doi:10.3389/fneur.2019.00713

Filice, F., Vörckel, K. J., Sungur, A. Ö., Wöhr, M. & Schwaller, B. (2016). Reduction in parvalbumin expression not loss of the parvalbumin-expressing GABA interneuron subpopulation in genetic parvalbumin and shank mouse models of autism. *Molecular Brain, 9*(1), 10. doi:10.1186/s13041-016-0192-8

Fox, G. B., Fan, L., LeVasseur, R. A. & Faden, A. I. (1998). Effect of traumatic brain injury on mouse spatial and nonspatial learning in the Barnes circular maze. *J Neurotrauma, 15*(12), 1037-1046. doi:10.1089/neu.1998.15.1037

Frotscher, M. (2010). Role for Reelin in stabilizing cortical architecture. *Trends Neurosci, 33*(9), 407-414. doi:10.1016/j.tins.2010.06.001

Gage, F. H., Kempermann, G., Palmer, T. D., Peterson, D. A. & Ray, J. (1998). Multipotent progenitor cells in the adult dentate gyrus. *J Neurobiol, 36*(2), 249-266.

Gao, X., Wang, X., Xiong, W. & Chen, J. (2016). In vivo reprogramming reactive glia into iPSCs to produce new neurons in the cortex following traumatic brain injury. *Scientific Reports, 6*, 22490. doi:10.1038/srep22490

Gardner, R. C., Burke, J. F., Nettiksimmons, J., Goldman, S., Tanner, C. M. & Yaffe, K. (2015). Traumatic brain injury in later life increases risk for Parkinson disease. *Ann Neurol, 77*(6), 987-995. doi:10.1002/ana.24396

Gentleman, S. M., Leclercq, P. D., Moyes, L., Graham, D. I., Smith, C., Griffin, W. S. & Nicoll, J. A. (2004). Long-term intracerebral inflammatory response after traumatic brain injury. *Forensic Sci Int, 146*(2-3), 97-104. doi:10.1016/j.forsciint.2004.06.027

Gentleman, S. M., Nash, M. J., Sweeting, C. J., Graham, D. I. & Roberts, G. W. (1993). Beta-amyloid precursor protein (beta APP) as a marker for axonal injury after head injury. *Neurosci Lett, 160*(2), 139-144. doi:10.1016/0304-3940(93)90398-5

Goldstein, L. E., Fisher, A. M., Tagge, C. A., Zhang, X. L., Velisek, L., Sullivan, J. A., . . . McKee, A. C. (2012). Chronic traumatic encephalopathy in blast-exposed military veterans and a blast neurotrauma mouse model. *Sci Transl Med, 4*(134), 134ra160. doi:10.1126/scitranslmed.3003716

Gong, C., Wang, T. W., Huang, H. S. & Parent, J. M. (2007). Reelin regulates neuronal progenitor migration in intact and epileptic hippocampus. *J Neurosci, 27*(8), 1803-1811. doi:10.1523/jneurosci.3111-06.2007

Guidotti, A., Grayson, D. R. & Caruncho, H. J. (2016). Epigenetic RELN Dysfunction in Schizophrenia and Related Neuropsychiatric Disorders. *Front Cell Neurosci, 10*, 89. doi:10.3389/fncel.2016.00089

Gultekin, R., Huang, S., Clavisi, O., Pattuwage, L., Konig, T. C. & Gruen, R. (2016). Pharmacological interventions in traumatic brain injury: Can we rely on systematic reviews for evidence? *Injury, 47*(3), 516-524. doi:10.1016/j.injury.2015.10.011

Hall, E. D., Sullivan, P. G., Gibson, T. R., Pavel, K. M., Thompson, B. M. & Scheff, S. W. (2005). Spatial and temporal characteristics of neurodegeneration after controlled cortical impact in mice: more than a focal brain injury. *J Neurotrauma, 22*(2), 252-265. doi:10.1089/neu.2005.22.252

Hasan, A., Deeb, G., Rahal, R., Atwi, K., Mondello, S., Marei, H. E., . . . Sleiman, E. (2017). Mesenchymal Stem Cells in the Treatment of Traumatic Brain Injury. *Front Neurol, 8*, 28. doi:10.3389/fneur.2017.00028

Hatton, J., Rosbolt, B., Empey, P., Kryscio, R. & Young, B. (2008). Dosing and safety of cyclosporine in patients with severe brain injury. *J Neurosurg, 109*(4), 699-707. doi:10.3171/jns/2008/109/10/0699

Heinrich, C., Nitta, N., Flubacher, A., Müller, M., Fahrner, A., Kirsch, M., . . . Haas, C. A. (2006). Reelin Deficiency and Displacement of Mature Neurons, But Not Neurogenesis, Underlie the Formation of Granule Cell Dispersion in the Epileptic Hippocampus. *The Journal of Neuroscience, 26*(17), 4701-4713. doi:10.1523/jneurosci.5516-05.2006

Hethorn, W. R., Ciarlone, S. L., Filonova, I., Rogers, J. T., Aguirre, D., Ramirez, R. A., . . . Weeber, E. J. (2015). Reelin supplementation recovers synaptic plasticity and cognitive deficits in a mouse model for Angelman syndrome. *Eur J Neurosci, 41*(10), 1372-1380. doi:10.1111/ejn.12893

Hevner, R. F. (2008). Reelin and the Cerebellum. In S. H. Fatemi (Ed.), *Reelin Glycoprotein: Structure, Biology and Roles in Health and Disease* (pp. 141-158). New York, NY: Springer New York.

Hiebert, J. B., Shen, Q., Thimmesch, A. R. & Pierce, J. D. (2015). Traumatic brain injury and mitochondrial dysfunction. *Am J Med Sci, 350*(2), 132-138. doi:10.1097/maj.0000000000000506

Hiesberger, T., Trommsdorff, M., Howell, B. W., Goffinet, A., Mumby, M. C., Cooper, J. A. & Herz, J. (1999). Direct binding of Reelin to VLDL receptor and ApoE receptor 2 induces tyrosine phosphorylation of disabled-1 and modulates tau phosphorylation. *Neuron, 24*(2), 481-489.

Hinzman, J. M., Thomas, T. C., Burmeister, J. J., Quintero, J. E., Huettl, P., Pomerleau, F., . . . Lifshitz, J. (2010). Diffuse brain injury elevates tonic glutamate levels and potassium-evoked glutamate release in discrete brain regions at two days post-injury: an enzyme-based microelectrode array study. *J Neurotrauma, 27*(5), 889-899. doi:10.1089/neu.2009.1238

Honda, T. & Nakajima, K. (2016). Proper Level of Cytosolic Disabled-1, Which Is Regulated by Dual Nuclear Translocation Pathways, Is Important for Cortical Neuronal Migration. *Cereb Cortex, 26*(7), 3219-3236. doi:10.1093/cercor/bhv162

Hong, S. E., Shugart, Y. Y., Huang, D. T., Shahwan, S. A., Grant, P. E., Hourihane, J. O., . . . Walsh, C. A. (2000). Autosomal recessive lissencephaly with cerebellar hypoplasia is associated with human RELN mutations. *Nat Genet, 26*(1), 93-96. doi:10.1038/79246

Hossini, A. M., Quast, A. S., Plotz, M., Grauel, K., Exner, T., Kuchler, J., . . . Zouboulis, C. C. (2016). PI3K/AKT Signaling Pathway Is Essential for Survival of Induced Pluripotent Stem Cells. *PLoS One, 11*(5), e0154770. doi:10.1371/journal.pone.0154770

Howell, B. W., Hawkes, R., Soriano, P. & Cooper, J. A. (1997). Neuronal position in the developing brain is regulated by mouse disabled-1. *Nature, 389*(6652), 733-737. doi:10.1038/39607

Hu, Q., Manaenko, A., Xu, T., Guo, Z., Tang, J. & Zhang, J. H. (2016). Hyperbaric oxygen therapy for traumatic brain injury: bench-to-bedside. *Med Gas Res, 6*(2), 102-110. doi:10.4103/2045-9912.184720

Hue, C. D., Cho, F. S., Cao, S., Nicholls, R. E., Vogel Iii, E. W., Sibindi, C., . . . Morrison Iii, B. (2016). Time Course and Size of Blood-Brain Barrier Opening in a Mouse Model of Blast-Induced Traumatic Brain Injury. *J Neurotrauma, 33*(13), 1202-1211. doi:10.1089/neu.2015.4067

Humphreys, I., Wood, R. L., Phillips, C. J. & Macey, S. (2013). The costs of traumatic brain injury: a literature review. *Clinicoecon Outcomes Res, 5*, 281-287. doi:10.2147/ceor.S44625

Hyder, A. A., Wunderlich, C. A., Puvanachandra, P., Gururaj, G. & Kobusingye, O. C. (2007). The impact of traumatic brain injuries: a global perspective. *NeuroRehabilitation, 22*(5), 341-353.

Ikonomidou, C. & Turski, L. (2002). Why did NMDA receptor antagonists fail clinical trials for stroke and traumatic brain injury? *Lancet Neurol, 1*(6), 383-386.

Israelsson, C., Bengtsson, H., Lobell, A., Nilsson, L. N., Kylberg, A., Isaksson, M., . . . Ebendal, T. (2010). Appearance of Cxcl10-expressing cell clusters is common for traumatic brain injury and neurodegenerative disorders. *Eur J Neurosci, 31*(5), 852-863. doi:10.1111/j.1460-9568.2010.07105.x

Israelsson, C., Wang, Y., Kylberg, A., Pick, C. G., Hoffer, B. J. & Ebendal, T. (2009). Closed head injury in a mouse model results in molecular changes indicating inflammatory responses. *J Neurotrauma, 26*(8), 1307-1314. doi:10.1089/neu.2008-0676
10.1089/neu.2008.0676

Jassam, Y. N., Izzy, S., Whalen, M., McGavern, D. B. & El Khoury, J. (2017). Neuroimmunology of Traumatic Brain Injury: Time for a Paradigm Shift. *Neuron, 95*(6), 1246-1265. doi:10.1016/j.neuron.2017.07.010

Jiang, Y., Gavrilovici, C., Chansard, M., Liu, R. H., Kiroski, I., Parsons, K., . . . Nguyen, M. D. (2016). Ndel1 and Reelin Maintain Postnatal CA1 Hippocampus Integrity. *The Journal of Neuroscience, 36*(24), 6538-6552. doi:10.1523/jneurosci.2869-15.2016

Johnson, V. E., Stewart, W. & Smith, D. H. (2013). Axonal pathology in traumatic brain injury. *Exp Neurol, 246*, 35-43. doi:10.1016/j.expneurol.2012.01.013

Jones, K. J., Templet, S., Zemoura, K., Kuzniewska, B., Pena, F. X., Hwang, H., . . . Xu, W. (2018). Rapid, experience-dependent translation of neurogranin enables memory encoding. *Proceedings of the National Academy of Sciences, 115*(25), E5805-E5814. doi:10.1073/pnas.1716750115

Jorolemon MR, K. D. (2019). Blast Injuries *In: StatPearls [Internet]. Treasure Island (FL): StatPearls Publishing; 2019 Jan-. Available from: https://www.ncbi.nlm.nih.gov/books/NBK430914/*.

Jossin, Y., Gui, L. & Goffinet, A. M. (2007). Processing of Reelin by embryonic neurons is important for function in tissue but not in dissociated cultured neurons. *J Neurosci, 27*(16), 4243-4252. doi:10.1523/jneurosci.0023-07.2007

Jossin, Y., Ignatova, N., Hiesberger, T., Herz, J., Lambert de Rouvroit, C. & Goffinet, A. M. (2004). The central fragment of Reelin, generated by proteolytic processing in vivo, is critical to its function during cortical plate development. *J Neurosci, 24*(2), 514-521. doi:10.1523/jneurosci.3408-03.2004

Kalish, B. T. & Whalen, M. J. (2016). Weight Drop Models in Traumatic Brain Injury. *Methods Mol Biol, 1462*, 193-209. doi:10.1007/978-1-4939-3816-2_12

Karlsson, M., Pukenas, B., Chawla, S., Ehinger, J. K., Plyler, R., Stolow, M., . . . Kilbaugh, T. (2018). Neuroprotective Effects of Cyclosporine in a Porcine Pre-Clinical Trial of Focal Traumatic Brain Injury. *J Neurotrauma*. doi:10.1089/neu.2018.5706

Karve, I. P., Taylor, J. M. & Crack, P. J. (2016). The contribution of astrocytes and microglia to traumatic brain injury. *Br J Pharmacol, 173*(4), 692-702. doi:10.1111/bph.13125

Kim, M. J., Jo, D. G., Hong, G. S., Kim, B. J., Lai, M., Cho, D. H., . . . Jung, Y. K. (2002). Calpain-dependent cleavage of cain/cabin1 activates calcineurin to mediate calcium-triggered cell death. *Proc Natl Acad Sci U S A, 99*(15), 9870-9875. doi:10.1073/pnas.152336999

Kim, Y., Fu, A. H., Tucker, L. B., Liu, J. & McCabe, J. T. (2018). Characterization of controlled cortical impact devices by high-speed image analysis. *J Neurosci Res, 96*(4), 501-511. doi:10.1002/jnr.24099

Kinder, H. A., Baker, E. W. & West, F. D. (2019). The pig as a preclinical traumatic brain injury model: current models, functional outcome measures, and translational detection strategies. *Neural Regen Res, 14*(3), 413-424. doi:10.4103/1673-5374.245334

Kohno, T., Honda, T., Kubo, K.-i., Nakano, Y., Tsuchiya, A., Murakami, T., . . . Hattori, M. (2015). Importance of Reelin C-Terminal Region in the Development and Maintenance of the Postnatal Cerebral Cortex and Its Regulation by Specific Proteolysis. *The Journal of Neuroscience, 35*(11), 4776-4787. doi:10.1523/jneurosci.4119-14.2015

Kokiko-Cochran, O. N. & Godbout, J. P. (2018). The Inflammatory Continuum of Traumatic Brain Injury and Alzheimer's Disease. *Front Immunol, 9*, 672. doi:10.3389/fimmu.2018.00672

Kuo, G., Arnaud, L., Kronstad-O'Brien, P. & Cooper, J. A. (2005). Absence of Fyn and Src causes a reeler-like phenotype. *J Neurosci, 25*(37), 8578-8586. doi:10.1523/jneurosci.1656-05.2005

Kwak, S. & Nakamura, R. (1995). Acute and late neurotoxicity in the rat spinal cord in vivo induced by glutamate receptor agonists. *J Neurol Sci, 129 Suppl*, 99-103. doi:10.1016/0022-510x(95)00076-e

Lambert de Rouvroit, C., de Bergeyck, V., Cortvrindt, C., Bar, I., Eeckhout, Y. & Goffinet, A. M. (1999). Reelin, the extracellular matrix protein deficient in reeler mutant mice, is processed by a metalloproteinase. *Exp Neurol, 156*(1), 214-217. doi:10.1006/exnr.1998.7007

Lambert de Rouvroit, C. & Goffinet, A. M. (1998). The reeler mouse as a model of brain development. *Adv Anat Embryol Cell Biol, 150*, 1-106.

Lane-Donovan, C., Philips, G. T., Wasser, C. R., Durakoglugil, M. S., Masiulis, I., Upadhaya, A., . . . Herz, J. (2015). Reelin protects against amyloid beta toxicity in vivo. *Sci Signal, 8*(384), ra67. doi:10.1126/scisignal.aaa6674

Lee, G. H., Chhangawala, Z., von Daake, S., Savas, J. N., Yates, J. R., 3rd, Comoletti, D. & D'Arcangelo, G. (2014). Reelin induces Erk1/2 signaling in cortical neurons through a non-canonical pathway. *J Biol Chem, 289*(29), 20307-20317. doi:10.1074/jbc.M114.576249

Li, G., Fang, L., Fernandez, G. & Pleasure, S. J. (2013). The ventral hippocampus is the embryonic origin for adult neural stem cells in the dentate gyrus. *Neuron, 78*(4), 658-672. doi:10.1016/j.neuron.2013.03.019

Liu, S., Li, Z., Fu, J., Sun, L., Xu, F., Harada, T., . . . Wu, S. (2014). The effects of harvesting media on biological characteristics and repair potential of neural stem cells after traumatic brain injury. *PLoS One, 9*(9), e107865. doi:10.1371/journal.pone.0107865

Liu, W. S., Pesold, C., Rodriguez, M. A., Carboni, G., Auta, J., Lacor, P., . . . Costa, E. (2001). Down-regulation of dendritic spine and glutamic acid decarboxylase 67 expressions in the reelin haploinsufficient heterozygous reeler mouse. *Proc Natl Acad Sci U S A, 98*(6), 3477-3482. doi:10.1073/pnas.051614698

Lu, L. & Mao, H. (2019). Quantifying the Effect of Repeated Impacts and Lateral Tip Movements on Brain Responses during Controlled Cortical Impact. *J Neurotrauma, 36*(11), 1828-1835. doi:10.1089/neu.2018.5929

Ma, X., Aravind, A., Pfister, B. J., Chandra, N. & Haorah, J. (2019). Animal Models of Traumatic Brain Injury and Assessment of Injury Severity. *Mol Neurobiol, 56*(8), 5332-5345. doi:10.1007/s12035-018-1454-5

Marmarou, A., Foda, M. A., van den Brink, W., Campbell, J., Kita, H. & Demetriadou, K. (1994). A new model of diffuse brain injury in rats. Part I: Pathophysiology and biomechanics. *J Neurosurg, 80*(2), 291-300. doi:10.3171/jns.1994.80.2.0291

Mayeux, R., Ottman, R., Maestre, G., Ngai, C., Tang, M. X., Ginsberg, H., . . . Shelanski, M. (1995). Synergistic effects of traumatic head injury and apolipoprotein-epsilon 4 in patients with Alzheimer's disease. *Neurology, 45*(3 Pt 1), 555-557. doi:10.1212/wnl.45.3.555

Mazzeo, A. T., Beat, A., Singh, A. & Bullock, M. R. (2009). The role of mitochondrial transition pore, and its modulation, in traumatic brain injury and delayed neurodegeneration after TBI. *Exp Neurol, 218*(2), 363-370. doi:10.1016/j.expneurol.2009.05.026

Mena, J. H., Sanchez, A. I., Rubiano, A. M., Peitzman, A. B., Sperry, J. L., Gutierrez, M. I. & Puyana, J. C. (2011). Effect of the modified Glasgow Coma Scale score criteria for mild traumatic brain injury on mortality prediction: comparing classic and modified Glasgow Coma Scale score model scores of 13. *J Trauma, 71*(5), 1185-1192; discussion 1193. doi:10.1097/TA.0b013e31823321f8

Miao, G. G., Smeyne, R. J., D'Arcangelo, G., Copeland, N. G., Jenkins, N. A., Morgan, J. I. & Curran, T. (1994). Isolation of an allele of reeler by insertional mutagenesis. *Proc Natl Acad Sci U S A, 91*(23), 11050-11054. doi:10.1073/pnas.91.23.11050

Mouzon, B., Chaytow, H., Crynen, G., Bachmeier, C., Stewart, J., Mullan, M., . . . Crawford, F. (2012). Repetitive mild traumatic brain injury in a mouse model produces learning and memory deficits accompanied by histological changes. *J Neurotrauma, 29*(18), 2761-2773. doi:10.1089/neu.2012.2498

Nakano, Y., Kohno, T., Hibi, T., Kohno, S., Baba, A., Mikoshiba, K., . . . Hattori, M. (2007). The extremely conserved C-terminal region of Reelin is not necessary for secretion but is required for efficient activation of downstream signaling. *J Biol Chem, 282*(28), 20544-20552. doi:10.1074/jbc.M702300200

Nichols, J., Bjorklund, G. R., Newbern, J. & Anderson, T. (2018). Parvalbumin fast-spiking interneurons are selectively altered by paediatric traumatic brain injury. *J Physiol, 596*(7), 1277-1293. doi:10.1113/jp275393

Nikolaeva, I., Crowell, B., Valenziano, J., Meaney, D. & D'Arcangelo, G. (2016). Beneficial Effects of Early mTORC1 Inhibition after Traumatic Brain Injury. *J Neurotrauma, 33*(2), 183-193. doi:10.1089/neu.2015.3899

Niu, S., Renfro, A., Quattrocchi, C. C., Sheldon, M. & D'Arcangelo, G. (2004). Reelin promotes hippocampal dendrite development through the VLDLR/ApoER2-Dab1 pathway. *Neuron, 41*(1), 71-84.

O'Meara, E. S., Kukull, W. A., Sheppard, L., Bowen, J. D., McCormick, W. C., Teri, L., . . . Larson, E. B. (1997). Head injury and risk of Alzheimer's disease by apolipoprotein E genotype. *Am J Epidemiol, 146*(5), 373-384. doi:10.1093/oxfordjournals.aje.a009290

Okie, S. (2005). Traumatic brain injury in the war zone. *N Engl J Med, 352*(20), 2043-2047. doi:10.1056/NEJMp058102

Okonkwo, D. O., Yue, J. K., Puccio, A. M., Panczykowski, D. M., Inoue, T., McMahon, P. J., . . . Manley, G. T. (2013). GFAP-BDP as an acute diagnostic marker in traumatic brain injury: results from the prospective transforming research and clinical knowledge in traumatic brain injury study. *J Neurotrauma, 30*(17), 1490-1497. doi:10.1089/neu.2013.2883

Orcinha, C., Munzner, G., Gerlach, J., Kilias, A., Follo, M., Egert, U. & Haas, C. A. (2016). Seizure-Induced Motility of Differentiated Dentate Granule Cells Is Prevented by the Central Reelin Fragment. *Front Cell Neurosci, 10*, 183. doi:10.3389/fncel.2016.00183

Osier, N. & Dixon, C. E. (2016). The Controlled Cortical Impact Model of Experimental Brain Trauma: Overview, Research Applications, and Protocol. *Methods Mol Biol, 1462*, 177-192. doi:10.1007/978-1-4939-3816-2_11

Osier, N. D. & Dixon, C. E. (2016). The Controlled Cortical Impact Model: Applications, Considerations for Researchers, and Future Directions. *Frontiers in Neurology, 7*(134). doi:10.3389/fneur.2016.00134

Plummer, S., Van den Heuvel, C., Thornton, E., Corrigan, F. & Cappai, R. (2016). The Neuroprotective Properties of the Amyloid Precursor Protein Following Traumatic Brain Injury. *Aging Dis, 7*(2), 163-179. doi:10.14336/ad.2015.0907

Pohlkamp, T., David, C., Cauli, B., Gallopin, T., Bouche, E., Karagiannis, A., . . . Bock, H. H. (2014). Characterization and distribution of Reelin-positive interneuron subtypes in the rat barrel cortex. *Cereb Cortex, 24*(11), 3046-3058. doi:10.1093/cercor/bht161

Prince, C. & Bruhns, M. E. (2017). Evaluation and Treatment of Mild Traumatic Brain Injury: The Role of Neuropsychology. *Brain Sci, 7*(8). doi:10.3390/brainsci7080105

Prins, M., Greco, T., Alexander, D. & Giza, C. C. (2013). The pathophysiology of traumatic brain injury at a glance. *Dis Model Mech, 6*(6), 1307-1315. doi:10.1242/dmm.011585

Pujadas, L., Gruart, A., Bosch, C., Delgado, L., Teixeira, C. M., Rossi, D., . . . Soriano, E. (2010). Reelin regulates postnatal neurogenesis and enhances spine hypertrophy and long-term potentiation. *J Neurosci, 30*(13), 4636-4649. doi:10.1523/jneurosci.5284-09.2010

Pulido, J. S., Sugaya, I., Comstock, J. & Sugaya, K. (2007). Reelin expression is upregulated following ocular tissue injury. *Graefes Arch Clin Exp Ophthalmol, 245*(6), 889-893. doi:10.1007/s00417-006-0458-4

Ramos-Cejudo, J., Wisniewski, T., Marmar, C., Zetterberg, H., Blennow, K., de Leon, M. J. & Fossati, S. (2018). Traumatic Brain Injury and Alzheimer's Disease: The Cerebrovascular Link. *EBioMedicine, 28*, 21-30. doi:10.1016/j.ebiom.2018.01.021

Risling, M., Smith, D., Stein, T. D., Thelin, E. P., Zanier, E. R., Ankarcrona, M. & Nilsson, P. (2019). Modelling human pathology of traumatic brain injury in animal models. *J Intern Med, 285*(6), 594-607. doi:10.1111/joim.12909

Rogers, J. T., Rusiana, I., Trotter, J., Zhao, L., Donaldson, E., Pak, D. T., . . . Weeber, E. J. (2011). Reelin supplementation enhances cognitive ability, synaptic plasticity, and dendritic spine density. *Learn Mem, 18*(9), 558-564. doi:10.1101/lm.2153511

Rogers, J. T. & Weeber, E. J. (2008). Reelin and apoE actions on signal transduction, synaptic function and memory formation. *Neuron Glia Biol, 4*(3), 259-270. doi:10.1017/s1740925x09990184

Rolfe, A. & Sun, D. (2015). Frontiers in Neuroengineering Stem Cell Therapy in Brain Trauma: Implications for Repair and Regeneration of Injured Brain in Experimental TBI Models. In F. H. Kobeissy (Ed.), *Brain Neurotrauma: Molecular, Neuropsychological, and Rehabilitation Aspects*. Boca Raton (FL): CRC Press/Taylor & Francis (c) 2015 by Taylor & Francis Group, LLC.

Romine, J., Au - Gao, X. & Au - Chen, J. (2014). Controlled Cortical Impact Model for Traumatic Brain Injury. *JoVE*(90), e51781. doi:doi:10.3791/51781

Royaux, I., Lambert de Rouvroit, C., D'Arcangelo, G., Demirov, D. & Goffinet, A. M. (1997). Genomic organization of the mouse reelin gene. *Genomics, 46*(2), 240-250.

Rubenstein, R., Chang, B., Yue, J. K., Chiu, A., Winkler, E. A., Puccio, A. M., . . . Vassar, M. J. (2017). Comparing Plasma Phospho Tau, Total Tau, and Phospho Tau-Total Tau Ratio as Acute and Chronic Traumatic Brain Injury Biomarkers. *JAMA Neurol, 74*(9), 1063-1072. doi:10.1001/jamaneurol.2017.0655

Sabbagh, J. J. & Dickey, C. A. (2016). The Metamorphic Nature of the Tau Protein: Dynamic Flexibility Comes at a Cost. *Frontiers in Neuroscience, 10*(3). doi:10.3389/fnins.2016.00003

Sahler, C. S. & Greenwald, B. D. (2012). Traumatic brain injury in sports: a review. *Rehabil Res Pract, 2012*, 659652. doi:10.1155/2012/659652

Schwulst, S. J. & Au - Islam, M. B. A. R. (2019). Murine Model of Controlled Cortical Impact for the Induction of Traumatic Brain Injury. *JoVE*(150), e60027. doi:doi:10.3791/60027

Shaefi, S., Mittel, A. M., Hyam, J. A., Boone, M. D., Chen, C. C. & Kasper, E. M. (2016). Hypothermia for severe traumatic brain injury in adults: Recent lessons from randomized controlled trials. *Surg Neurol Int, 7*, 103. doi:10.4103/2152-7806.194816

Shapira, Y., Shohami, E., Sidi, A., Soffer, D., Freeman, S. & Cotev, S. (1988). Experimental closed head injury in rats: mechanical, pathophysiologic, and neurologic properties. *Crit Care Med, 16*(3), 258-265. doi:10.1097/00003246-198803000-00010

Sheldon, M., Rice, D. S., D'Arcangelo, G., Yoneshima, H., Nakajima, K., Mikoshiba, K., . . . Curran, T. (1997). Scrambler and yotari disrupt the disabled gene and produce a reeler-like phenotype in mice. *Nature, 389*(6652), 730-733. doi:10.1038/39601

Siebold, L., Obenaus, A. & Goyal, R. (2018). Criteria to define mild, moderate, and severe traumatic brain injury in the mouse controlled cortical impact model. *Exp Neurol, 310*, 48-57. doi:10.1016/j.expneurol.2018.07.004

Silverberg, N. D. & Iverson, G. L. (2011). Etiology of the post-concussion syndrome: Physiogenesis and Psychogenesis revisited. *NeuroRehabilitation, 29*(4), 317-329. doi:10.3233/nre-2011-0708

Smith, D. H., Chen, X. H., Nonaka, M., Trojanowski, J. Q., Lee, V. M., Saatman, K. E., . . . Meaney, D. F. (1999). Accumulation of amyloid beta and tau and the formation of neurofilament inclusions following diffuse brain injury in the pig. *J Neuropathol Exp Neurol, 58*(9), 982-992. doi:10.1097/00005072-199909000-00008

Stary, C. M., Xu, L., Sun, X., Ouyang, Y. B., White, R. E., Leong, J., . . . Giffard, R. G. (2015). MicroRNA-200c contributes to injury from transient focal cerebral ischemia by targeting Reelin. *Stroke, 46*(2), 551-556. doi:10.1161/strokeaha.114.007041

Stein, D. G., Sayeed, I., Espinosa-Garcia, C., Atif, F. & Sergeeva, E. G. (2017). Goldstein et al.'s Secondary Analysis of Progesterone Clinical Trial for Traumatic Brain Injury Can

Only Reflect the Same Trial Design Flaws: A Response to "Very Early Administration of Progesterone Does Not Improve Neuropsychological Outcomes in Subjects with Moderate to Severe Traumatic Brain Injury". *J Neurotrauma, 34*(13), 2192-2193. doi:10.1089/neu.2016.4949

Sun, D. (2014). The potential of endogenous neurogenesis for brain repair and regeneration following traumatic brain injury. *Neural Regen Res, 9*(7), 688-692. doi:10.4103/1673-5374.131567

Sun, D., Colello, R. J., Daugherty, W. P., Kwon, T. H., McGinn, M. J., Harvey, H. B. & Bullock, M. R. (2005). Cell proliferation and neuronal differentiation in the dentate gyrus in juvenile and adult rats following traumatic brain injury. *J Neurotrauma, 22*(1), 95-105. doi:10.1089/neu.2005.22.95

Tang-Schomer, M. D., Johnson, V. E., Baas, P. W., Stewart, W. & Smith, D. H. (2012). Partial interruption of axonal transport due to microtubule breakage accounts for the formation of periodic varicosities after traumatic axonal injury. *Exp Neurol, 233*(1), 364-372. doi:10.1016/j.expneurol.2011.10.030

Taylor, C. A., Bell, J. M., Breiding, M. J. & Xu, L. (2017). Traumatic Brain Injury-Related Emergency Department Visits, Hospitalizations, and Deaths - United States, 2007 and 2013. *MMWR Surveill Summ, 66*(9), 1-16. doi:10.15585/mmwr.ss6609a1

Teasdale, G. M., Murray, G. D. & Nicoll, J. A. (2005). The association between APOE epsilon4, age and outcome after head injury: a prospective cohort study. *Brain, 128*(Pt 11), 2556-2561. doi:10.1093/brain/awh595

Teixeira, C. M., Kron, M. M., Masachs, N., Zhang, H., Lagace, D. C., Martinez, A., . . . Soriano, E. (2012). Cell-autonomous inactivation of the reelin pathway impairs adult neurogenesis in the hippocampus. *J Neurosci, 32*(35), 12051-12065. doi:10.1523/jneurosci.1857-12.2012

Trommsdorff, M., Gotthardt, M., Hiesberger, T., Shelton, J., Stockinger, W., Nimpf, J., . . . Herz, J. (1999). Reeler/Disabled-like disruption of neuronal migration in knockout mice lacking the VLDL receptor and ApoE receptor 2. *Cell, 97*(6), 689-701. doi:10.1016/s0092-8674(00)80782-5

Trotter, J., Lee, G. H., Kazdoba, T. M., Crowell, B., Domogauer, J., Mahoney, H. M., . . . D'Arcangelo, G. (2013). Dab1 is required for synaptic plasticity and associative learning. *J Neurosci, 33*(39), 15652-15668. doi:10.1523/jneurosci.2010-13.2013

Trotter, J., Lee, G. H., Kazdoba, T. M., Crowell, B., Domogauer, J., Mahoney, H. M., . . . D'Arcangelo, G. (2013). Dab1 Is Required for Synaptic Plasticity and Associative Learning. *The Journal of Neuroscience, 33*(39), 15652-15668. doi:10.1523/jneurosci.2010-13.2013

Turtzo, L. C., Budde, M. D., Dean, D. D., Gold, E. M., Lewis, B. K., Janes, L., . . . Frank, J. A. (2015). Failure of intravenous or intracardiac delivery of mesenchymal stromal cells to improve outcomes after focal traumatic brain injury in the female rat. *PLoS One, 10*(5), e0126551. doi:10.1371/journal.pone.0126551

Turtzo, L. C., Budde, M. D., Gold, E. M., Lewis, B. K., Janes, L., Yarnell, A., . . . Frank, J. A. (2013). The evolution of traumatic brain injury in a rat focal contusion model. *NMR Biomed, 26*(4), 468-479. doi:10.1002/nbm.2886

Utsunomiya-Tate, N., Kubo, K.-i., Tate, S.-i., Kainosho, M., Katayama, E., Nakajima, K. & Mikoshiba, K. (2000). Reelin molecules assemble together to form a large protein complex, which is inhibited by the function-blocking CR-50 antibody. *Proceedings of the National Academy of Sciences, 97*(17), 9729-9734. doi:10.1073/pnas.160272497

Van Putten, H. P., Bouwhuis, M. G., Muizelaar, J. P., Lyeth, B. G. & Berman, R. F. (2005). Diffusion-weighted imaging of edema following traumatic brain injury in rats: effects of secondary hypoxia. *J Neurotrauma, 22*(8), 857-872. doi:10.1089/neu.2005.22.857

Ventruti, A., Kazdoba, T. M., Niu, S. & D'Arcangelo, G. (2011). Reelin deficiency causes specific defects in the molecular composition of the synapses in the adult brain. *Neuroscience, 189*, 32-42. doi:10.1016/j.neuroscience.2011.05.050

Vergouwen, M. D., Vermeulen, M. & Roos, Y. B. (2006). Effect of nimodipine on outcome in patients with traumatic subarachnoid haemorrhage: a systematic review. *Lancet Neurol, 5*(12), 1029-1032. doi:10.1016/s1474-4422(06)70582-8

Wan, X., Gan, C., You, C., Fan, T., Zhang, S., Zhang, H., . . . Lei, T. (2019). Association of APOE epsilon4 with progressive hemorrhagic injury in patients with traumatic intracerebral hemorrhage. *J Neurosurg*, 1-8. doi:10.3171/2019.4.Jns183472

Wang, F., Wang, X., Shapiro, L. A., Cotrina, M. L., Liu, W., Wang, E. W., . . . Huang, J. H. (2017). NKCC1 up-regulation contributes to early post-traumatic seizures and increased post-traumatic seizure susceptibility. *Brain Struct Funct, 222*(3), 1543-1556. doi:10.1007/s00429-016-1292-z

Washington, P. M., Forcelli, P. A., Wilkins, T., Zapple, D. N., Parsadanian, M. & Burns, M. P. (2012). The effect of injury severity on behavior: a phenotypic study of cognitive and emotional deficits after mild, moderate, and severe controlled cortical impact injury in mice. *J Neurotrauma, 29*(13), 2283-2296. doi:10.1089/neu.2012.2456

Wasser, C. R. & Herz, J. (2017). Reelin: Neurodevelopmental Architect and Homeostatic Regulator of Excitatory Synapses. *J Biol Chem, 292*(4), 1330-1338. doi:10.1074/jbc.R116.766782

Weber, J. T., Rzigalinski, B. A. & Ellis, E. F. (2001). Traumatic injury of cortical neurons causes changes in intracellular calcium stores and capacitative calcium influx. *J Biol Chem, 276*(3), 1800-1807. doi:10.1074/jbc.M009209200

Wei, Y., Shin, M. R. & Sesti, F. (2018). Oxidation of KCNB1 channels in the human brain and in mouse model of Alzheimer's disease. *Cell Death & Disease, 9*(8), 820. doi:10.1038/s41419-018-0886-1

Werner, C. & Engelhard, K. (2007). Pathophysiology of traumatic brain injury. *Br J Anaesth, 99*(1), 4-9. doi:10.1093/bja/aem131

Weston, N. M. & Sun, D. (2018). The Potential of Stem Cells in Treatment of Traumatic Brain Injury. *Curr Neurol Neurosci Rep, 18*(1), 1. doi:10.1007/s11910-018-0812-z

Wible, E. F. & Laskowitz, D. T. (2010). Statins in traumatic brain injury. *Neurotherapeutics, 7*(1), 62-73. doi:10.1016/j.nurt.2009.11.003

Xiong, Y., Mahmood, A. & Chopp, M. (2013). Animal models of traumatic brain injury. *Nat Rev Neurosci, 14*(2), 128-142. doi:10.1038/nrn3407

Xiong, Y., Mahmood, A. & Chopp, M. (2018). Current understanding of neuroinflammation after traumatic brain injury and cell-based therapeutic opportunities. *Chin J Traumatol, 21*(3), 137-151. doi:10.1016/j.cjtee.2018.02.003

Xu, H., Wang, Z., Li, J., Wu, H., Peng, Y., Fan, L., . . . Chen, G. (2017). The Polarization States of Microglia in TBI: A New Paradigm for Pharmacological Intervention. *Neural Plast, 2017*, 5405104. doi:10.1155/2017/5405104

Yasui, N., Nogi, T., Kitao, T., Nakano, Y., Hattori, M. & Takagi, J. (2007). Structure of a receptor-binding fragment of reelin and mutational analysis reveal a recognition mechanism similar to endocytic receptors. *Proceedings of the National Academy of Sciences, 104*(24), 9988-9993. doi:10.1073/pnas.0700438104

Zanier, E. R., Montinaro, M., Vigano, M., Villa, P., Fumagalli, S., Pischiutta, F., . . . De Simoni, M. G. (2011). Human umbilical cord blood mesenchymal stem cells protect mice brain after trauma. *Crit Care Med, 39*(11), 2501-2510. doi:10.1097/CCM.0b013e31822629ba

Zhang, X., Chen, Y., Jenkins, L. W., Kochanek, P. M. & Clark, R. S. (2005). Bench-to-bedside review: Apoptosis/programmed cell death triggered by traumatic brain injury. *Crit Care, 9*(1), 66-75. doi:10.1186/cc2950

Zheng, W., ZhuGe, Q., Zhong, M., Chen, G., Shao, B., Wang, H., . . . Jin, K. (2013). Neurogenesis in adult human brain after traumatic brain injury. *J Neurotrauma, 30*(22), 1872-1880. doi:10.1089/neu.2010.1579